NUREG/CR-6800
ORNL/TM-2002/6

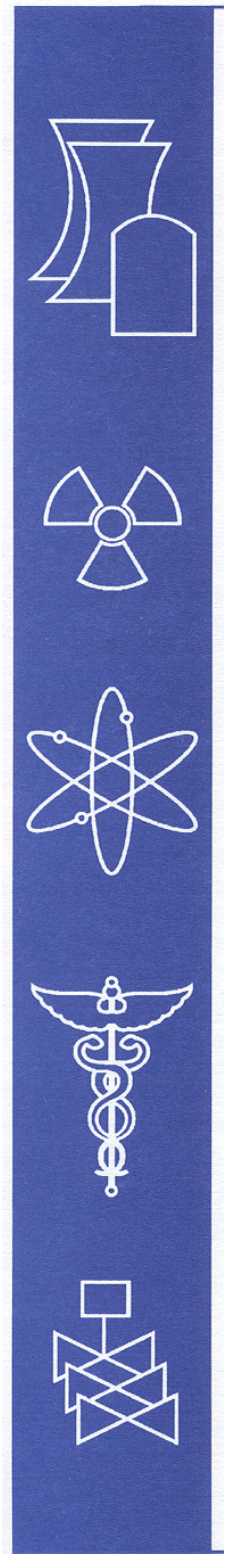

Assessment of Reactivity Margins and Loading Curves for PWR Burnup-Credit Cask Designs

Prepared by
J. C. Wagner and C. E. Sanders, ORNL

Oak Ridge National Laboratory

U.S. Nuclear Regulatory Commission
Office of Nuclear Regulatory Research
Washington, DC 20555-0001

AVAILABILITY OF REFERENCE MATERIALS IN NRC PUBLICATIONS

NRC Reference Material

As of November 1999, you may electronically access NUREG-series publications and other NRC records at NRC's Public Electronic Reading Room at http://www.nrc.gov/reading-rm.html. Publicly released records include, to name a few, NUREG-series publications; *Federal Register* notices; applicant, licensee, and vendor documents and correspondence; NRC correspondence and internal memoranda; bulletins and information notices; inspection and investigative reports; licensee event reports; and Commission papers and their attachments.

NRC publications in the NUREG series, NRC regulations, and *Title 10, Energy*, in the Code of *Federal Regulations* may also be purchased from one of these two sources:

1. The Superintendent of Documents
   U.S. Government Printing Office
   P.O. Box SSOP
   Washington, DC 20402–0001
   Internet: bookstore.gpo.gov
   Telephone: 202–512–1800
   Fax: 202-512-2250
2. The National Technical Information Service
   Springfield, VA 22161–0002
   www.ntis.gov
   1–800–553–6847 or, locally, 703–605–6000

A single copy of each NRC draft report for comment is available free, to the extent of supply, upon written request as follows:

Address: Office of the Chief Information Officer,
Reproduction and Distribution
Services Section
U.S. Nuclear Regulatory Commission
Washington, DC 20555–0001
E-mail: DISTRIBUTION@nrc.gov
Facsimile: 301–415–2289

Some publications in the NUREG series that are posted at NRC's Web site address http://www.nrc.gov/reading-rm/doc-collections/nuregs are updated periodically and may differ from the last printed version. Although references to material found on a Web site bear the date the material was accessed, the material available on the date cited may subsequently be removed from the site.

Non-NRC Reference Material

Documents available from public and special technical libraries include all open literature items, such as books, journal articles, and transactions, *Federal Register* notices, Federal and State legislation, and congressional reports. Such documents as theses, dissertations, foreign reports and translations, and non-NRC conference proceedings may be purchased from their sponsoring organization.

Copies of industry codes and standards used in a substantive manner in the NRC regulatory process are maintained at—

The NRC Technical Library
Two White Flint North
11545 Rockville Pike
Rockville, MD 20852–2738

These standards are available in the library for reference use by the public. Codes and standards are usually copyrighted and may be purchased from the originating organization or, if they are American National Standards, from—

American National Standards Institute
11 West 42nd Street
New York, NY 10036–8002
www.ansi.org
212–642–4900

Legally binding regulatory requirements are stated only in laws; NRC regulations; licenses, including technical specifications; or orders, not in NUREG-series publications. The views expressed in contractor-prepared publications in this series are not necessarily those of the NRC.

The NUREG series comprises (1) technical and administrative reports and books prepared by the staff (NUREG/XXXX) or agency contractors (NUREG/CR-XXXX), (2) proceedings of conferences (NUREG/CP-XXXX), (3) reports resulting from international agreements (NUREG/IA-XXXX), (4) brochures (NUREG/BR-XXXX), and (5) compilations of legal decisions and orders of the Commission and Atomic and Safety Licensing Boards and of Directors' decisions under Section 2.206 of NRC's regulations (NUREG-0750).

NUREG/CR–6800
ORNL/TM–2002/6

Assessment of Reactivity Margins and Loading Curves for PWR Burnup-Credit Cask Designs

Manuscript Completed: November 2002
Date Published: March 2003

Prepared by
J. C. Wagner and C. E. Sanders, ORNL

Oak Ridge National Laboratory
Managed by UT-Battelle, LLC
Oak Ridge, TN 37831–6370

R. Y. Lee, NRC Project Manager

Prepared for
Division of System Analysis and Regulatory Effectiveness
Office of Nuclear Regulatory Research
U.S. Nuclear Regulatory Commission
Washington, DC 20555–0001
NRC Job Code W6479

ABSTRACT

This report presents studies to assess reactivity margins and loading curves for pressurized water reactor (PWR) burnup-credit criticality safety evaluations. The studies are based on a generic high-density 32-assembly cask and systematically vary individual calculational (depletion and criticality) assumptions to demonstrate the impact on the predicted effective neutron multiplication factor, k_{eff}, and burnup-credit loading curves. The purpose of this report is to provide a greater understanding of the importance of input parameter variations and quantify the impact of calculational assumptions on the outcome of a burnup-credit evaluation. This study should provide guidance to regulators and industry on the technical areas where improved information will most enhance the estimation of accurate subcritical margins. Based on these studies, areas where future work may provide the most benefit are identified. The report also includes an evaluation of the degree of burnup credit needed for high-density casks to transport the current spent nuclear fuel inventory. By comparing PWR discharge data to actinide-only based loading curves and determining the number of assemblies that meet the loading criteria, this evaluation finds that additional negative reactivity (through either increased credit for fuel burnup or cask design/utilization modifications) is necessary to accommodate the majority of current spent fuel assemblies in high-capacity casks. Assemblies that are not acceptable for loading in the prototypic high-capacity cask may be stored or transported by other means (e.g., lower capacity casks that utilize flux traps and/or increased fixed poison concentrations or high-capacity casks with design/utilization modifications).

CONTENTS

Page

CONTENTS (continued)

LIST OF FIGURES

LIST OF FIGURES (continued)

LIST OF FIGURES (continued)

LIST OF TABLES

FOREWORD

In 1999 the United States Nuclear Regulatory Commission (U.S. NRC) issued initial recommended guidance for using reactivity credit due to fuel irradiation (i.e., burnup credit) in the criticality safety analysis of spent pressurized-water-reactor (PWR) fuel in storage and transportation packages. This guidance was issued by the NRC Spent Fuel Project Office (SFPO) as Revision 1 to Interim Staff Guidance 8 (ISG8R1) and published in the *Standard Review Plan for Transportation Packages for Spent Nuclear Fuel*, NUREG-1617 (March 2000). With this initial guidance as a basis, the NRC Office of Nuclear Regulatory Research initiated a program to provide the SFPO with technical information that would:

- enable realistic estimates of the subcritical margin for systems with spent nuclear fuel (SNF) and an increased understanding of the phenomena and parameters that impact the margin, and
- support the development of technical bases and recommendations for effective implementation of burnup credit and provide realistic SNF acceptance criteria while maintaining an adequate margin of safety.

A significant number of domestic and international studies have been performed to help understand the components that influence the negative reactivity available with burnup credit. However, most of these studies have focused on a specific technical issue and a comparison between studies is often difficult due to the use of different calculational assumptions (e.g., nuclide sets, cask models, etc.). This report presents comprehensive parametric studies to demonstrate the effect of variations in the calculational assumptions (depletion and criticality) required for a PWR burnup-credit safety evaluation on the predicted effective neutron multiplication factor, k_{eff}, and ultimately on burnup-credit loading curves. The purpose of this report is to provide a greater understanding of the importance of input parameter variations on k_{eff} values and loading curves and identify the impact of the calculational assumptions on the outcome of burnup-credit criticality safety evaluations. Such information is valuable to help guide implementation of burnup credit by focusing efforts on areas that will best contribute to achieving accurate and realistic estimates of the subcritical margin. Improved estimates of the subcritical margin will make it possible to increase the applicability of burnup credit to a greater population of present and future SNF for PWRs. The use of burnup-credit results in fewer casks needing to be transported, thereby reducing regulatory burden on licensees while maintaining safety for transporting SNF. Lastly, this effort will contribute to making effective, efficient, and realistic regulatory decisions.

Farouk Eltawila, Director
Division of Systems Analysis and Regulatory Effectiveness

ACKNOWLEDGEMENTS

This work was performed under contract with the Office of Nuclear Regulatory Research, U.S. Nuclear Regulatory Commission (NRC). The authors gratefully acknowledge C. V. Parks of Oak Ridge National Laboratory (ORNL) for providing guidance for this work and valuable comments/suggestions on the draft report. We would like to thank C. J. Withee of the NRC Spent Fuel Project Office for useful discussions, suggestions, and review of this document. In addition, the thorough review of the draft manuscript by M. D. DeHart and I. C. Gauld is very much appreciated. Finally, the authors are thankful to W. C. Carter for her preparation and formatting of the final report.

1 INTRODUCTION

This report presents the results of parametric studies to evaluate the impact of variations in the calculational assumptions (depletion and criticality) required for a pressurized-water-reactor (PWR) burnup-credit safety evaluation on the effective neutron multiplication factor, k_{eff}. The final product of a burnup-credit safety evaluation is a loading curve, which specifies loading criteria in terms of the minimum required assembly burnup as a function of assembly-initial enrichment. A loading curve represents combinations of burnup and initial fuel enrichment that correspond to a single value of k_{eff} for a given configuration (e.g., a burnup-credit cask). An illustrative loading curve is shown in Figure 1. Because loading curves dictate acceptability of spent nuclear fuel (SNF) assemblies for cask loading, it is important to understand how variations in analysis assumptions influence calculated loading curves. This understanding will assist in the prudent selection of calculational assumptions, identify areas where future work may provide the most benefit, and identify assumptions that have negligible impact. As the uncertainties in burnup-credit analyses are better understood and reduced, the population of SNF qualified for loading in high-capacity casks can be increased while adequate safety margins are maintained.

1.1 BACKGROUND

In the past, criticality safety analyses for commercial light-water-reactor (LWR) SNF storage and transportation canisters assumed the spent fuel to be fresh (unirradiated) fuel with uniform isotopic compositions corresponding to the maximum allowable enrichment and without fixed burnable absorbers.[1] This *fresh-fuel assumption* provides a well-defined, bounding approach to the criticality safety analysis that eliminates concerns related to the fuel operating history, and thus considerably simplifies the safety analysis. However, because this assumption ignores the inherent decrease in reactivity as a result of irradiation, it is very conservative. The concept of taking credit for the reduction in reactivity due to fuel burnup is commonly referred to as *burnup credit.* Numerous publications (e.g., Refs. 2, 3, 4) have demonstrated that increases in SNF cask capacities from the use of burnup credit can enable a reduction in the number of casks and shipments, and thus have considerable financial and safety-related benefits. A review of the technical issues associated with burnup credit for LWR fuel is available in Ref. 5.

The reduction in reactivity that occurs with fuel burnup is due to the change in concentration (net reduction) of fissile nuclides and the production of actinide and fission-product neutron absorbers. Consequently, it has been recognized that if criticality calculations are performed based on all fissile nuclides and a limited subset of absorbers, the calculated k_{eff} value is conservative (i.e., k_{eff} is overestimated). To date, the proposed approach for burnup credit in storage and transportation casks has been to qualify calculated isotopic predictions via validation against destructive assay measurements from SNF samples and qualify criticality analysis methods via validation against applicable critical experiments. Thus, the nuclides in a safety analysis process have been primarily limited by the availability of measured assay data and applicable critical experiments.

The use of burnup credit necessitates that the reactor operating conditions experienced by the fuel be considered. Consequently, in comparison to analyses based on the fresh-fuel assumption, additional information and assumptions are needed for input to a burnup-credit evaluation. A related complication lies in the desire for storage and transportation casks for a given reactor type, PWR or boiling-water reactor (BWR), to be qualified to accept SNF assemblies from all (or many) United States (U.S.) utilities,

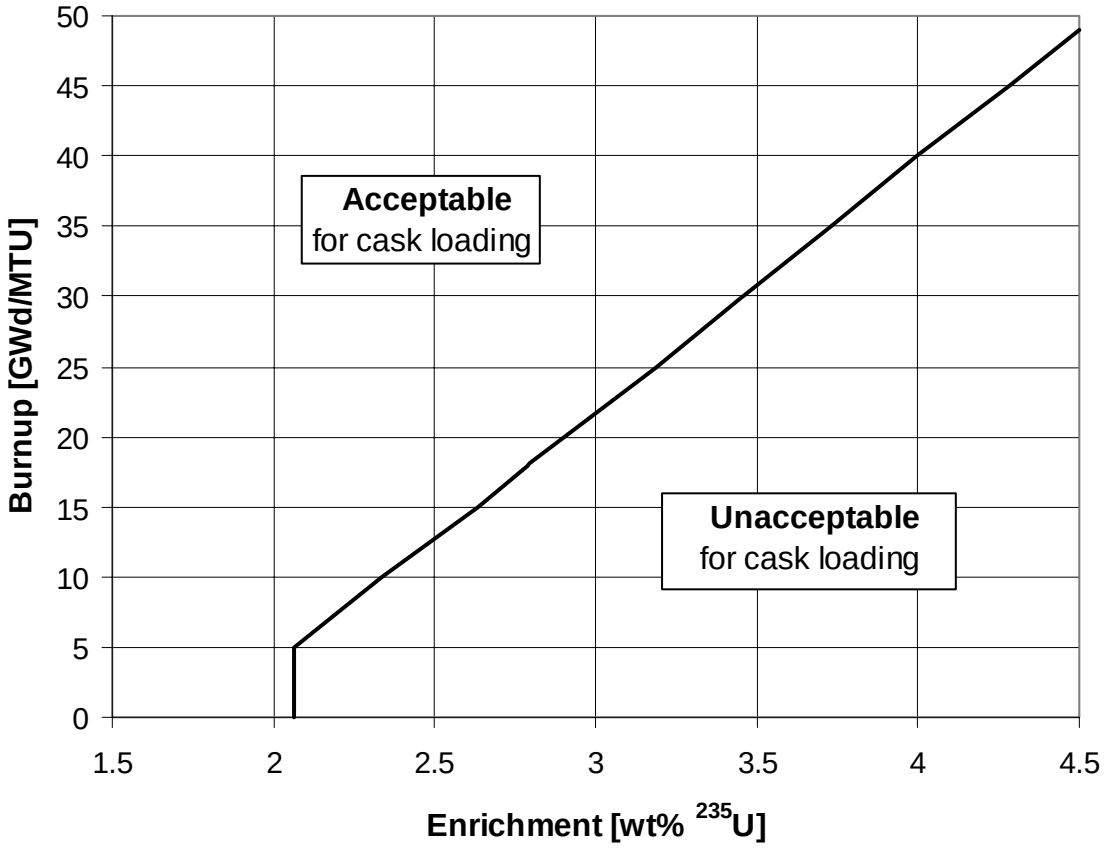

Figure 1 Illustrative burnup-credit loading curve depicting initial enrichment and minimum burnup combinations that define the boundary for loading acceptability. All points on the curve represent burnup and enrichment combinations that yield the same value of k_{eff}. [The vertical portion of the loading curve (at low burnup) corresponds to a region in which the reduction in reactivity due to burnup is overwhelmed by the increase in reactivity associated with the conservatism in the burnup-credit evaluation. Hence, no credit is taken for burnup in this region.]

and thus accept fuel that has experienced varying reactor operating conditions. Such broad qualification on cask contents requires an understanding of the effects of variations in reactor operating conditions and fuel assembly design characteristics on the reactivity of SNF to establish justifiable assumptions for a burnup-credit evaluation. Although a large number of studies (e.g., Refs. 6–15) have been performed, a consensus has not been reached on many of the important analysis assumptions. This situation is largely attributed to the difficulties associated with the accurate estimation of uncertainties for such a complex problem. A requirement for analyses to account for extreme or atypical reactor operating conditions can introduce significant conservatism with respect to typical SNF. Additionally, there remains an incomplete understanding of the impact of variations in many modeling assumptions on the final outcome of a burnup-credit evaluation (a burnup-enrichment loading curve).

To date, there has been no regulatory experience in the U.S. with licensing of a PWR or BWR cask using burnup credit. As mentioned, studies performed in the U.S. and abroad have provided an advanced understanding of the issues and a basis for developing approaches for a safety evaluation. Based on these technical investigations, the Spent Fuel Project Office (SFPO) of the Nuclear Regulatory Commission (NRC) issued Revision 1 of Interim Staff Guidance 8 (ISG-8)[16] on burnup credit in July 1999. A discussion of the technical considerations that helped form the development of ISG-8 can be found in Ref. 17. Subsequently, the recommendations in ISG-8 were incorporated into the NRC Standard Review Plan for transportation casks.[18]

This regulatory guidance[16,18] recommends limiting the amount of burnup credit to that available from actinide compositions in SNF with an assembly-averaged burnup of 40 GWd/MTU or less. Regarding modeling assumptions, it is recommended that the applicant ensure that the actinide compositions used in analyzing the licensing safety basis are calculated using fuel design and in-reactor operating parameters selected to provide conservative estimates of the k_{eff} value under cask conditions. Furthermore, it is recommended that the calculation of the k_{eff} value be performed using cask models, appropriate analysis assumptions, and code inputs that allow adequate representation of the physics of the spent fuel cask environment.

A small shift (up or down) in a cask loading curve can have a significant impact on the number of SNF assemblies that are acceptable for loading. Consequently, reductions in analysis uncertainties or increases in allowable burnup credit can lower the burnup-enrichment loading curve and notably expand the applicability of burnup credit. This point is demonstrated by comparing the illustrative loading curve in Figure 1 to the PWR SNF discharge data shown in Figure 2. Cask design characteristics (e.g., assembly separation, fixed poison loading, and the use of assembly inserts) can also be optimized to lower burnup-credit loading curves. Assemblies that are not qualified for loading in a high-capacity cask (i.e., do not meet the minimum burnup requirement for its initial enrichment value) may be stored or transported by other means. These include (1) lower capacity (e.g., 24-assembly) casks that utilize flux traps and/or increased fixed poison concentrations and (2) high-capacity casks with design/utilization modifications, such as increased assembly separation and neutron poison concentration or the use of absorber rods that are inserted into assemblies.

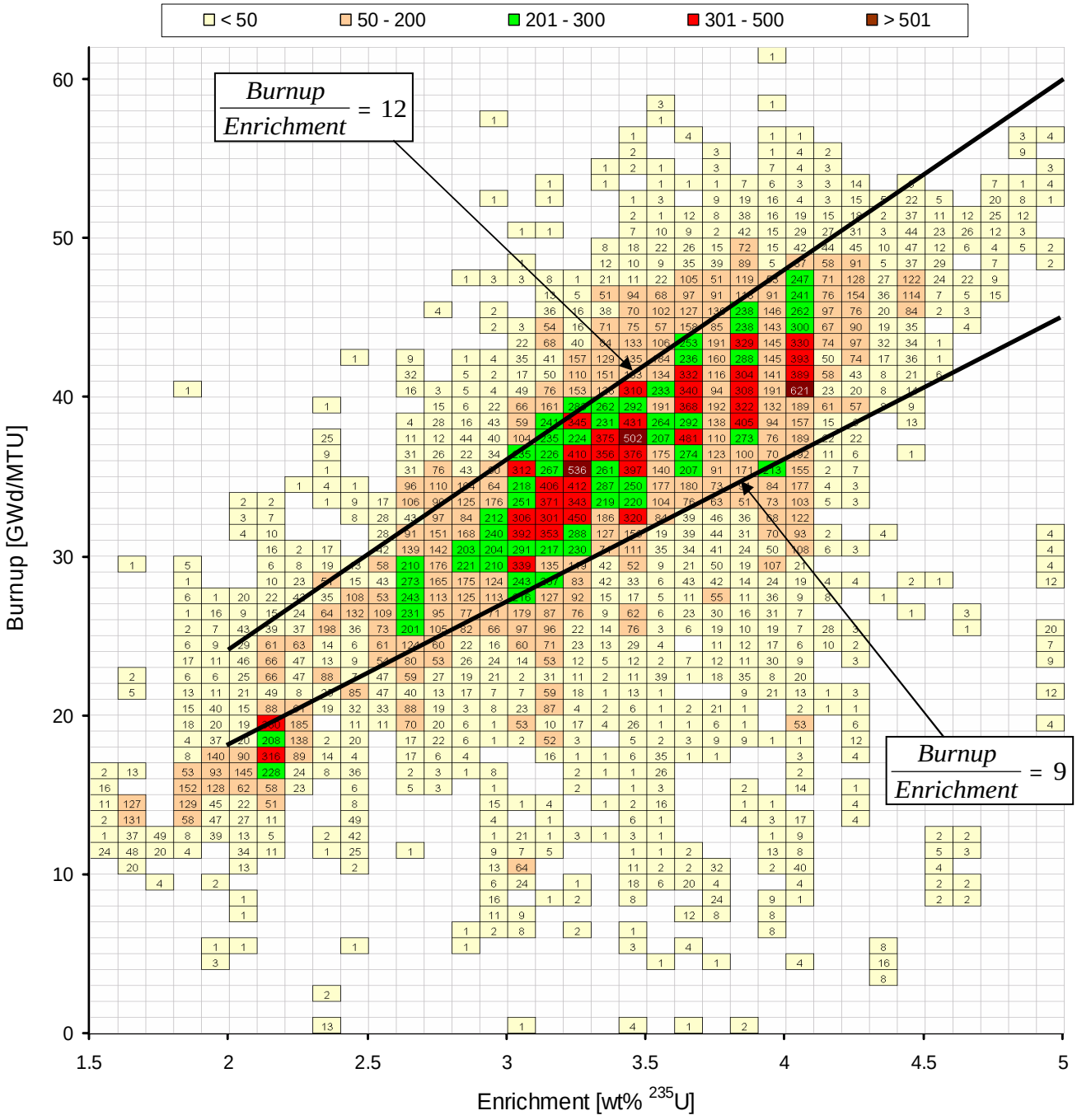

Figure 2 PWR SNF data illustrating the range of typical enrichment and discharge burnup combinations (Ref. 19). Numerical values in legend and on figure correspond to the number of SNF assemblies.

1.2 PURPOSE

The purpose of this report is to use a prototypic high-capacity 32-assembly cask as a basis to investigate and quantify the effect of variations in burnup-credit analysis assumptions on the value of k_{eff}, and subsequently on burnup-credit loading curves. The use of a single representative storage/transportation cask design to investigate the variation in analysis assumptions enables the relative value of the assumptions to be better understood. This information may assist NRC staff reviewers in their evaluation of the calculational assumptions used in burnup-credit applications and provide guidance with respect to technical areas where improved information will most improve the accuracy of burnup-credit analyses margin estimates.

1.3 OUTLINE

The remainder of this report is organized as follows: Section 2 describes the computational methods and codes used for the analyses. Section 3 provides a physical description of the cask used for the studies and describes the reference calculational models. Results are presented in Section 4 for fresh fuel conditions to establish a baseline for comparisons. The effects of variations in depletion parameters/conditions on k_{eff} values are investigated in Section 5. Studies of the effects of the important criticality modeling assumptions are provided in Section 6. Finally, the effectiveness of using burnup credit to accommodate SNF in a high-capacity cask is evaluated by comparing SNF discharge data to loading curves in Section 7, followed by conclusions in Section 8.

2 COMPUTATIONAL METHODS

The burnup-credit analysis process involves depletion calculations to determine the SNF isotopic compositions, extracting SNF isotopic compositions from the depletion output for use in a criticality model, and a criticality calculation to determine the k_{eff} value. Additionally, the generation of a loading curve requires a series of depletion and criticality calculations to determine burnup and enrichment combinations that correspond to a given value of k_{eff}. To simplify this process, an analysis sequence[20] has been developed to automate burnup-credit analyses by coupling the depletion and criticality modules of SCALE.[21] This sequence, referred to as STARBUCS,[20, 22] was used for the analyses presented in this report.

The STARBUCS sequence couples a number of SCALE code modules, including ARP, ORIGEN-S, CSASI, WAX, and KENO V.a, to achieve the automation. The ARP code prepares cross sections for each burnup step based on interpolation for fuel enrichment and mid-cycle burnup from a user-supplied ARP library that contains problem-dependent cross sections. The ORIGEN-ARP methodology offers a faster alternative to the SAS2H depletion analysis sequence[23] in SCALE, while maintaining calculational accuracy.[24] Several ARP libraries are available with the SCALE code package, or the user may generate their own problem-specific libraries. The generation of ARP libraries is straightforward and is explained in detail in Ref. 25. For the analyses presented in this report, numerous problem-specific ARP libraries were generated with the SAS2H sequence and the SCALE 44-group library.

Using an ARP-generated cross-section library, ORIGEN-S performs the depletion calculations to generate fuel compositions for all unique fuel regions (e.g., different axial- and/or horizontal-burnup regions). The CSASI module is used to automate resonance self-shielding calculations and prepare macroscopic fuel cross sections for each unique fuel region. Sequentially with CSASI, the WAX modules are executed to append the cross sections into a single cross-section library. Finally, the STARBUCS module executes the three-dimensional (3-D) KENO V.a Monte Carlo criticality code[26] using the generated cross sections and isotopic compositions. To ensure proper convergence and reduce statistical uncertainty, the KENO V.a calculations simulated 1100 generations, with 2000 neutron histories per generation, and skipped the first 100 generations before averaging; thus, each calculated k_{eff} value is based on 2 million neutron histories. The KENO V.a calculations utilized the SCALE 238-group cross-section library.

The objective of a burnup-credit evaluation is the generation of burnup-enrichment loading curves, which represent burnup and enrichment combinations that correspond to a given k_{eff} value for a given fuel/cask design. The determination of these burnup-enrichment combinations requires a number of depletion and criticality calculations associated with an iterative search and/or interpolation. The development of the STARBUCS sequence has enabled the automation of the generation of loading curves through the addition of a search capability[22] that allows repeated STARBUCS calculations to be performed, using a least-squares analysis of the results to automatically adjust enrichment until a desired k_{eff} value is obtained within a desired tolerance for a series of burnup steps. Although this search capability is computationally intensive (each data point on a loading curve requires ~5 iterations), it completely automates the process, and therefore is not user-time intensive. Hence, this capability has facilitated studies to evaluate the effect of calculational assumptions on loading curves. For calculations utilizing this search capability, the target k_{eff} value was 0.94 with a convergence criterion of $\pm$ 0.002. Therefore, all loading curves presented in this report correspond to $k_{eff} = 0.940 \pm 0.002$. Note that the loading curves generated for this report are intended to only demonstrate the effects of various analysis assumptions, and thus may not include all of the conservative assumptions that would be required for a licensing evaluation.

3 CASK DESCRIPTION AND MODELS

In a separate effort[27] related to burnup credit, a generic high-capacity burnup-credit-style cask, designated GBC-32, was defined as a computational benchmark to provide a reference configuration for the estimation of reactivity margins available from fission products and minor actinides. The generic cask design includes features from several U.S. cask vendor's designs (e.g., similar canister inside diameter and Boral[†] for fixed neutron poison), as well as features from an internationally specified benchmark cask,[14] and will accommodate 32 PWR fuel assemblies. Hence, the GBC-32 cask was used for all of the studies presented in this report. The boron loading in the Boral panels is 0.0225 g $^{10}B/cm^2$, which, per regulatory guidance,[1] is 75% of the 0.0300 g $^{10}B/cm^2$ loading that corresponds to the modeled Boral panel thickness. Detailed specifications for the GBC-32 cask are available in Ref. 27.

3.1 CALCULATIONAL MODELS FOR THE GBC-32 CASK

Three calculational models of the GBC-32 cask were developed for KENO V.a. The first model is the GBC-32 cask with uniform axial and horizontal fuel composition. This model was used for fresh fuel calculations and for various comparisons to cases with non-uniform axial and/or horizontal burnup. Cross-sectional views of the computational model, as generated by KENO V.a, are shown in Figure 3 and Figure 4. The second model includes the active fuel length divided into 18 equally-spaced axial regions to enable representation of the variation in axial composition due to axial burnup. The third model has additional modeling detail to represent the horizontal variation in burnup. For conservatism, the assemblies are oriented such that the lower burnup regions of neighboring assemblies are adjacent. Although this is anticipated to be the most-reactive assembly orientation, no studies were performed to confirm this expectation. A cross-sectional view of this model, which indicates the fuel assembly orientation, is shown in Figure 5. In all cases, all of the assemblies in the cask models are the same (i.e., the same initial enrichment, assembly-averaged burnup, and cooling time).

To enable comparisons of various assumptions, a **reference model** was defined for the criticality calculations. The reference model includes an axial-burnup distribution and assumes 5-year cooling time, but does not include horizontal burnup or isotopic correction factors (used to "correct" predicted isotopic compositions to that determined from comparisons with measured assay data). The axial-burnup profile used in the reference model corresponds to the bounding profile suggested in Ref. 6 for PWR fuel with assembly-averaged discharge burnup greater than 30 GWd/MTU. The profile is plotted in Figure 6 and the specifications necessary for modeling the profile are provided in Table 1. The fuel design used in the reference model is the Westinghouse (WE) 17×17 assembly.

It is also necessary to define the nuclides included in the criticality models. The use of a subset of possible actinides in burnup-credit calculations is referred to as "actinide-only" burnup credit. The use of a subset of possible actinides and fission products is referred to herein as "actinide + fission product" burnup credit. The actinide and fission product nuclides used here for actinide + fission product calculations are consistent with those identified in Ref. 5 as being the most important for criticality calculations. Table 2 lists the nuclides included for the two classifications of burnup credit. These "classes" of burnup-credit nuclides are defined here for the purpose of these studies; other terminology and nuclide sets have been defined and used by others studying burnup-credit phenomena.

[†] Boral is a clad composite of aluminum and boron carbide. A Boral panel or plate consists of three distinct layers. The outer layers are aluminum cladding which form a sandwich with a central layer that consists of a uniform aggregate of fine boron carbide particles within an aluminum alloy matrix.

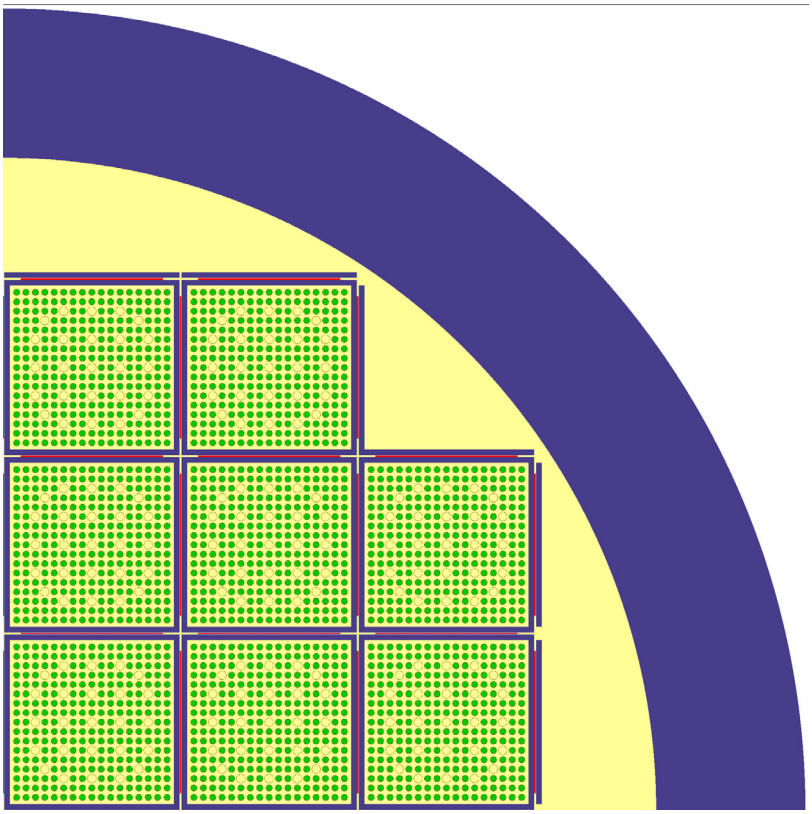

Figure 3 Radial cross section of one quarter of the KENO V.a model of the GBC-32 cask

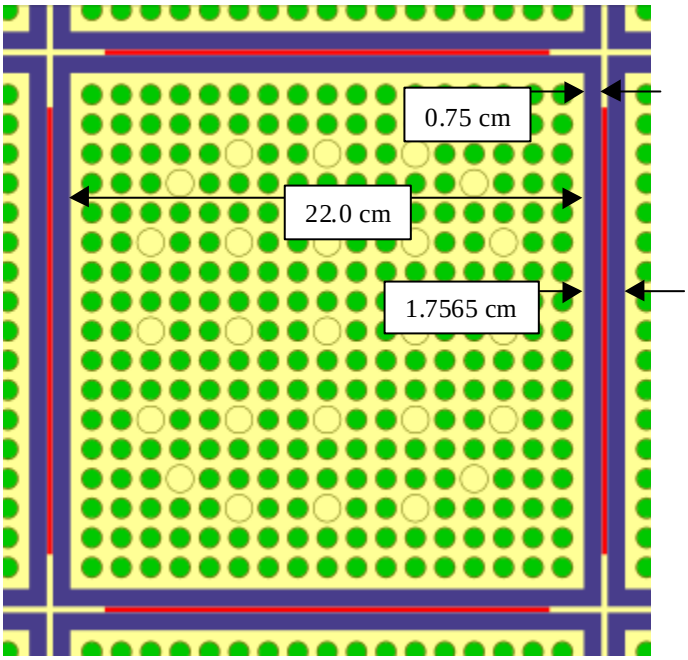

Figure 4 Cross-sectional view of an assembly cell in the KENO V.a model of the GBC-32 cask

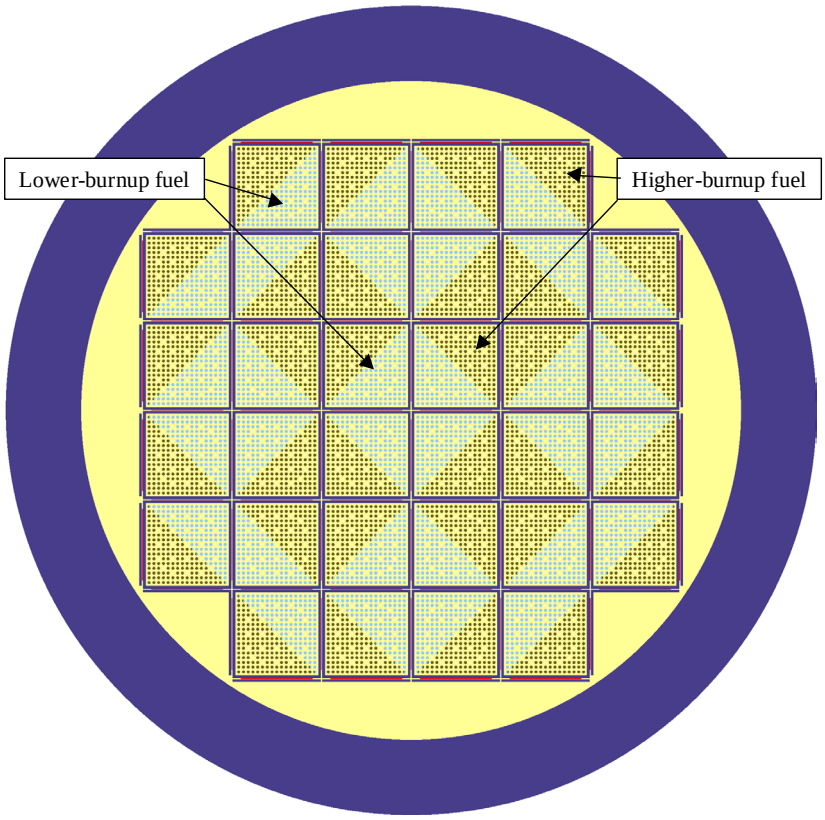

Figure 5 GBC-32 cask model with binary variation in horizontal burnup

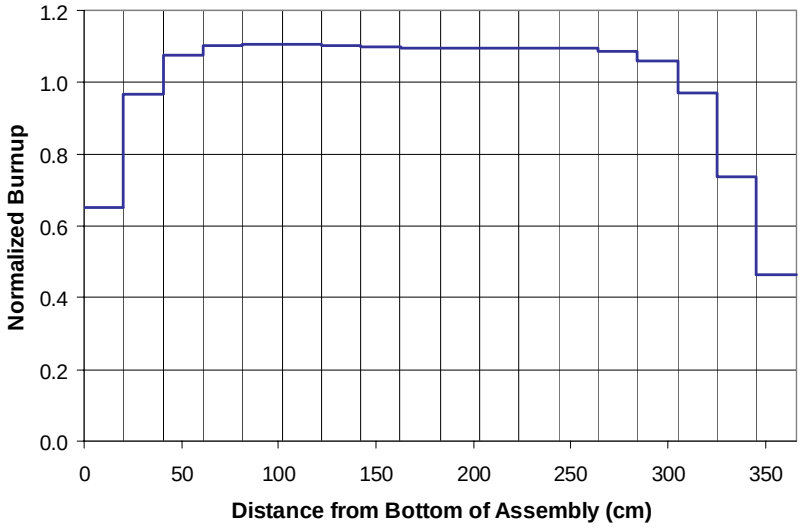

Figure 6 Axial-burnup profile used in the reference model (*Source*: Ref. 6)

Table 1 Axial-burnup profile used in the reference model (*Source*: Ref. 6)

Upper bound of axial region, measured from bottom of active fuel (cm)	Normalized burnup
20.32	0.652
40.64	0.967
60.95	1.074
81.27	1.103
101.61	1.108
121.93	1.106
142.28	1.102
162.60	1.097
182.88	1.094
203.20	1.094
223.52	1.095
243.83	1.096
264.15	1.095
284.49	1.086
304.81	1.059
325.12	0.971
345.44	0.738
365.76	0.462

Table 2 Nuclides associated with the classifications of burnup credit used for analysis

Set 1: Actinide-only burnup-credit nuclides (10 total)									
U-234	U-235	U-238	Pu-238	Pu-239	Pu-240	Pu-241	Pu-242	Am-241	O[†]
Set 2: Actinide + fission product burnup-credit nuclides (29 total)									
U-234	U-235	U-236	U-238	Pu-238	Pu-239	Pu-240	Pu-241	Pu-242	Am-241
Am-243	Np-237	Mo-95	Tc-99	Ru-101	Rh-103	Ag-109	Cs-133	Sm-147	Sm-149
Sm-150	Sm-151	Sm-152	Nd-143	Nd-145	Eu-151	Eu-153	Gd-155	O[†]	

[†]Oxygen is neither an actinide nor a fission product, but is included in this list because it is an integral part of the fuel, and hence included in the calculations.

3.2 CALCULATIONAL MODELS FOR DEPLETION ANALYSES

The WE 17×17 fuel assembly was used as the reference fuel assembly for both depletion and criticality models. For the determination of the SNF isotopic compositions, a number of different operating conditions were evaluated. To enable comparisons of the various conditions, reference depletion conditions were defined. Neglecting the presence of control rods and burnable poison rods, these conditions correspond to values judged to be bounding based on available reactor operational data and are discussed in the following section. The presence of control rods and burnable poison rods are evaluated as a variation and their effect is determined based on comparison to the reference conditions.

4 FRESH FUEL CALCULATIONS

Before proceeding on to the various parametric studies, results are presented in this section for fresh fuel conditions to establish a baseline for comparison. The k_{eff} values as a function of enrichment for the GBC-32 cask are plotted in Figure 7. Note that 1-σ error bars are included on the figure but are sufficiently small that they are difficult to distinguish from the data symbols. An important point to note from this figure is that, in the absence of burnup credit, assemblies with enrichments greater than ~ 2.0 wt % ^{235}U (the majority of PWR SNF assemblies, see Figure 2) exceed the recommended 0.95 limit[1, 18] for k_{eff}, and thus would not be acceptable for loading into the GBC-32 cask.

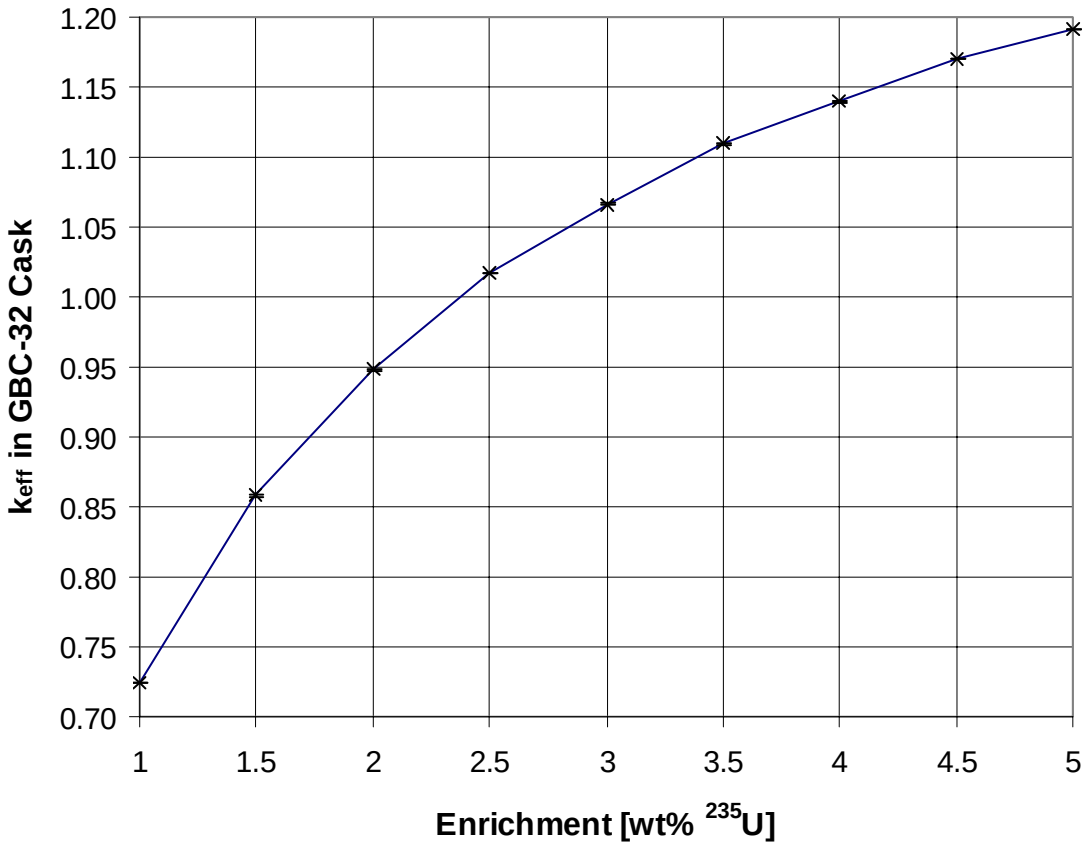

Figure 7 k_{eff} as a function of initial enrichment in GBC-32 cask

5 EFFECTS OF DEPLETION MODELING

It is anticipated that burnup credit will be applied for a wide variety of fuel types irradiated under a variety of reactor operating conditions (temperature, soluble boron concentration, burnable poison usage, etc.). If a cask design is to accept such a variety of fuel assemblies, analyses must account for the variations in the depletion conditions to ensure that the composition of the SNF will provide a bounding reactivity. Several studies (e.g., Refs. 8–10) have been performed to assess the effect of depletion modeling assumptions on SNF calculated isotopic compositions. In these studies, the calculated isotopic compositions were used to calculate neutron multiplication factors for infinite SNF pin lattices and generic casks loaded with SNF. Trends in neutron multiplication were then examined as a function of each parameter to determine the conservative direction (e.g., high temperature versus low temperature) for that parameter, and the magnitude of the effect over a realistic operating range. A summary of these findings (taken from Ref. 5) is provided in Table 3.

Table 3 Summary of information on depletion modeling parameters (*Source*: Ref. 5)

Parameter	Bounding condition	Estimated sensitivity[†]	Recommended value/model
Fuel temperature	Highest temperature	4–5 pcm Δk/K	Maximum pellet-average temperature
Moderator temperature	Highest temperature	35–90 pcm Δk/K	Maximum core outlet temperature
Soluble boron concentration	Highest concentration	3–3.5 pcm Δk /ppm	Maximum cycle-averaged concentration
Operating history	High power late in life (actinide-only)	N/A	Assume simple operating history, with margin of 200 pcm or more
Specific power	High specific power (actinide-only)	N/A	High but credible specific power
Fixed absorbers	Absorbers present during depletion	N/A	May not be excessive to assume absorbers present, but further study is warranted.

[†]pcm (per cent mille) = 10^{-5}

For each parameter studied, the sensitivity of the neutron multiplication to changes in the parameter increases with increasing burnup. Furthermore, with the exception of specific power/operating history effects, all of the trends are related to spectral hardening. Spectral hardening results in an increased production rate of plutonium from increased fast neutron capture in ^{238}U. The increased production of plutonium and decreased fission of ^{235}U have the effect of increasing the reactivity of the fuel at discharge and beyond. The mechanisms that result in spectral hardening for various operating conditions are discussed in Refs. 5 and 8.

In practice, an operational extreme in one parameter may result in an opposite extreme for a coupled parameter. However, simultaneous use of bounding parameter values in a depletion model provides a simple bounding approach to the modeling process since it is unlikely that any fuel would be depleted under all such conditions simultaneously. With previous work having established the trends in the neutron multiplication factor for each of the relevant depletion environment parameters/conditions, analyses are presented in the following subsections to determine the impact of the bounding assumptions, as compared to nominal conditions.

The use of parameters in a safety evaluation that cannot be justified as bounding may necessitate loading restrictions to ensure that the SNF assemblies loaded in the cask are not more reactive than those considered in the safety evaluation. In most cases, such loading restrictions are considered undesirable, thus motivating the determination and use of justifiable bounding parameters for the safety evaluation. Bounding parameters may be dictated by relatively few assemblies, while they are subsequently applied to all assemblies in a burnup-credit safety evaluation. Therefore, it has been suggested (e.g., Ref. 28) that future work consider the use of risk-informed approaches to develop criteria for selecting bounding parameters. For example, approaches to allow the use of more representative parameters (e.g., parameters that bound 95% of the SNF) could be investigated.

5.1 DEPLETION PARAMETERS

Studies in this section provide an estimate of the reactivity effect associated with simultaneously using bounding values for the following depletion environment parameters: soluble boron concentration, moderator temperature, fuel temperature and specific power. Variation in operating history (e.g., downtimes and variations in power) have been considered elsewhere[8,9] and are not considered in this study; continuous burnup and constant power were assumed. All criticality calculations were performed for the GBC-32 cask for the reference model identified in Section 3.1 (5-year cooling, axial-burnup distribution included). Finally, note that the calculations assume constant depletion conditions as a function of burnup.

The use of bounding values is compared to the use of nominal values to evaluate the effect on k_{eff} with respect to typical or nominal fuel. To perform this comparison, nominal and bounding PWR operating conditions for soluble boron concentration, moderator temperature, fuel temperature and specific power were determined and are given in Table 4. The parameters were determined based on a limited review of reactor operating-history data that are available as a result of efforts performed under the Office of Civilian Radioactive Waste Management to analyze commercial reactor criticals for the Yucca Mountain Project[29] and other related studies (e.g., Refs. 8, 10). Where axial variations exist in a parameter (e.g., moderator temperature/density), the value was selected based on the most conservative region for that parameter (e.g., nominal and bounding values for moderator temperature correspond to the core exit, where they are at their maximum). The authors exercised judgement in the selection of these values and acknowledge that a more thorough review of plant data may result in differences in the actual values. It is recognized that the nominal value for specific power may be too high, [10] but the sensitivity is relatively small. The remaining selected values are considered to be reasonable, and should enable useful comparisons (i.e., the comparisons should not be sensitive to minor variations in the parameter values). However, the results will be sensitive to major variations in the parameter values (e.g., significant increases or decreases in the difference between bounding and nominal values).

Table 4 Summary of parameters used for the depletion calculations

Parameter	Value used in analysis for "nominal" conditions	Value used in analysis for "bounding" conditions
Moderator temperature, density (K, g/cm^3)	595, 0.68	610, 0.63
Fuel temperature (K)	850	1100
Power density (MW/MTU)	40	60
Moderator boron concentration (ppm)	600	1000

First, separate ARP libraries were generated for the nominal and bounding depletion conditions. Then, depletion calculations were performed for both nominal and bounding conditions for various initial fuel enrichments. The differences, Δk values, between the bounding and nominal conditions, as a function of burnup and enrichment, are shown in Figure 8 for cases with and without the major fission products included. The results show that the increase in k_{eff} associated with the use of bounding parameters increases with burnup and decreases with initial fuel enrichment. The results with and without the major fission products present are similar, but the Δk values are smaller when the major fission products are included. In both cases the results show that the increase in k_{eff} is . 2% Δk for typical discharge burnup and enrichment combinations. The ratio of burnup and enrichment is approximately constant for typical discharged SNF, and is generally within the range of 9–12 [units of (GWd/MTU)/wt % ^{235}U)] (e.g., 4.0 wt % fuel typically achieves a burnup between 36 and 48 GWd/MTU). This point is illustrated in Figure 2, which shows a graphical representation of enrichment and burnup combinations for discharged PWR SNF and provides a frame of reference for *typical* enrichment and discharge burnup combinations.

A series of calculations was also performed in which each parameter was individually set to the nominal value, while the remaining parameters were set to their respective bounding value. The results from these calculations, in terms of Δk values, are provided in Figure 9 for actinide-only and actinide + fission product conditions. The results demonstrate that the increase in k_{eff} associated with the simultaneous use of bounding parameters is (1) dominated by the bounding value for moderator temperature/density, (2) notably and similarly impacted by the bounding values for soluble boron concentration and fuel temperature, and (3) relatively insensitive to the bounding value for specific power. These results are generally consistent with, but are smaller in magnitude than, the sensitivities listed in Table 3. Approximately one half of the total Δk value is associated with the moderator temperature/density, while the remaining half is nearly equally divided between the bounding assumptions for the soluble boron concentration and the fuel temperature. The maximum moderator temperature in a reactor occurs near the top of the fuel where the burnup is reduced due to leakage (see Figure 6). Consequently, the maximum moderator temperature in this region, which dominates the reactivity in a burnup-credit cask, must be properly bounded.

Finally, to assess the impact on a burnup-credit evaluation for a high-capacity cask, separate loading curves were generated for the nominal and bounding depletion conditions. These loading curves are compared in Figure 10 for actinide-only and actinide + fission product burnup credit. The results indicate that bounding depletion parameters notably increase the minimum required burnup for a given initial

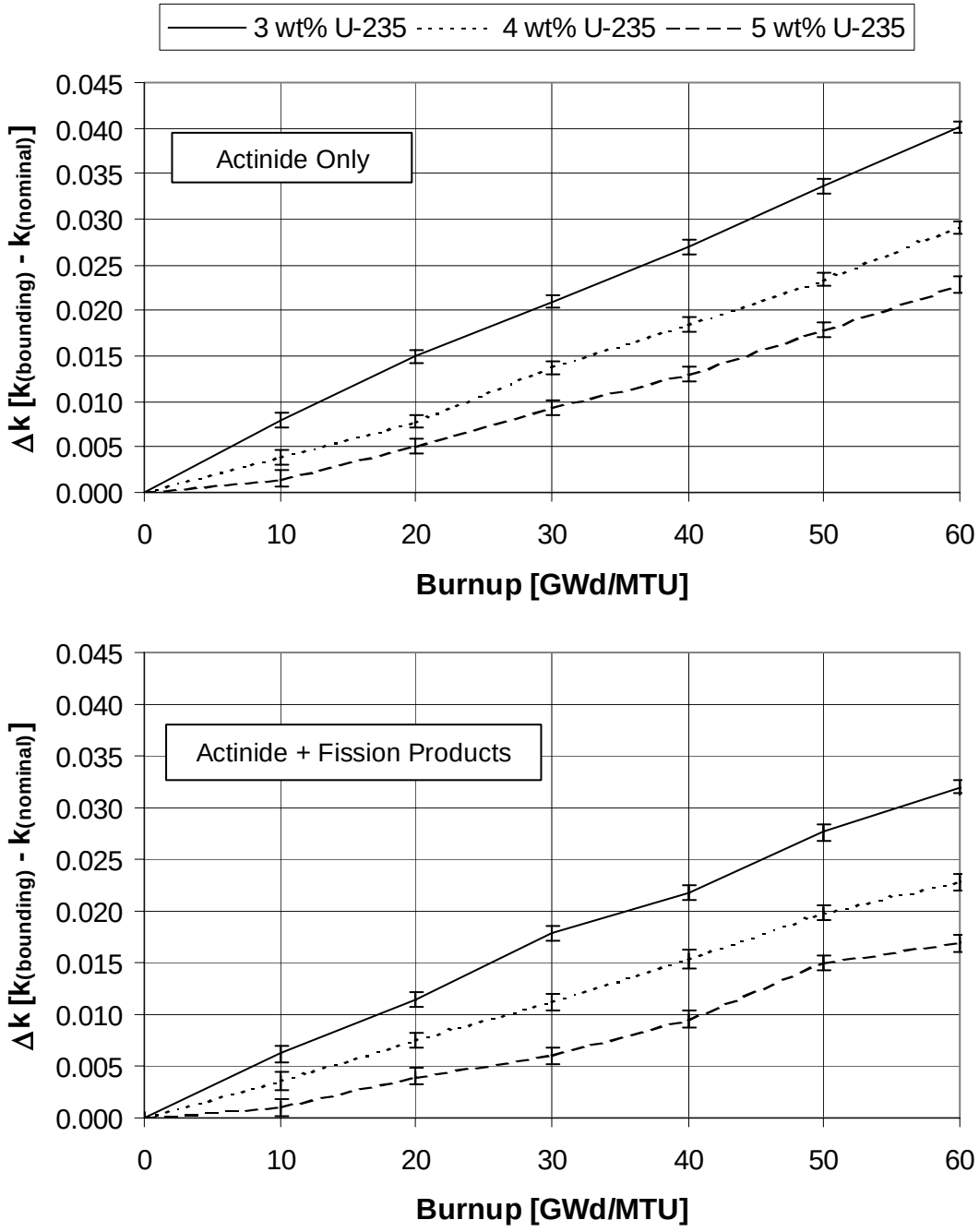

Figure 8 Comparison of Δ*k* values between cases with bounding and nominal depletion parameters for various initial fuel enrichments

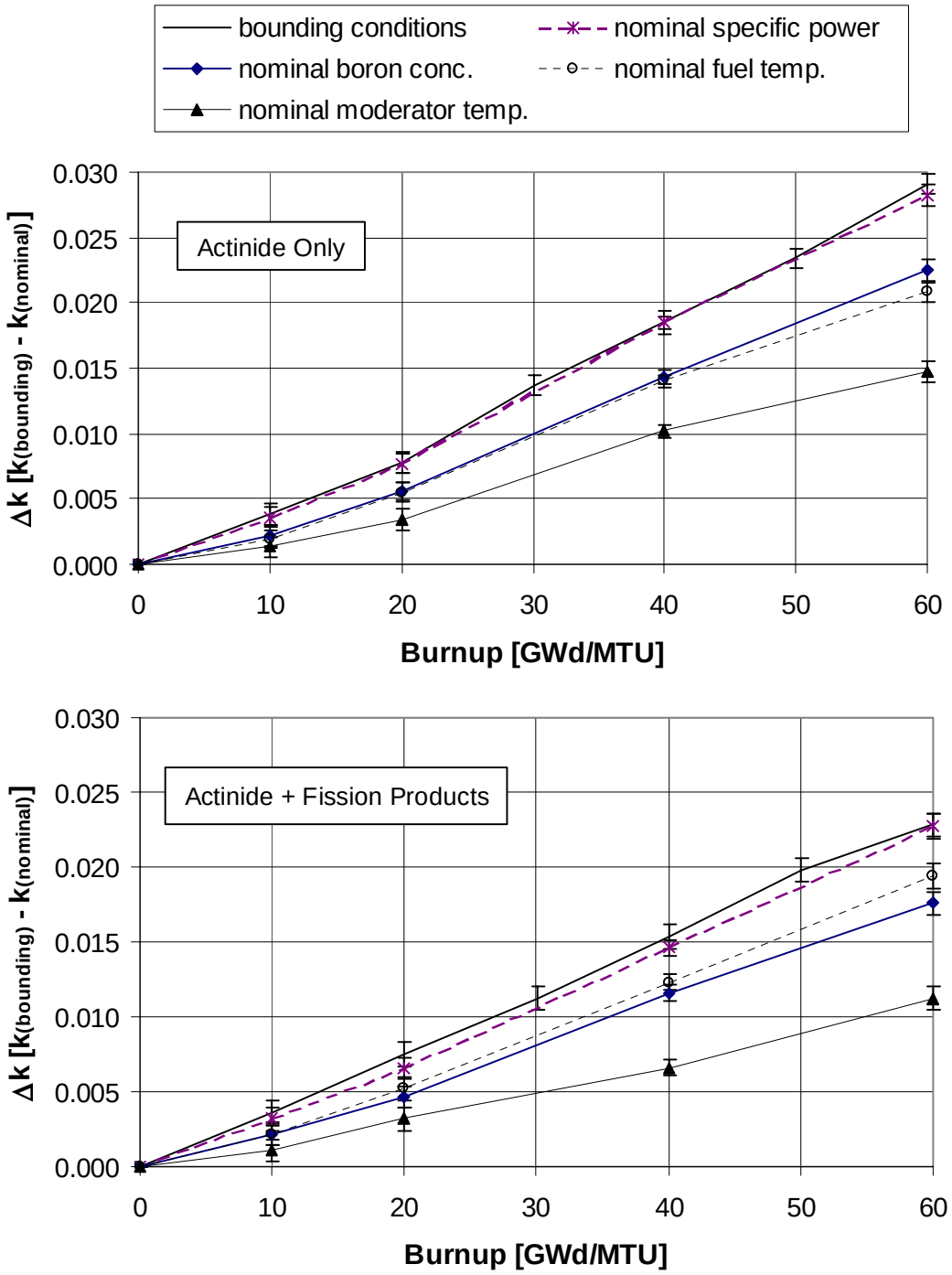

Figure 9 Comparison of Δ*k* values between a case with all bounding parameters and cases in which individual parameters are set equal to the defined nominal value. The effect of an individual parameter is approximately equal to the difference between the bounding condition curve and the nominal curve for that parameter. The results correspond to 4.0 wt % ^{235}U fuel.

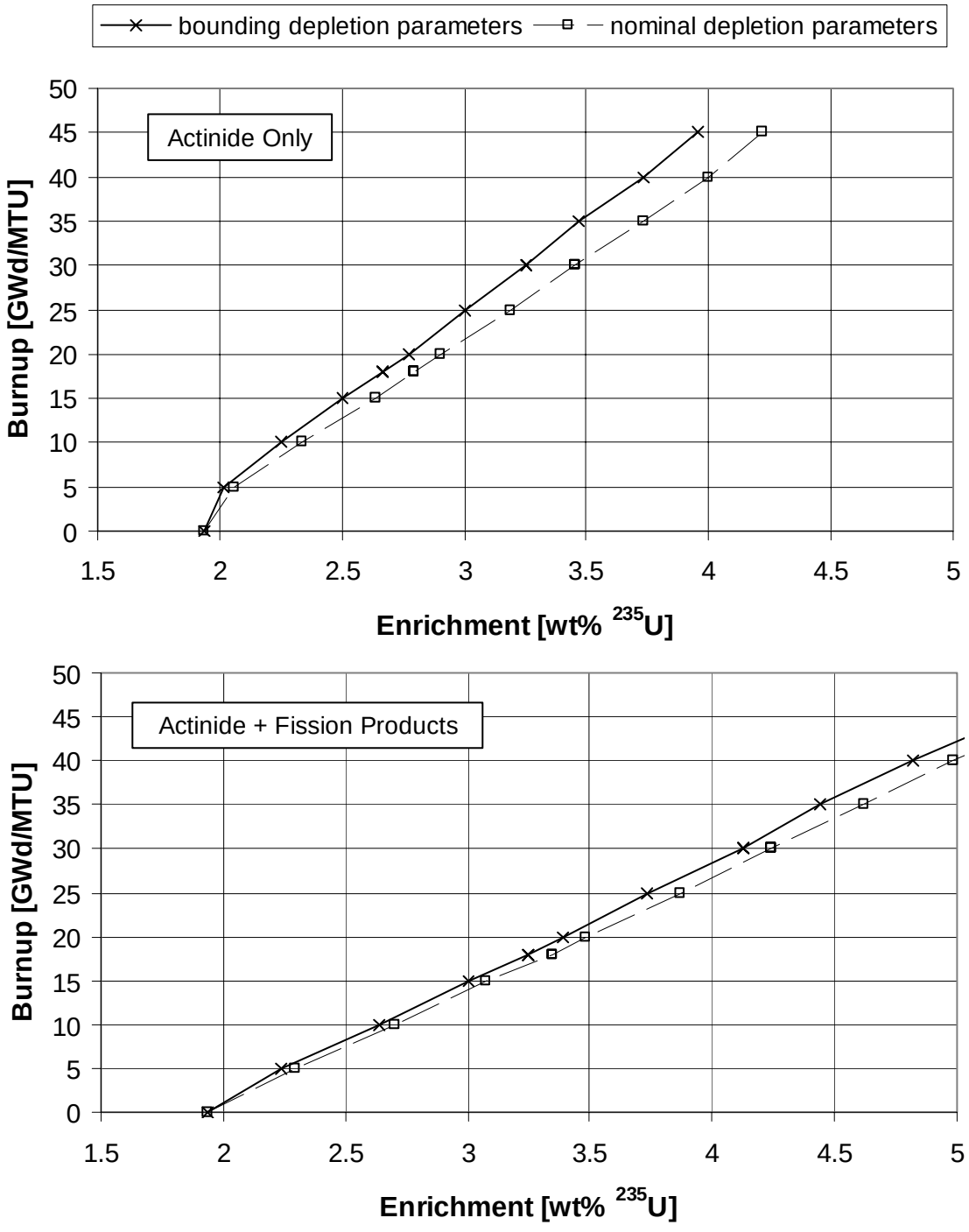

Figure 10 Comparison of the effect of depletion parameters on burnup-credit loading curves for the GBC-32 cask and 5-year cooling

enrichment (e.g., for actinide-only burnup credit, the minimum required burnup for 3.75 wt % ^{235}U enrichment is increased by ~5 GWd/MTU). The difference between the "bounding" and "nominal" loading curves is much less when the major fission products are included.

Note that from this point forward, unless explicitly stated otherwise, all calculations will correspond to the bounding depletion parameters.

5.2 BURNABLE POISON RODS

The presence of burnable poison rods (BPRs) during depletion hardens the neutron spectrum due to removal of thermal neutrons by capture and by displacement of moderator, resulting in enhanced production of fissile plutonium isotopes and diminished ^{235}U depletion. As a result, an assembly exposed to BPRs will have a higher reactivity for a given burnup than an assembly that has not used BPRs. Recent work[30] has provided detailed parametric studies to quantify the impact of BPRs on the reactivity of SNF. Those studies concluded that BPRs have a notable positive impact on the reactivity of SNF for typical operating practices, and thus should be addressed in a burnup-credit evaluation.

The effect of BPRs on reactivity is dependent upon the duration that the BPRs are present, the subsequent accumulated burnup, the BPR design, and the initial fuel enrichment. Thus, for a given BPR design, a burnup-credit analysis should include a justifiable assumption for the burnup duration in which the fuel is exposed to BPRs. Assuming BPR exposure during the entire depletion is a simple, conservative approach to bound the reactivity effect of BPRs. However, such an approach increases the SNF reactivity by ~1–2% Δk in comparison to the typical case in which the BPRs are removed after one cycle. More realistic approaches based on typical operating conditions and/or loading restriction(s) may be acceptable with supporting justification. For these approaches, it is necessary to define a maximum burnup for use as the BPR burnup exposure duration. Values of 20 and 30 GWd/MTU are reasonable possibilities. Hence, in this section, we examine the effect of BPR exposure during the first 20 and 30 GWd/MTU of burnup, and compare them to the condition without BPRs present and the condition in which BPRs are present during the entire depletion.

The WE Wet Annular Burnable Absorber (WABA) BPR design was used for this study, and the burnable poison rod assembly (BPRA) was assumed to include the maximum number of BPRs (i.e., 24 BPRs for the WE 17×17 assembly design). For a comparison of the impact of different BPR designs and design specifications, the reader is referred to Ref. 30. An ARP library was generated for each of the BPR exposure conditions considered (i.e., BPR exposure during first 20 GWd/MTU, first 30 GWd/MTU, and the entire depletion), using the bounding depletion parameters given in Table 4. Subsequently, STARBUCS calculations were performed for enrichments of 3, 4, and 5 wt % ^{235}U.

The differences, Δk values, between cases with and without BPRs present for each of the BPR exposures considered are given in Figure 11 for actinide-only burnup credit. The results with the major fission products present are provided in Figure 12. Finally, the impact of these BPR exposure assumptions on the loading curves for both actinide-only and actinide + fission product burnup credit is illustrated in Figure 13. The loading curves in Figure 13 show the conservatism associated with assuming BPR exposure for the entire depletion.

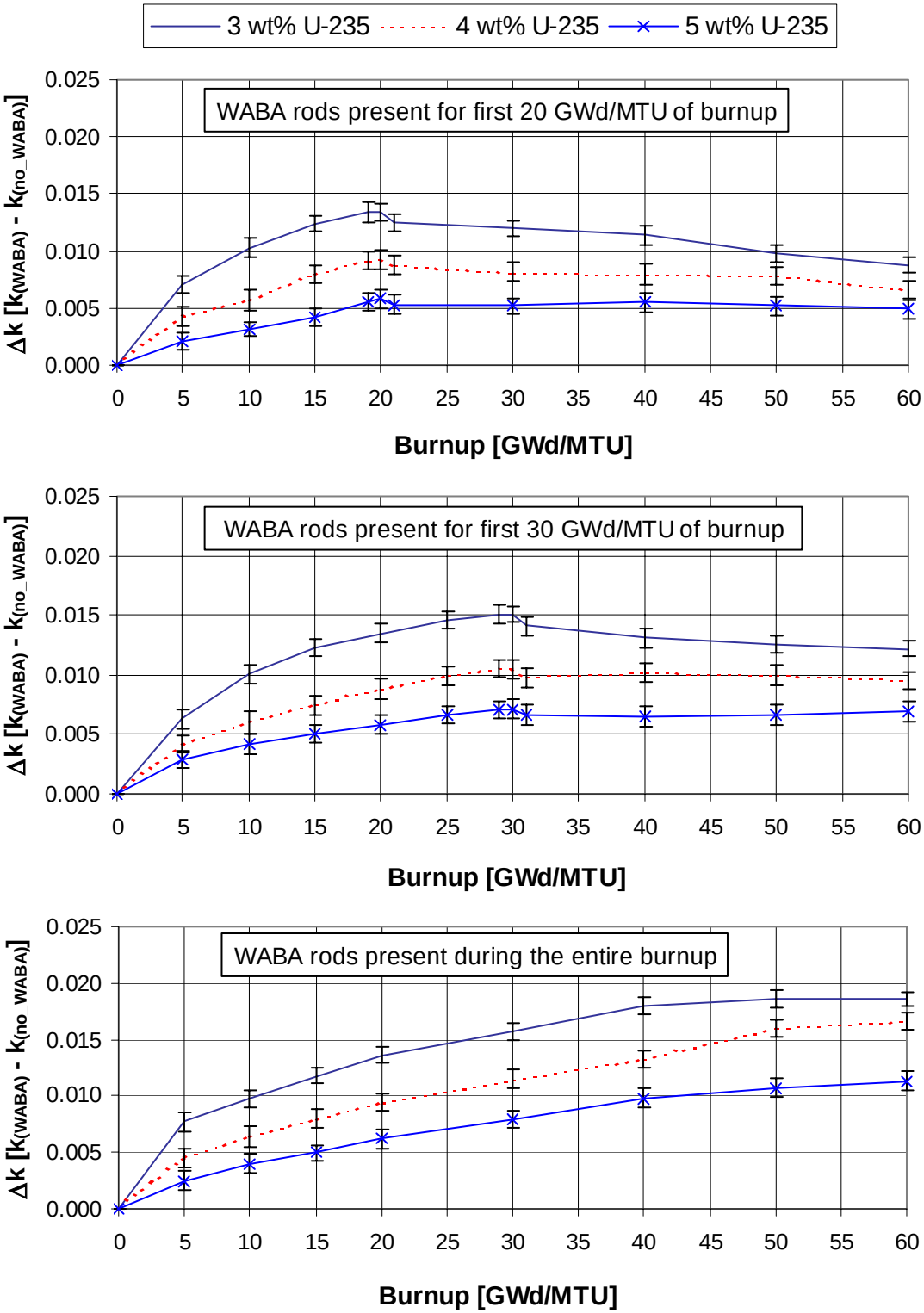

Figure 11 Comparison of Δ*k* values for fuel that has been exposed to WE WABA rods and actinide-only burnup credit

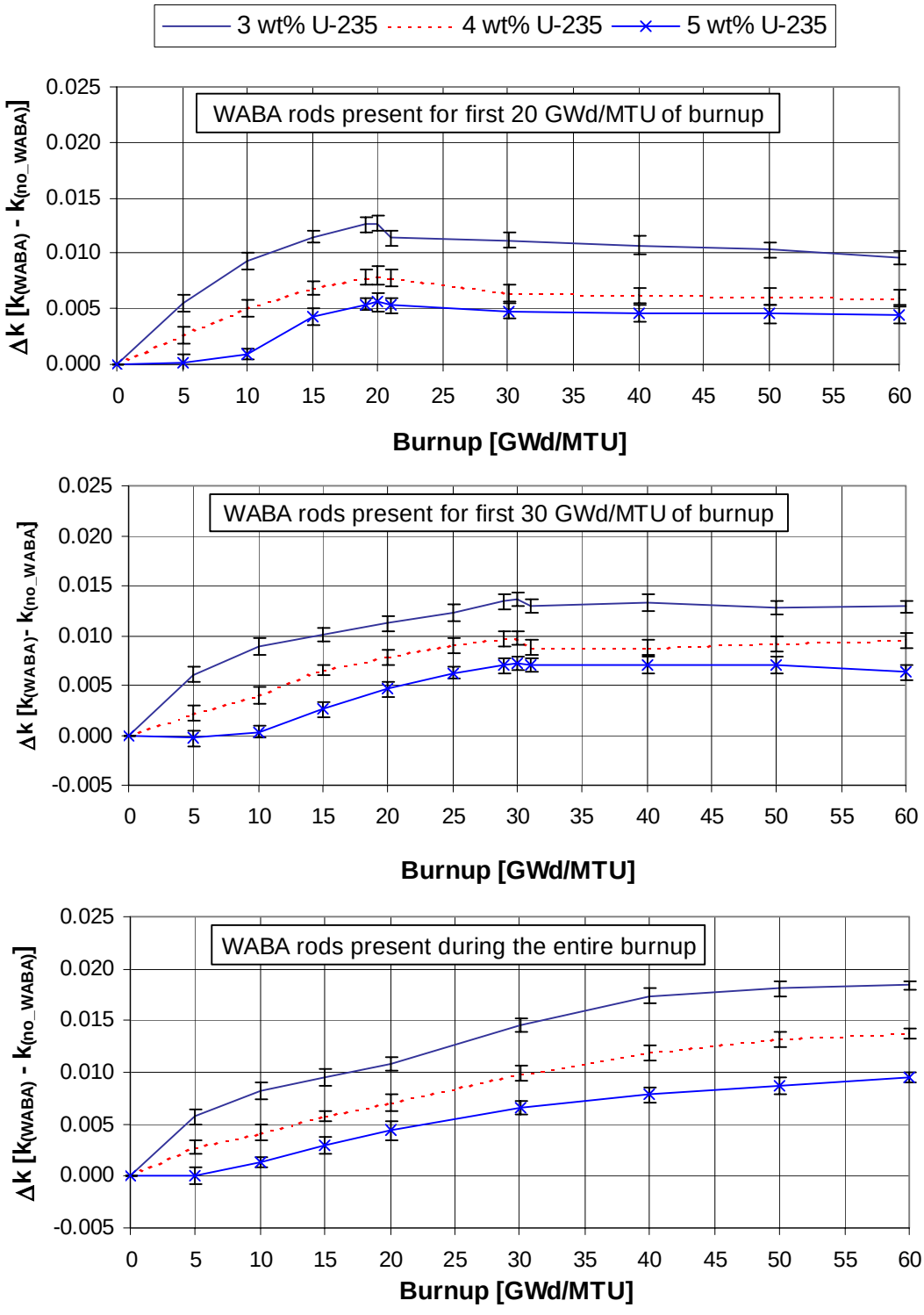

Figure 12 Comparison of Δ*k* values for fuel that has been exposed to WE WABA rods and actinide + fission product burnup credit

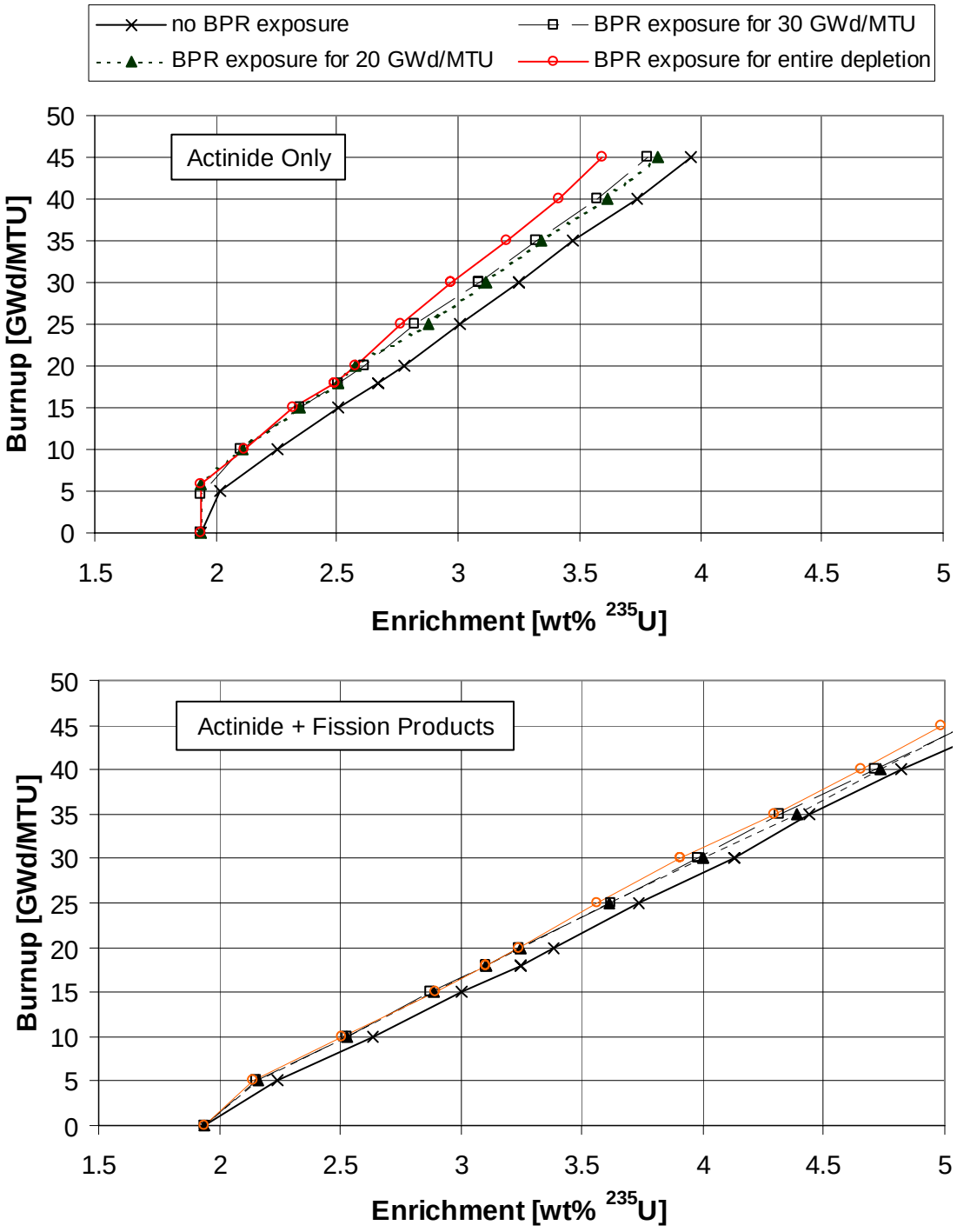

Figure 13 Effect of BPR exposure on burnup-credit loading curves for the GBC-32 cask

5.3 CONTROL RODS

In the U.S., PWRs currently operate with control rods (CRs) withdrawn or nearly withdrawn from the active fuel region and use soluble boron to control changes in reactivity with burnup. In contrast, French PWR operations involve long periods of CR insertion for reactor control, low-power operations and load-following.[31] Similarly, some early domestic operations included CR insertions of notable depths, usually for some portion of an assembly's first cycle of burnup.[32] Also, axial power shaping rods (APSRs) may be inserted during normal operations at B&W plants, but impact fewer assemblies (e.g., in Three Mile Island Unit-1, eight assemblies/core may contain APSRs, while 24 assemblies/core may contain CRs[33]). Fuel shuffling between cycles reduces the probability that a fuel assembly will be exposed to CR/APSR insertions during more than one cycle.

The presence of CRs and APSRs increases the reactivity of burned fuel by hardening the neutron spectrum (due to removal of thermal neutrons by capture and by displacement of moderator) and suppressing burnup in localized regions. The latter effect can lead to axial-burnup distributions characterized by significantly under-burned regions, as is apparent by examining the axial-burnup profiles in Ref. 34. Although the axial-burnup distribution is an important concern for burnup-credit evaluations, the effect of CR/APSR insertion on the axial-burnup profile is not addressed here because it is considered in the selection of bounding axial-burnup profile(s).[6, 35] Instead, this study examines the effect of CR/APSR insertion on reactivity due to the impact of spectral hardening on the spent-fuel isotopics only.

Recent work[36] has provided detailed parametric studies to quantify the impact of CRs and APSRs on the reactivity of SNF, including evaluations of full and partial insertion conditions for a variety of different designs. The study concluded that, based on the assumption that U.S. PWRs do not use CRs to a significant extent (i.e., CRs are not inserted deeper than the top ~20 cm of the active fuel and CRs are not inserted for extended periods of burnup), the effect of CRs on discharge reactivity is relatively small (less than 0.2% Δk). However, that study also demonstrated that if CRs are deeply inserted (e.g., full-axial insertion) into the active fuel region for an extended period of burnup, they have a notable positive impact on the reactivity of SNF.

Due to the large variability in CR and APSR usage, estimating the effect of CRs and APSRs in a generic manner is difficult. Based on operational arguments for U.S. PWRs, similar to those stated above, a previous study[6] considered full-axial insertion for one cycle (15 GWd/MTU) as an upper bound for assemblies exposed to CRs. For this evaluation, similar to the approach in the previous section for BPRs, parametric analyses were performed for a couple of full-axial insertion exposure scenarios to establish the effect on SNF reactivity. Specifically, the effect of CR insertions during the first 5 and 15 GWd/MTU of burnup are compared to conditions without CR insertion.

For this study, the WE Ag-In-Cd CR design, which is representative of other CR designs, was used. For a comparison of the impact of different CR designs and design specifications, the reader is referred to Ref. 36. An ARP library was generated for each of the two CR insertions conditions considered (i.e., full CR insertion during first 5 and 15 GWd/MTU of burnup), using the bounding depletion parameters given in Table 4. Subsequently, STARBUCS calculations were performed for enrichments of 3, 4, and 5 wt % ^{235}U.

The differences, Δk values, between cases with and without CRs inserted are given in Figure 14 for actinide-only burnup credit. The results with the major fission products present are provided in Figure 15. Finally, the impact of these CR exposure assumptions on loading curves is illustrated in Figure 16, where it can be seen that the assumption of CR exposure for 15 GWd/MTU has a very significant effect on the loading curve.

The insertion of BPRs and CRs cause similar reactivity effects. In terms of operations, BPRs are typically inserted into an assembly during its first cycle of operation, are always fully inserted, and are not withdrawn during power operations. In contrast, CRs may be used in a variety of ways, including full and partial insertions for brief periods of burnup. When fully inserted, CRs have a larger impact on reactivity than BPRs, but CRs are typically used for brief periods of burnup and are not typically fully inserted. Because it is not physically possible for a BPRA and a CR/APSR assembly to be simultaneously inserted into a fuel assembly, it may be possible to use the BPR modeling assumption to bound the effects of BPR and CR/APSR insertions. As an example, Figure 16 compares loading curves based on both BPR and CR insertions, and shows that the cases with 20 GWd/MTU BPR insertion and 5 GWd/MTU full CR insertion yield nearly identical loading curves over most of the burnup-enrichment range.

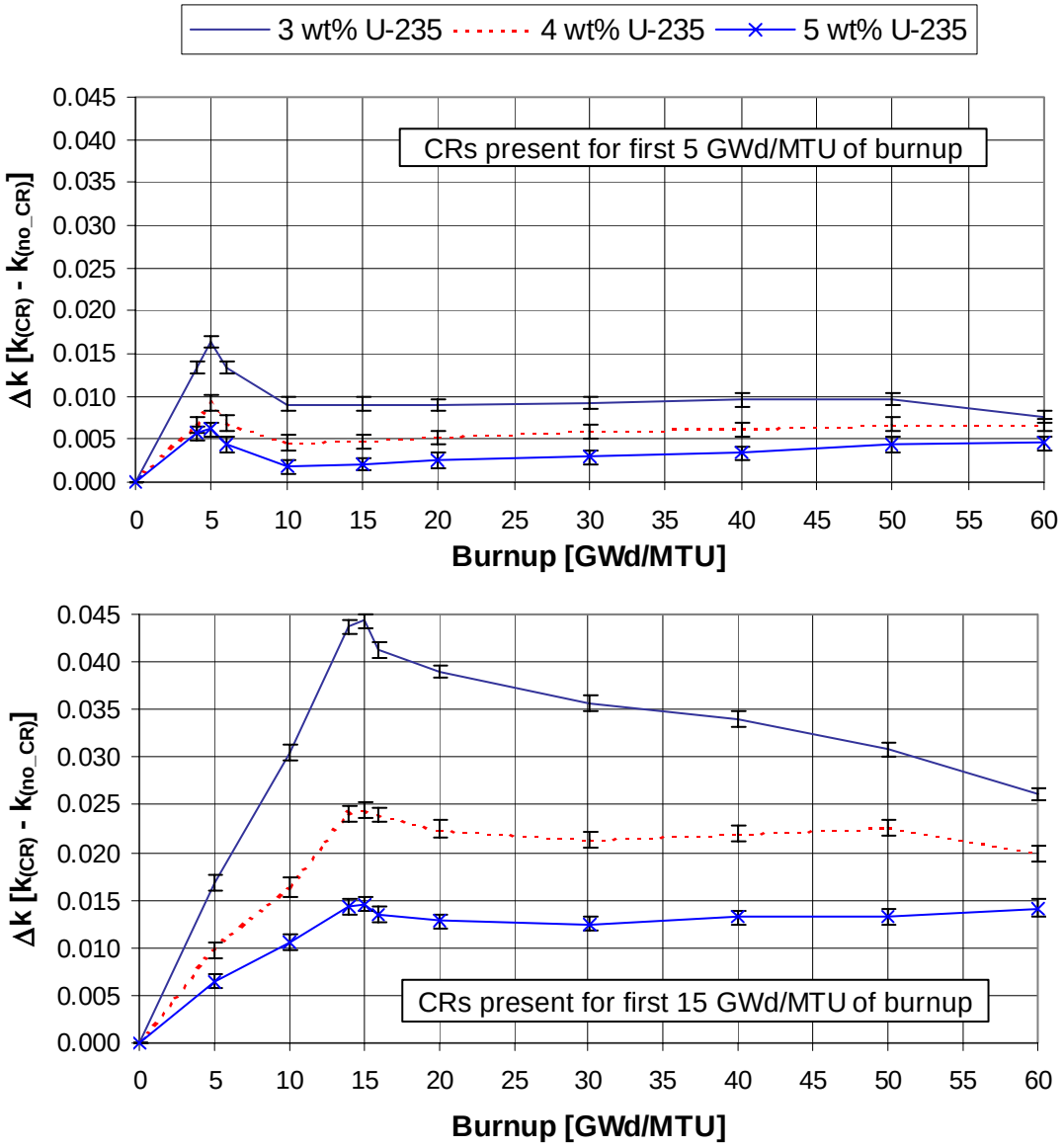

Figure 14 Comparison of Δ*k* values for fuel with and without Ag-In-Cd CR insertions and actinide-only burnup credit

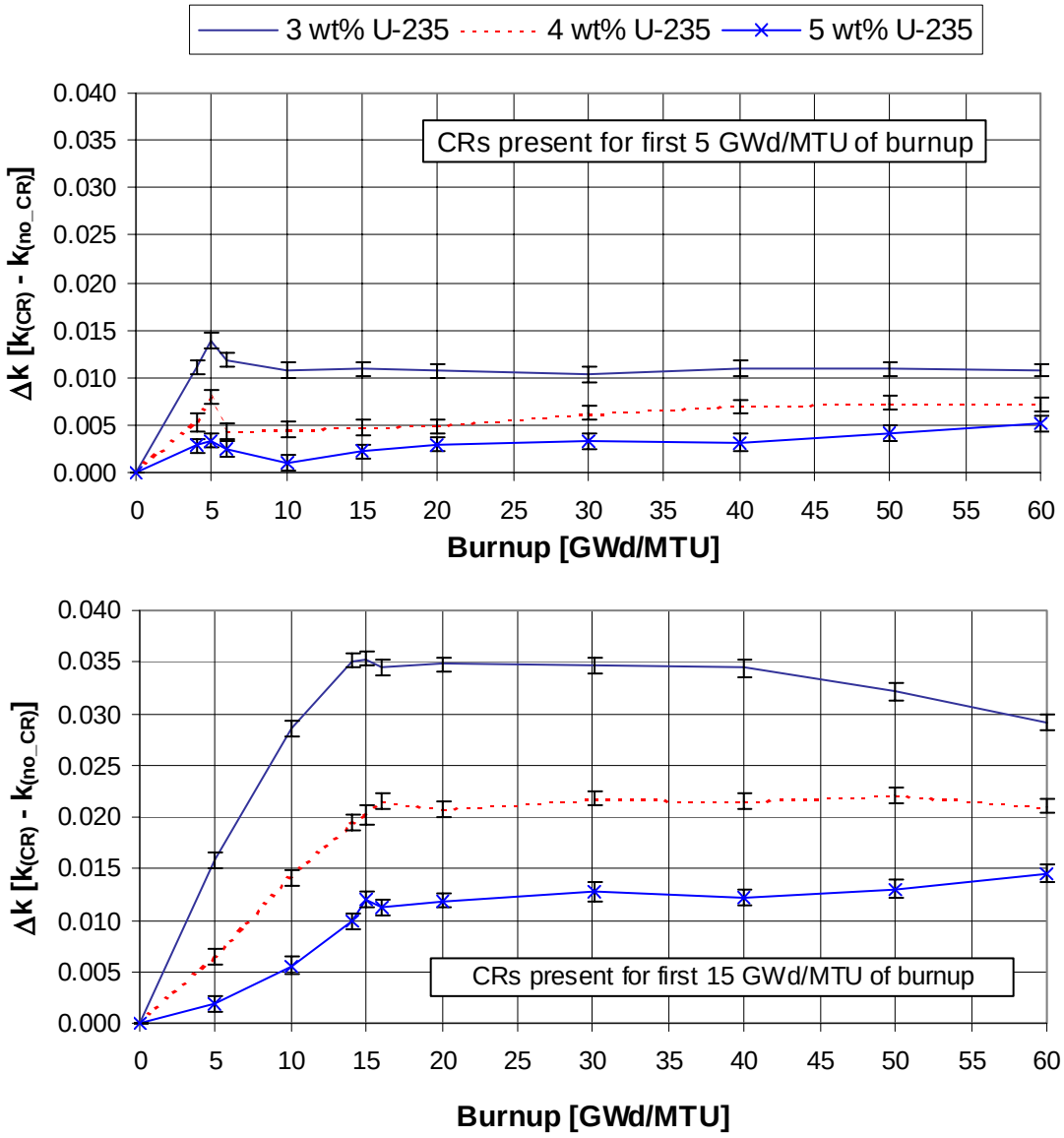

Figure 15 Comparison of Δ*k* values for fuel with and without Ag-In-Cd CR insertions and actinide + fission product burnup credit

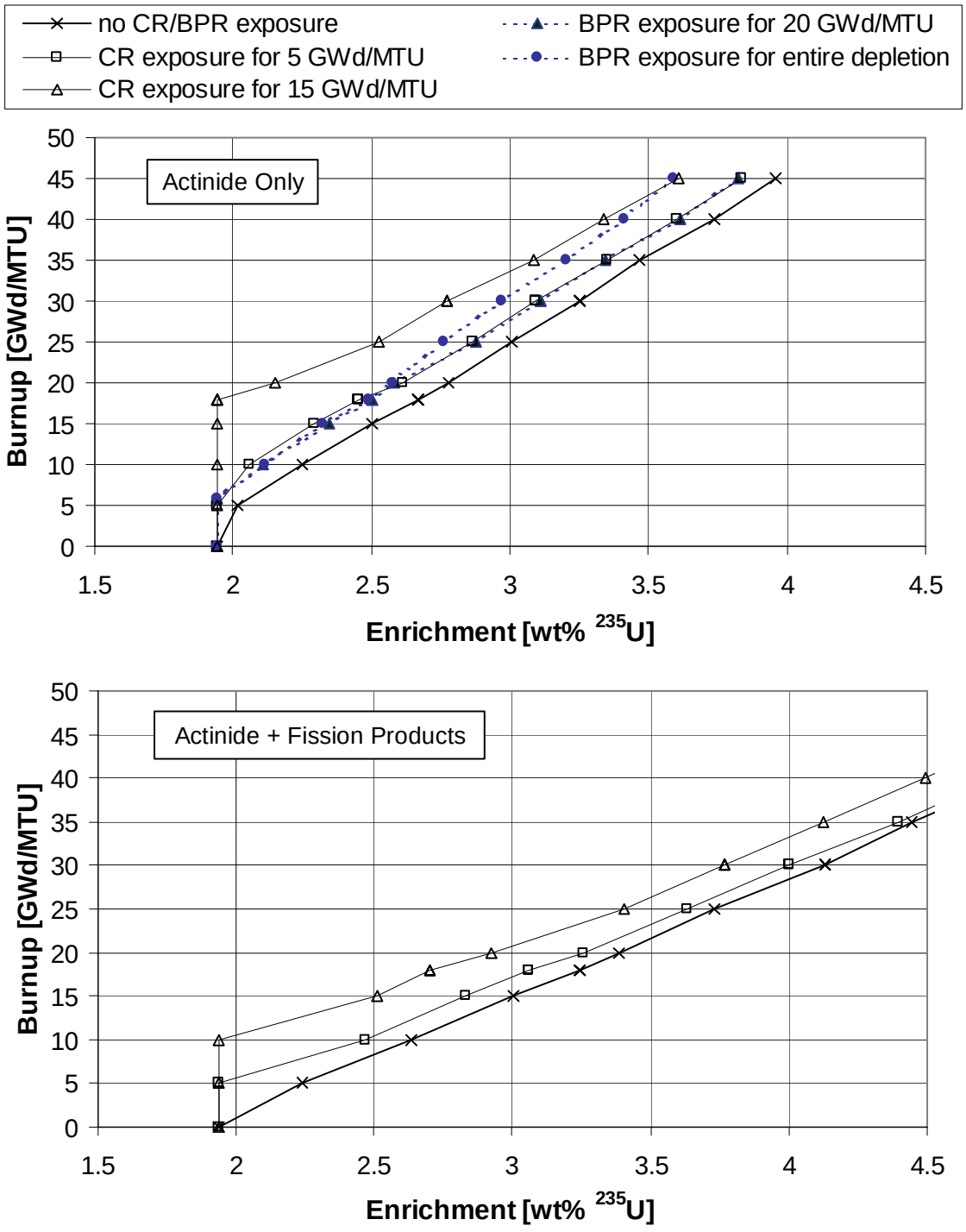

Figure 16 Comparison of the effects of CR and BPR insertion on burnup-credit loading curves for the GBC-32 cask

6 EFFECTS OF CRITICALITY MODELING

In this section, the criticality modeling assumptions of primary importance to burnup credit are evaluated. Unless explicitly stated otherwise, all calculations correspond to the reference model defined in Section 3.1 and the bounding depletion parameters defined in Table 4.

6.1 SPATIAL BURNUP DISTRIBUTIONS

In this subsection, the effects of spatial burnup distributions, including both axial and horizontal, on k_{eff} in the GBC-32 cask are investigated as a function of initial enrichment, burnup, and cooling time.

6.1.1 Axial Burnup

6.1.1.1 Background

Axial variations in flux result in a non-uniform burnup distribution along the axial length of SNF. The axial distribution is typically characterized by end regions that are significantly under-burned with respect to the assembly-averaged burnup. The shape of the distribution is dependent upon the accumulated burnup, as well as other characteristics of the assembly operating history (e.g., partial-length absorbers, APSRs, CRs, and non-uniform axial fuel enrichments). For fuels of moderate-to-high burnup (i.e., burnup beyond ~20 GWd/MTU), these under-burned regions are dominant in terms of reactivity, and must be represented to ensure subcritical margins.

To accurately calculate the reactivity of SNF, a calculational model must include the axial distribution, which is done by axially segmenting the model to approximate the isotopic compositions associated with the axial variation in burnup. The most reactive region of the spent fuel is near the assembly ends, where there exists a balance between increased multiplication due to lower burnup and increased leakage due to closer proximity to the fuel ends. The difference in k_{eff} between a calculation with explicit representation of the axial-burnup distribution and a calculation that assumes uniform axial burnup has become known as the "end effect." Although the assumption of uniform axial burnup has no physical validity for SNF, it has proven useful as a reference for comparison of the effect of the axial-burnup distribution.

Numerous studies have been performed to quantify the reactivity effect associated with axial burnup. A review of those studies is available in Ref. 37. In general, these studies have shown that assuming uniform axial burnup is conservative for low burnup, but becomes increasingly nonconservative as burnup increases. The transition between conservative and nonconservative is dependent on numerous factors (including enrichment, cooling time, and the nuclides included in the criticality model), but generally occurs in the burnup range of 15–25 GWd/MTU.

For a given axial-burnup profile, the end effect has been shown to be strongly dependent upon the cooling time and the use of fission products in the criticality model. Previous work (e.g., Ref. 35), has shown that the end effect (1) increases with burnup, (2) becomes positive later in burnup when fission products are not included, (3) is reduced when fission products are neglected, and (4) increases with cooling time. Although the end effect has been shown to be dependent upon many factors, it is primarily dependent on the slope of the burnup profile near the ends of the fuel, which is dependent on the fuel assembly design, burnup, and reactor operating environment (e.g., CR usage). While the accumulated burnup for a SNF assembly is readily available from plant data in terms of the assembly-averaged burnup, the axial-burnup profile may not be readily available.

To account for the axial-burnup distribution in a burnup-credit evaluation, an approach must be developed to address the impact in a general manner. One such approach is to identify and use axial-burnup profiles that are bounding in terms of the value of k_{eff}, and yet sufficiently realistic as to adequately represent the physics. The approach to date in the U.S. has been to determine bounding axial profiles from actual burnup profiles; either identifying specific profiles that are bounding or developing artificial bounding profiles based on the characteristics of actual bounding profiles.

Previous works (e.g., Refs. 8, 38) in this area have employed a relatively straightforward approach – perform criticality calculations for each burnup shape to determine the profile that produces the greatest end effect. The bounding profiles from Ref. 38, which are derived from the axial-burnup database of Ref. 34 are listed in Table 5 and designated the Set 1 burnup-dependent profiles. The burnup profile changes with burnup – tending to flatten with increasing burnup. Hence, axial-burnup profiles are often separated into burnup ranges in analyses for determining bounding profiles, as was done in Ref. 38.

The work of Ref. 38 was later expanded[39] to determine bounding profiles over coarser burnup ranges. The bounding profiles for three burnup ranges were determined (based on the 12 bounding profiles listed in Table 5) and suggested for use with a proposed actinide-only burnup-credit methodology.[6] For reference, the three profiles are provided in Table 6 and designated the Set 2 burnup-dependent profiles.

6.1.1.2 Analysis

STARBUCS calculations were performed to quantify the effect of axial burnup as a function of burnup, initial enrichment, cooling time, and nuclides included in the model. Unless explicitly stated otherwise, the calculations correspond to the reference model defined in Section 3.1 (i.e., 5-year cooling and the axial-burnup profile listed in Table 1).

Figure 17 shows the variation in the end effect with variations in initial enrichment for actinide-only and actinide + fission product burnup credit. These results are consistent with previous findings that the end effect is negative for low burnup, undergoes a transition, subsequently increases with increasing burnup, and is notably larger when fission products are included. As discussed in Ref. 37, previous studies have reached conflicting conclusions with regard to the behavior of the end effect with varying initial enrichment. The curves in Figure 17 reveal the cause of the previous conflicting observations – the end effect does not consistently increase or decrease as a function of initial enrichment. Rather, the behavior is dependent on burnup; for burnup values . 40 GWd/MTU the end effect is shown to remain relatively constant or decrease with increasing initial enrichment. In contrast, for burnup values / 40 GWd/MTU the end effect is shown to increase with increasing enrichment.

To demonstrate the impact of using different axial profiles, calculations were performed with each of the 3 burnup profiles listed in Table 6 for 4.0 wt % ^{235}U enrichment and 5-year cooling. The results are shown in Figure 18 and demonstrate significant difference in the end effect for these profiles. Note that the profiles from the lower burnup ranges yield the largest end effect. To demonstrate the effect of cooling time within the timeframe of interest to cask storage and transportation, Figure 19 shows the end effect for various cooling times. Consistent with previous findings (e.g., Ref. 40), the end effect increases notably with cooling time.

Finally, to demonstrate the impact of axial-burnup modeling on loading curves for the GBC-32 cask, loading curves were generated for each of the following modeling assumptions: (1) uniform axial burnup, (2) the reference axial-burnup profile (listed in Table 1), (3) the 12 burnup-dependent profiles listed in Table 5, and (4) the 3 burnup-dependent profiles listed in Table 6. In the last two cases, the burnup profiles are dependent on burnup, thus different profiles are applied in different burnup ranges, as

specified in Tables 5 and 6. The resulting loading curves are compared in Figure 20. The discontinuities in the cases based on burnup-dependent profiles occur at the boundaries between burnup ranges that utilize different profiles. The finer resolution burnup-dependent profiles (Set 1) provide a notable reduction in the loading curve above ~ 38 GWd/MTU, as compared to the Set 2 profiles, and minimal reduction for the remainder of the burnup range. Consequently, it appears there is little value associated with using the fine resolution profile for lower burnups.

Table 5 Set 1: Burnup-dependent bounding axial-burnup profiles (*Source*: Ref. 38)

Burnup group	1	2	3	4	5	6	7	8	9	10	11	12
Axial height (%)	Burnup ranges (GWd/MTU)											
	> 46	42–46	38–42	34–38	30–34	26–30	22–26	18–22	14–18	10–14	6–10	< 6
2.78	0.573	0.674	0.660	0.585	0.652	0.619	0.630	0.668	0.649	0.633	0.662	0.574
8.33	0.917	0.949	0.936	0.957	0.967	0.924	0.936	1.034	1.044	0.989	0.931	0.947
13.89	1.066	1.053	1.045	1.091	1.074	1.056	1.066	1.150	1.208	1.019	1.049	1.091
19.44	1.106	1.085	1.080	1.121	1.103	1.097	1.103	1.094	1.215	0.857	1.059	1.105
25.00	1.114	1.095	1.091	1.126	1.108	1.103	1.108	1.053	1.214	0.776	1.108	1.094
30.56	1.111	1.095	1.093	1.111	1.106	1.101	1.109	1.048	1.208	0.754	1.144	1.087
36.11	1.106	1.093	1.092	1.094	1.102	1.103	1.112	1.064	1.197	0.785	1.168	1.086
41.69	1.101	1.091	1.090	1.093	1.097	1.112	1.119	1.095	1.189	1.013	1.183	1.087
47.22	1.097	1.089	1.089	1.092	1.094	1.125	1.126	1.121	1.188	1.185	1.189	1.091
57.80	1.093	1.088	1.088	1.091	1.094	1.136	1.132	1.135	1.192	1.253	1.190	1.096
58.33	1.089	1.086	1.088	1.092	1.095	1.143	1.135	1.140	1.195	1.278	1.183	1.102
63.89	1.086	1.084	1.086	1.099	1.096	1.143	1.135	1.138	1.190	1.283	1.167	1.105
69.44	1.081	1.081	1.084	1.096	1.095	1.136	1.129	1.130	1.156	1.276	1.135	1.105
75.00	1.073	1.073	1.077	1.087	1.086	1.115	1.109	1.106	1.022	1.251	1.079	1.096
80.56	1.051	1.053	1.057	1.073	1.059	1.047	1.041	1.049	0.756	1.193	0.976	1.066
86.11	0.993	0.987	0.996	1.003	0.971	0.882	0.871	0.933	0.614	1.075	0.806	0.986
91.67	0.832	0.800	0.823	0.796	0.738	0.701	0.689	0.669	0.481	0.863	0.596	0.806
97.22	0.512	0.524	0.525	0.393	0.462	0.456	0.448	0.373	0.284	0.515	0.375	0.474

Table 6 Set 2: Burnup-dependent axial-burnup profiles (*Source*: Ref. 6)

Profile number	**1**	**2**	**3**
Burnup group	1	2	3
Axial	Burnup ranges (GWd/MTU)		
height (%)	<18	18–30	>30
2.78	0.649	0.668	0.652
8.33	1.044	1.034	0.967
13.89	1.208	1.150	1.074
19.44	1.215	1.094	1.103
25.00	1.214	1.053	1.108
30.56	1.208	1.048	1.106
36.11	1.197	1.064	1.102
41.69	1.189	1.095	1.097
47.22	1.188	1.121	1.094
57.80	1.192	1.135	1.094
58.33	1.195	1.14	1.095
63.89	1.190	1.138	1.096
69.44	1.156	1.130	1.095
75.00	1.022	1.106	1.086
80.56	0.756	1.049	1.059
86.11	0.614	0.933	0.971
91.67	0.481	0.669	0.738
97.22	0.284	0.373	0.462

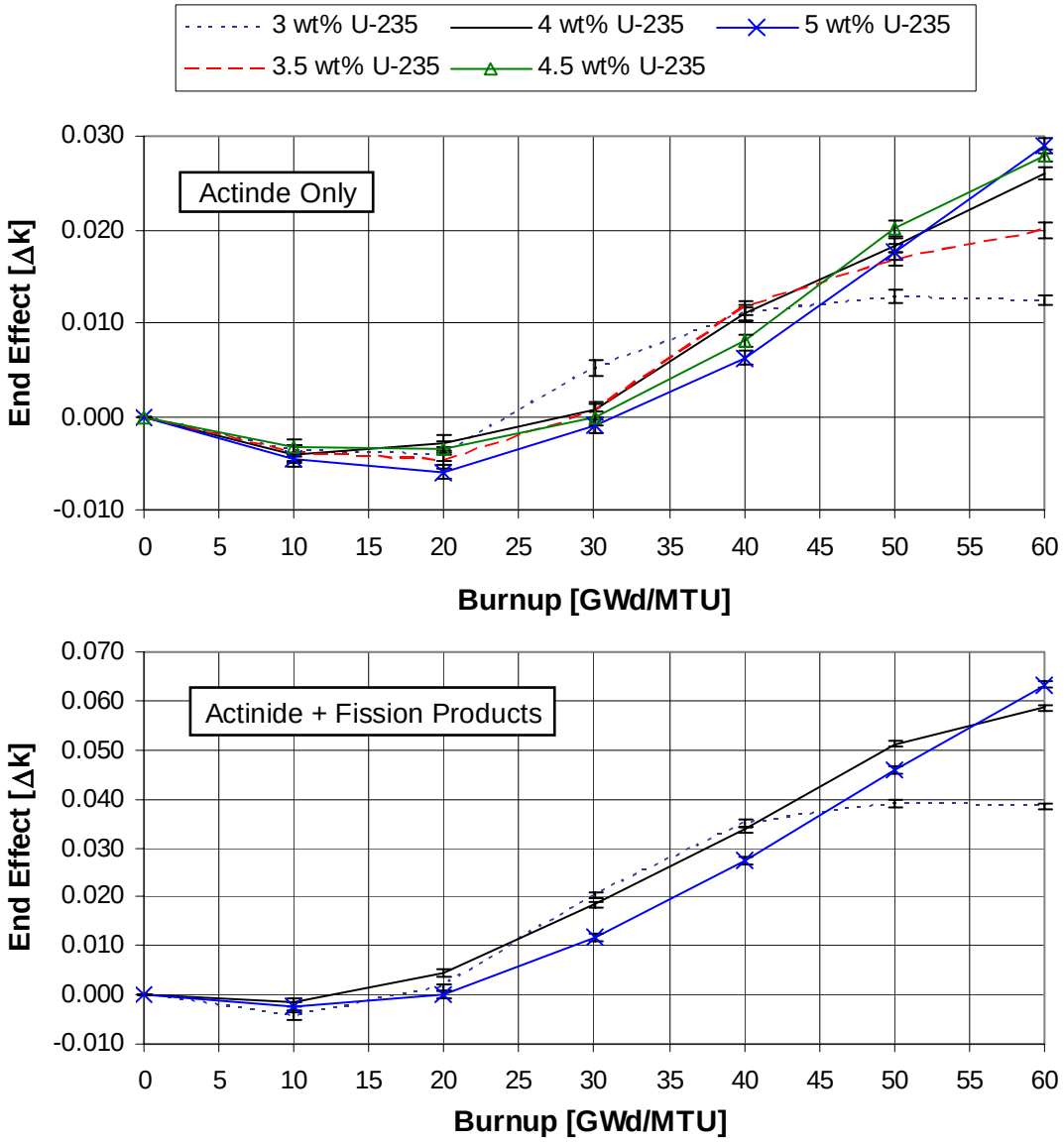

Figure 17 Comparison of the end effect using the reference axial profile of Table 1 for various initial fuel enrichments

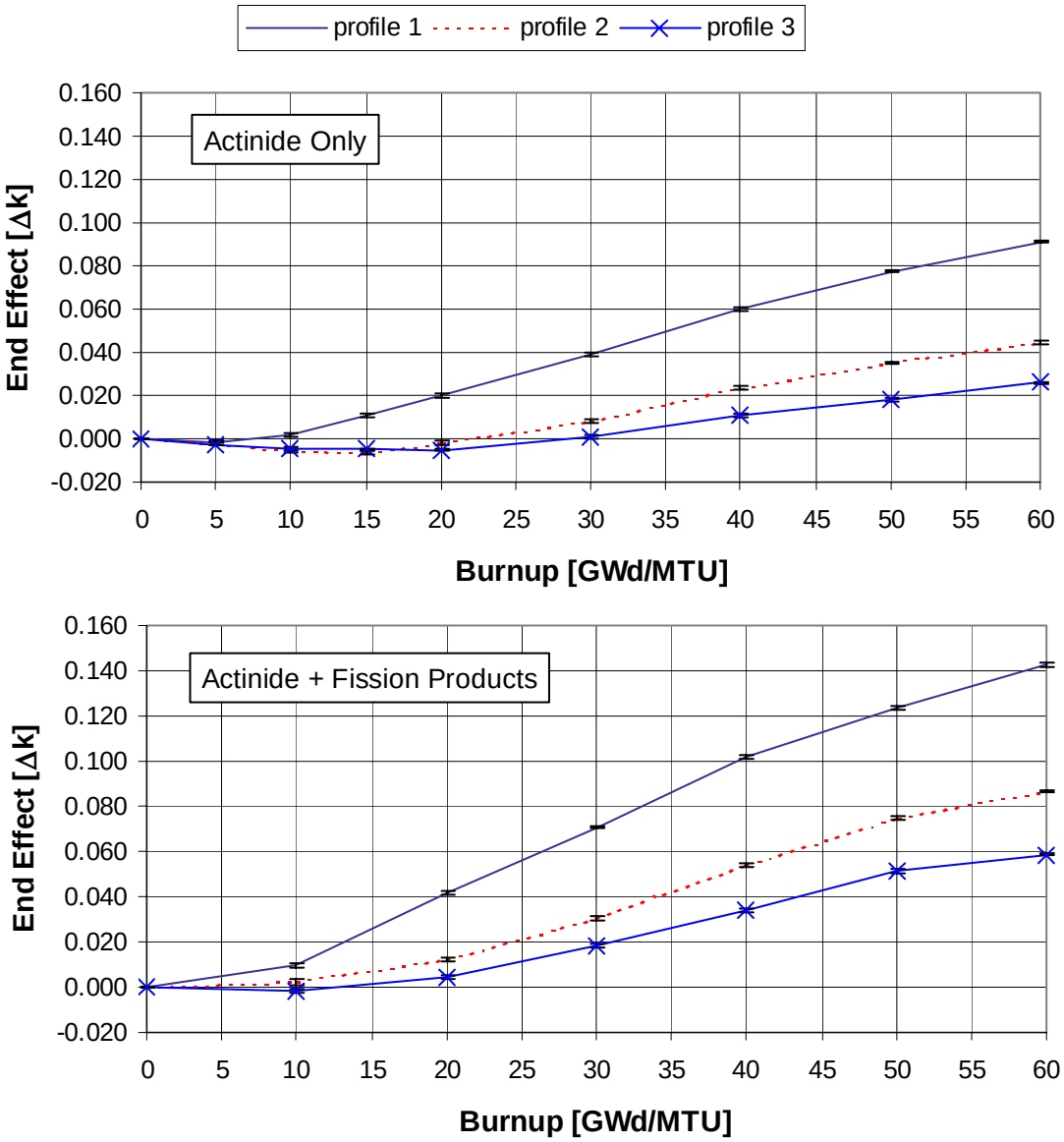

Figure 18 Comparison of the end effect for the Set 2 axial-burnup profiles of Table 6 and 4 wt % fuel

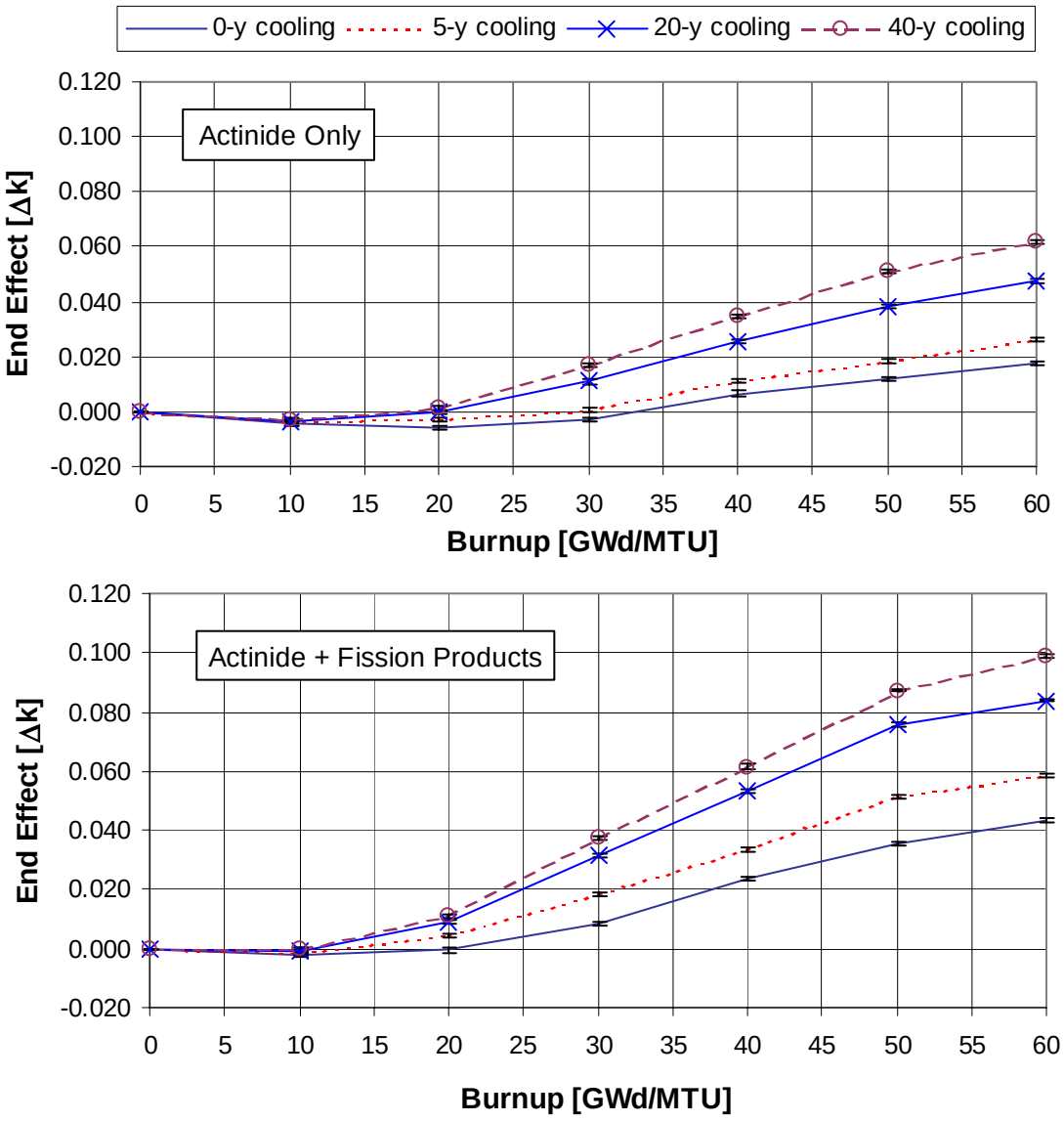

Figure 19 Comparison of the end effect as a function of cooling time using the reference axial profile of Table 1 and 4 wt % fuel

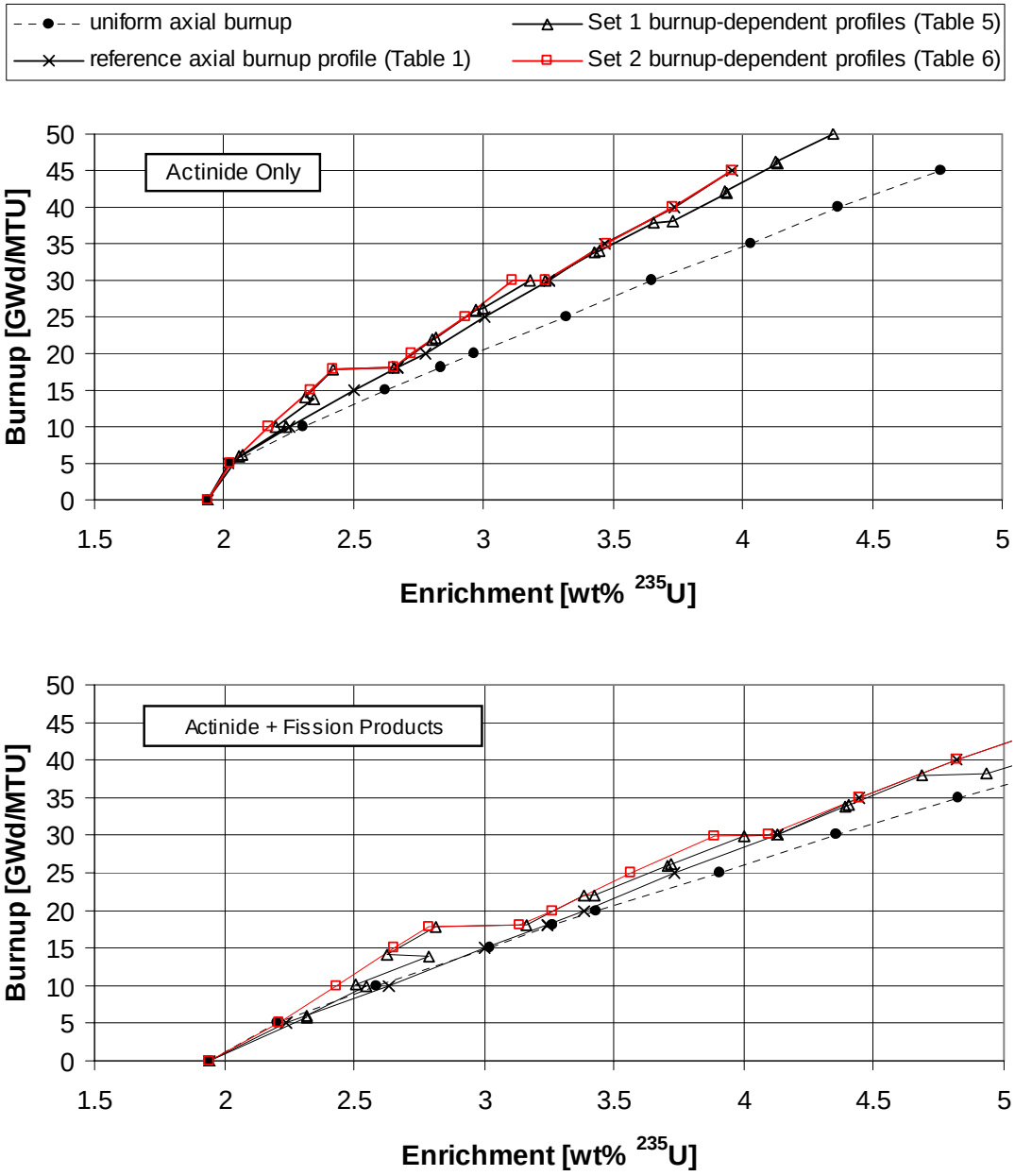

Figure 20 Comparison of the effect of axial-burnup profiles on burnup-credit loading curves for GBC-32 cask

6.1.2 Horizontal Burnup

6.1.2.1 Background

Radial variations in the neutron flux, which are mainly due to leakage at the core periphery, result in a non-uniform horizontal burnup distribution over the radial extent of the reactor core. As the reactor operates, the radial flux shape flattens due to fuel depletion and fission product poisoning near the core center. However, because of the high leakage, burnup drops off rapidly near the core periphery. At the end of a cycle, the individual assemblies located near the center of the core will have a relatively uniform horizontal burnup distribution, while the assemblies near the core periphery may have a significant horizontal variation in burnup.[41] Thus, it is possible for fuel rods on one side of an assembly to have experienced less burnup than fuel rods on the opposite side of the same assembly. To enhance fuel utilization, assemblies are relocated within the reactor core between cycles, which reduce the horizontal burnup gradient in typical discharged SNF. However, a periphery assembly discharged after a single cycle may exhibit a significant horizontal burnup gradient.[41]

A database containing quadrant-wise horizontal burnup gradients for 808 PWR assemblies (WE 17 × 17 and B&W 15 × 15) is available in Ref. 41. The database has been examined for trends with the number of operating cycles, accumulated burnup, and initial enrichment. No trend with initial enrichment was observed. However, the horizontal gradient was shown to be inversely proportional to accumulated burnup and number of cycles, which are obviously closely related. In other words, the horizontal variation in burnup decreases with increasing burnup. Axial variation of the horizontal burnup distribution has not been assessed.

The horizontal variation in burnup is a criticality safety concern in the event that two or more assemblies are placed in a configuration such that their low-burnup zones are adjacent, thus resulting in a potential increase in reactivity. This potential reactivity increase will be greatest in small cask designs — such as truck casks — where radial neutron leakage is significant. Although the effect is not expected to be significant in large rail-type casks and the probability of placing assemblies in such a configuration is small, this concern should be addressed in burnup-credit safety analyses, per regulatory guidance in Ref. 18.

Based on the horizontal burnup database,[41] Ref. 6 somewhat arbitrarily suggested bounding burnup-dependent values for horizontal burnup gradients to be used in actinide-only burnup-credit applications. These values are listed in Table 7. Further, it was proposed that these gradients be applied in conjunction with the most reactive loading configuration. Such an approach should be adequately bounding. However, studies have not been performed to quantify the effect on SNF reactivity associated with this approach, and subsequently assess the value of developing alternative approaches. Therefore, studies are presented in this section to quantify the effect of the proposed approach in terms of Δk values and loading curves.

6.1.2.2 Analysis

Using the GBC-32 cask model illustrated in Figure 5, along with the previously defined reference conditions (i.e., 5-year cooling, axial-burnup distribution included), STARBUCS calculations were performed to quantify the effect of horizontal burnup. Note that with the use of 18 axial regions to represent the axial-burnup variation and two radial regions to represent the horizontal burnup gradient, each SNF assembly is modeled with 36 sets of isotopic compositions. The effect of a 25% horizontal burnup gradient (with respect to the horizontal assembly-averaged) is shown in Figure 21 for various

initial enrichments. Consistent with the suggestions of Ref. 6, half of each assembly is modeled with a burnup of 25% less than the horizontal assembly-averaged burnup and the other half is modeled with 25% higher than the horizontal assembly-averaged burnup, resulting in a 50% gradient across the assembly. The horizontal gradient effect, which is defined here as the difference in k_{eff} between a calculation with explicit representation of the horizontal burnup gradient and a calculation that assumes uniform horizontal burnup, is shown to increase with decreasing fuel enrichment and is relatively insensitive to the inclusion of the major fission products. Even for this rather substantial burnup gradient, the effect is shown to be less than ~ 0.005 Δk for typical discharge burnup and enrichment combinations. Calculations were also performed with gradients of 10, 20, 25, and 33% for 4.0 wt % ^{235}U enriched fuel, and the results are shown in Figure 22. The results show that for medium-to-high burnup fuel (i.e., burnup / 30–60 GWd/MTU, depending on initial enrichment), where the horizontal burnup gradient is expected to be < 10% (Ref. 41), the horizontal gradient effect is small (i.e., < 0.002 Δk). Finally, the horizontal gradient effect was evaluated for various cooling times. The results, which correspond to a gradient of 25% and 4.0 wt % ^{235}U enriched fuel, are given in Figure 23 and show that the horizontal burnup gradient effect is fairly insensitive to cooling time.

To demonstrate the impact of horizontal burnup modeling on loading curves for the GBC-32 cask, loading curves were generated for the following two modeling assumptions: (1) uniform horizontal burnup, and (2) the 3 burnup-dependent horizontal gradients listed in Table 7. The resulting loading curves are compared in Figure 24, where it can be seen that this rather conservative approach for modeling the horizontal burnup gradient has a small impact on the loading curve, as compared to the uniform horizontal burnup assumption.

Table 7 Bounding burnup-dependent horizontal burnup gradients (*Source*: Ref. 6)

Assembly-averaged burnup (GWd/MTU)	Horizontal gradient (%)
< 18	33[†]
18 ≤ and < 30	25
30 ≤	20

[†]An assembly with assembly-averaged burnup of 15 GWd/MTU is modeled with 10 GWd/MTU (33% lower) in one half and 20 GWd/MTU (33% higher) in the other half, representing a 33% deviation in each half with respect to the assembly-averaged burnup.

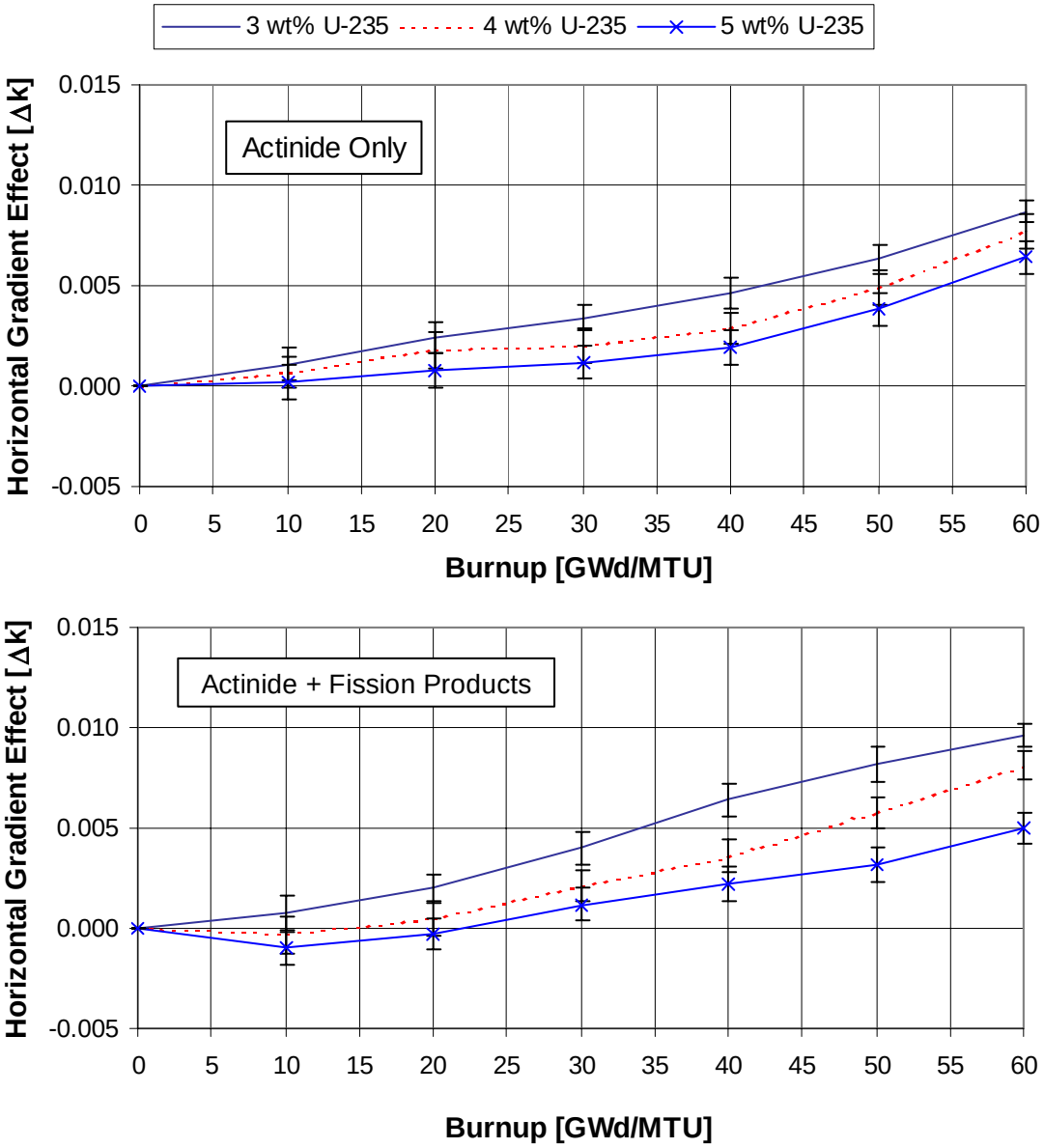

Figure 21 Effect of a 25% horizontal burnup gradient for various fuel enrichments

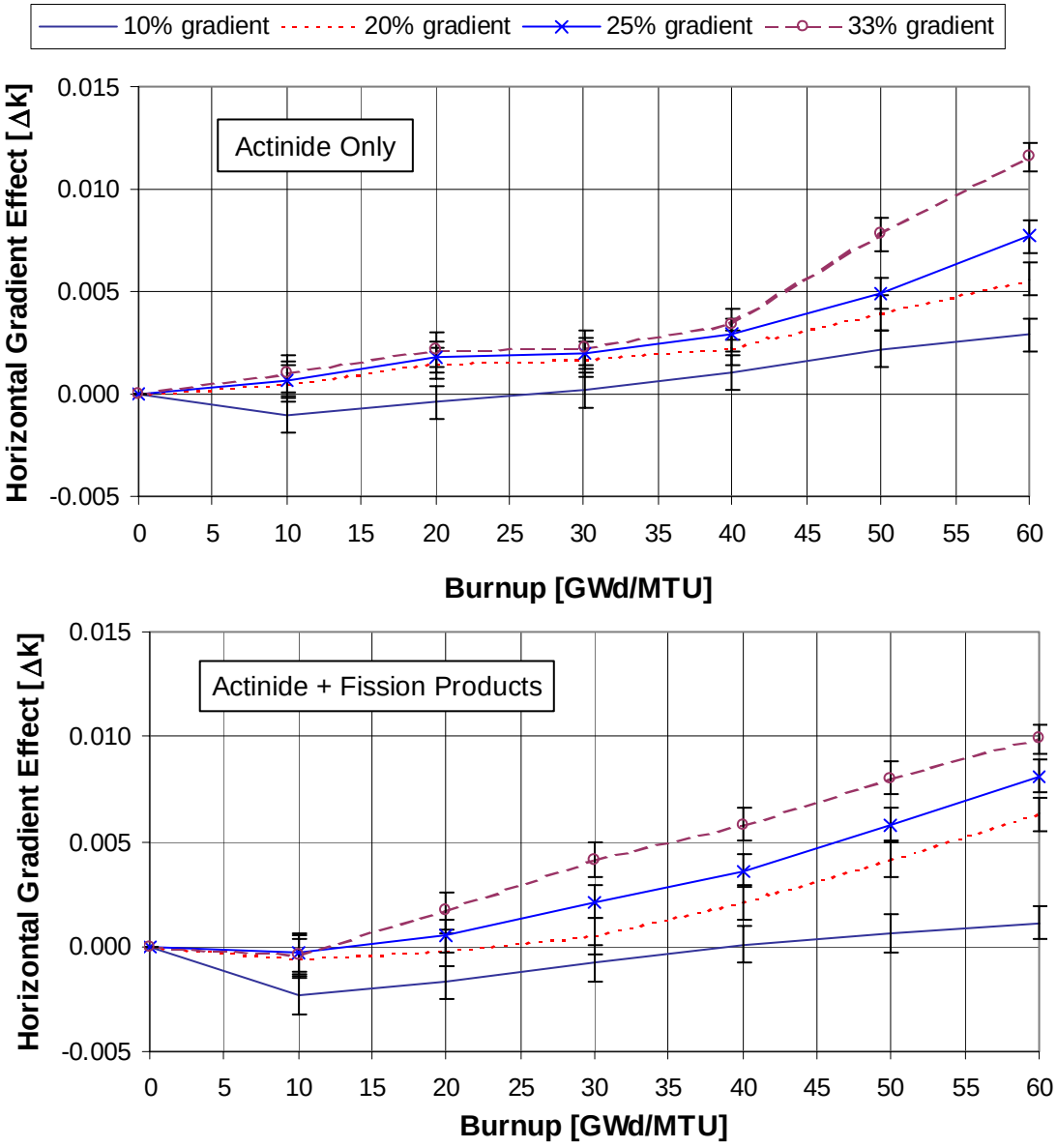

Figure 22 Effect of variations in the horizontal burnup gradient with 4.0 wt % ^{235}U fuel

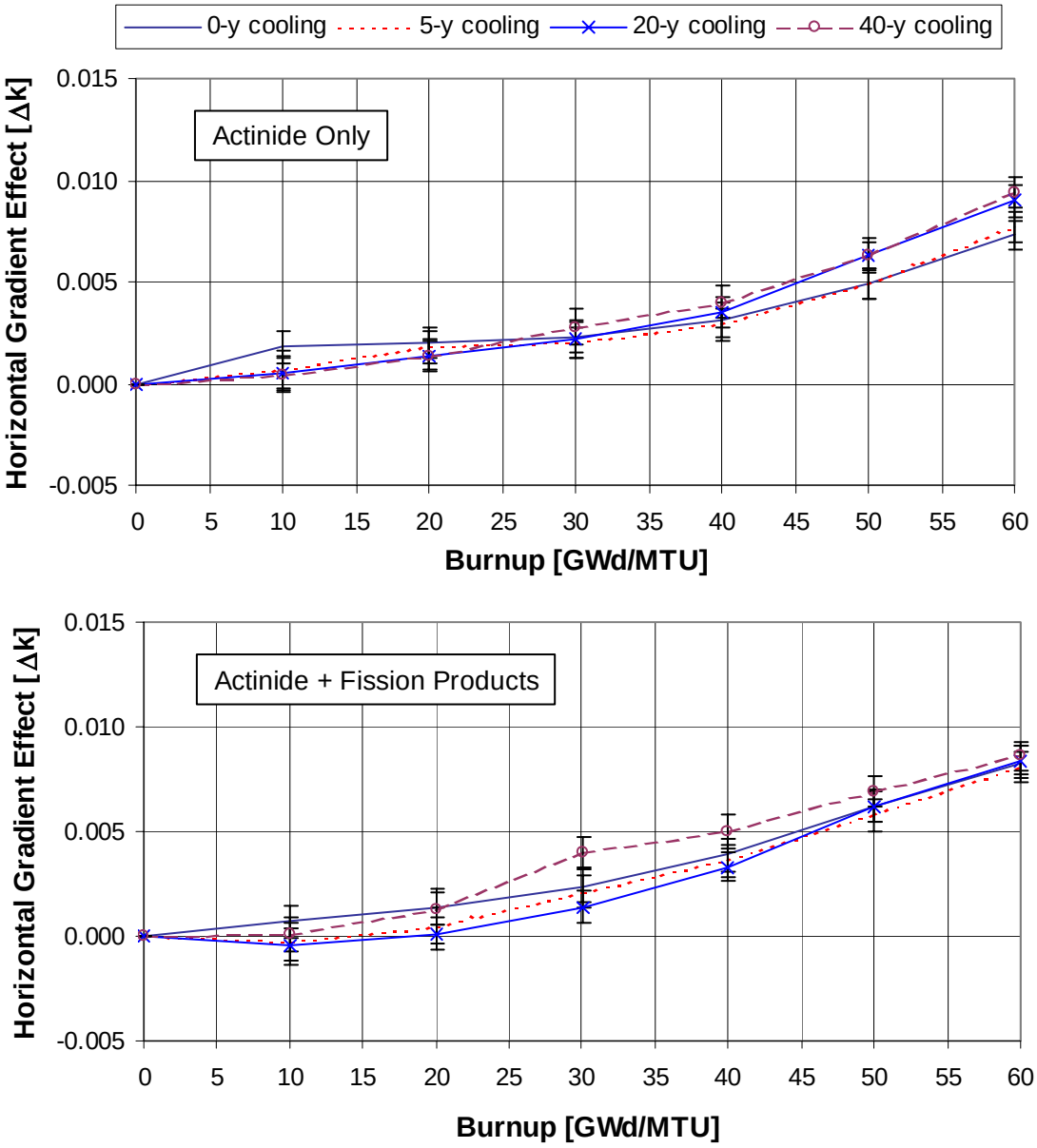

Figure 23 Comparison of the horizontal gradient (25%) effect as a function of cooling time with 4.0 wt % ^{235}U fuel

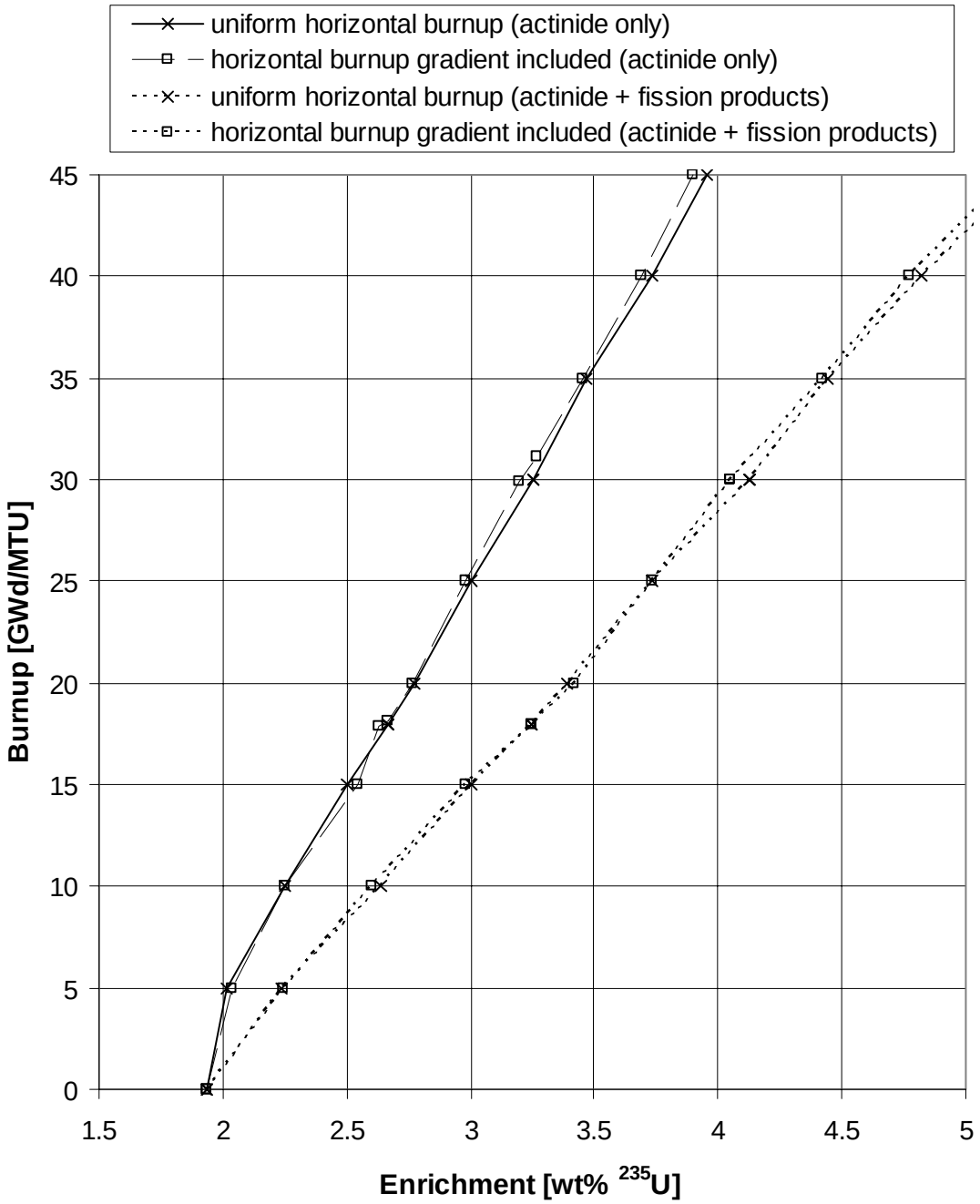

Figure 24 Comparison of the effect of horizontal burnup on burnup-credit loading curves for the GBC-32 cask

6.2 COOLING TIME

6.2.1 Background

Cooling time is an important parameter in a burnup-credit evaluation. It has been shown in numerous studies (e.g., Ref. 40) that SNF discharged from a reactor will increase in reactivity for approximately 100 hours after discharge due to the decrease in neutron absorption caused by the decay of very short-lived fission products. The decrease in reactivity from 100 hours to 100 years is driven by the buildup of the neutron absorbers ^{241}Am (from decay of ^{241}Pu) and ^{155}Gd (from ^{155}Eu which decays with $t_{1/2}$ = 4.7 years). After approximately 100 years, the reactivity begins to increase, governed primarily by the decay of two major neutron absorbers – ^{241}Am ($t_{1/2}$ = 432.7 years) and ^{240}Pu ($t_{1/2}$ = 6,560 years).

6.2.2 Analysis

The effect of cooling time, in terms of Δk values, as a function of burnup for cooling times within the 0-40 year timeframe is shown in Figure 25 for actinide-only and actinide + fission product burnup credit for 4.0 wt % ^{235}U fuel. The results show that the negative reactivity available from cooling time is significant, increases with burnup, and does not change significantly with the inclusion of the major fission products. The effect of cooling time for varying fuel enrichments is shown in Figure 26 for actinide-only burnup credit, where it may be observed that the negative reactivity margin available from cooling time (within the 0–40 year timeframe) decreases with increasing fuel enrichment (for a given burnup).

Finally, to demonstrate the impact of cooling time on loading curves for the GBC-32 cask, Figure 27 provides loading curves for cooling times of 5, 20, and 40 years. Increased cooling time is shown to substantially lower the loading curves. Therefore, credit for longer cooling times, beyond the current recommended limit of 5-years,[18] could be utilized in the future to expand the inventory of SNF that can be loaded into a cask.

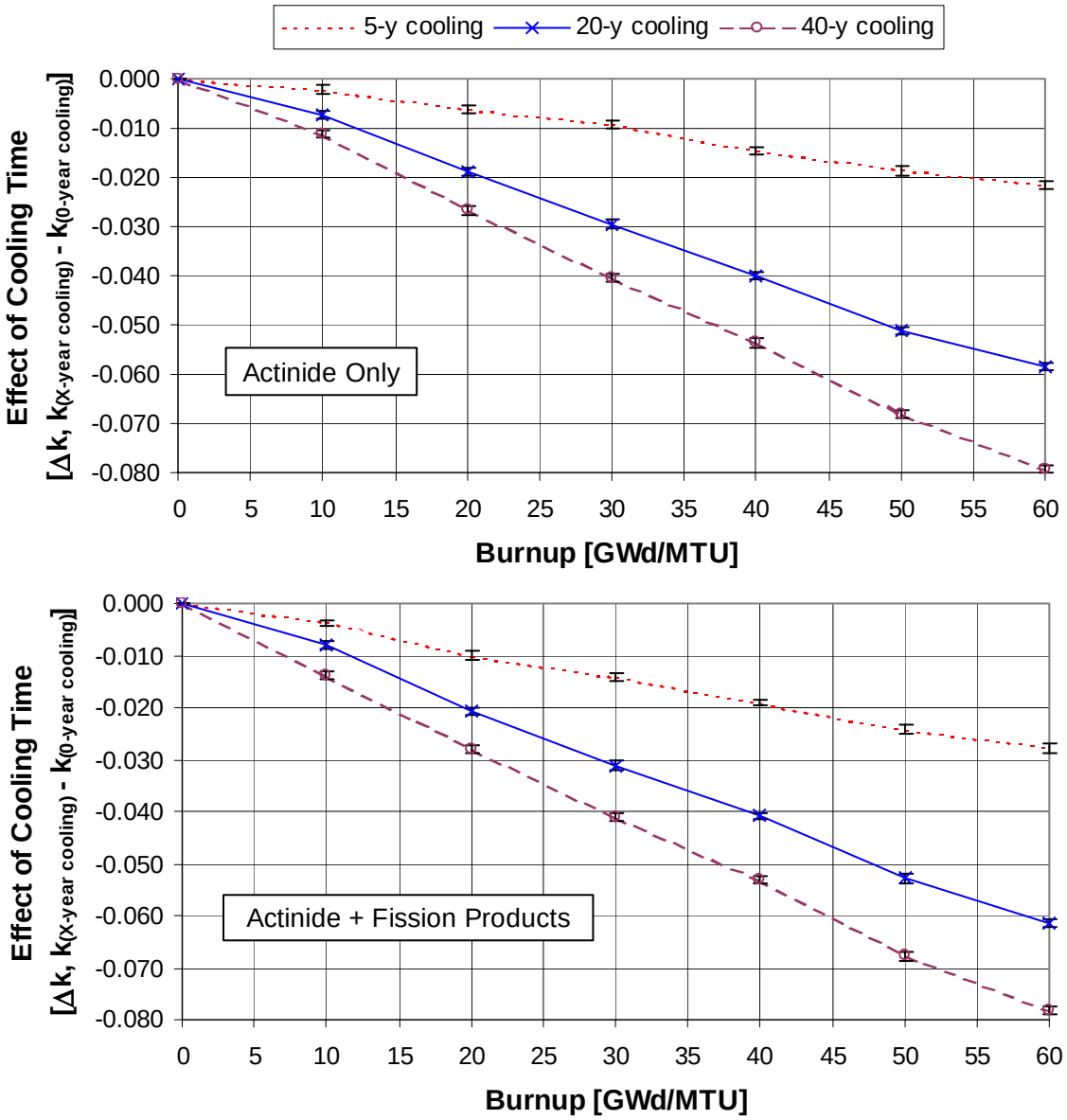

Figure 25 Effect of cooling time as a function of burnup with 4.0 wt % fuel

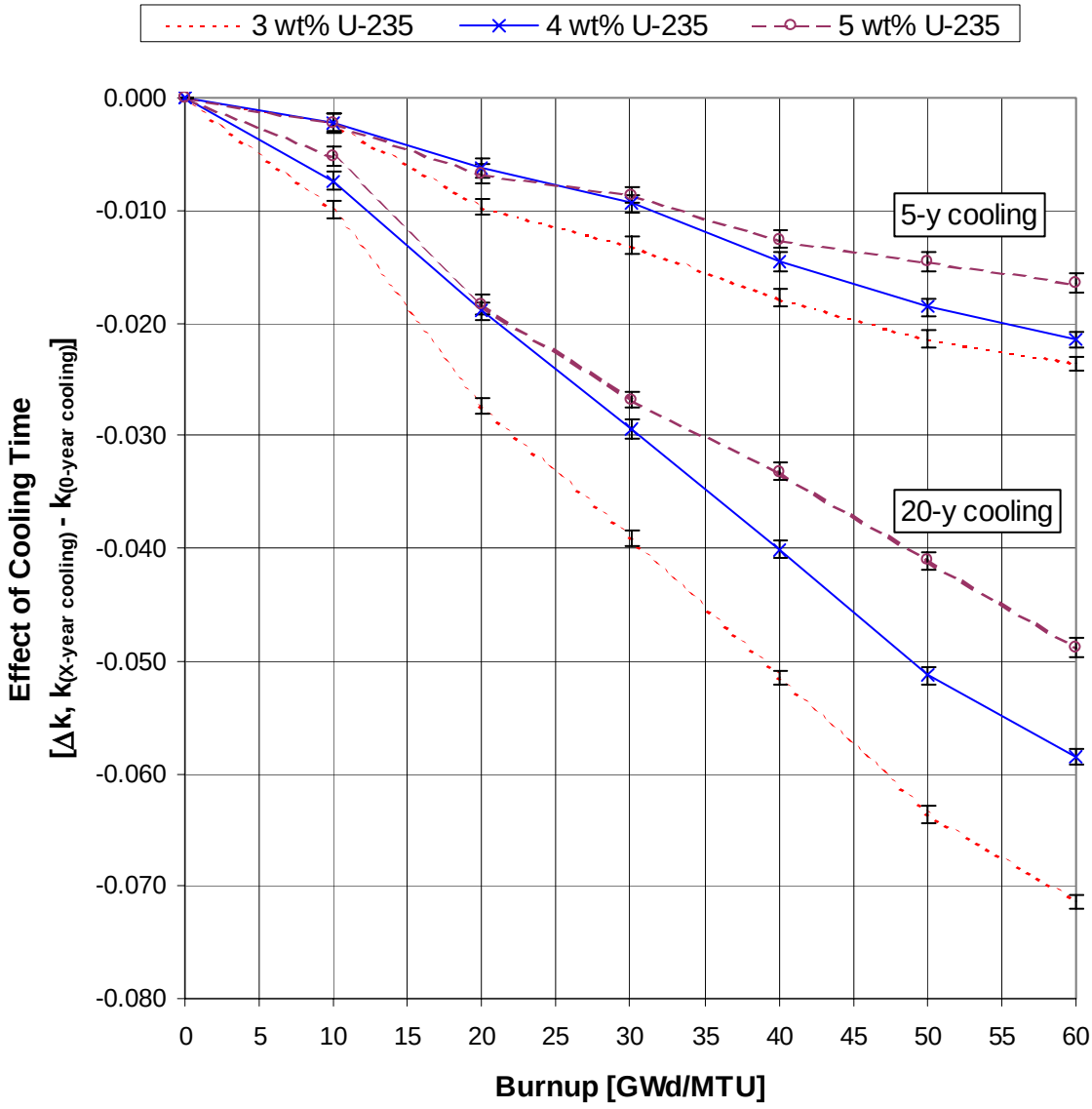

Figure 26 Effect of cooling time as a function of burnup for various initial fuel enrichments and actinide-only burnup credit

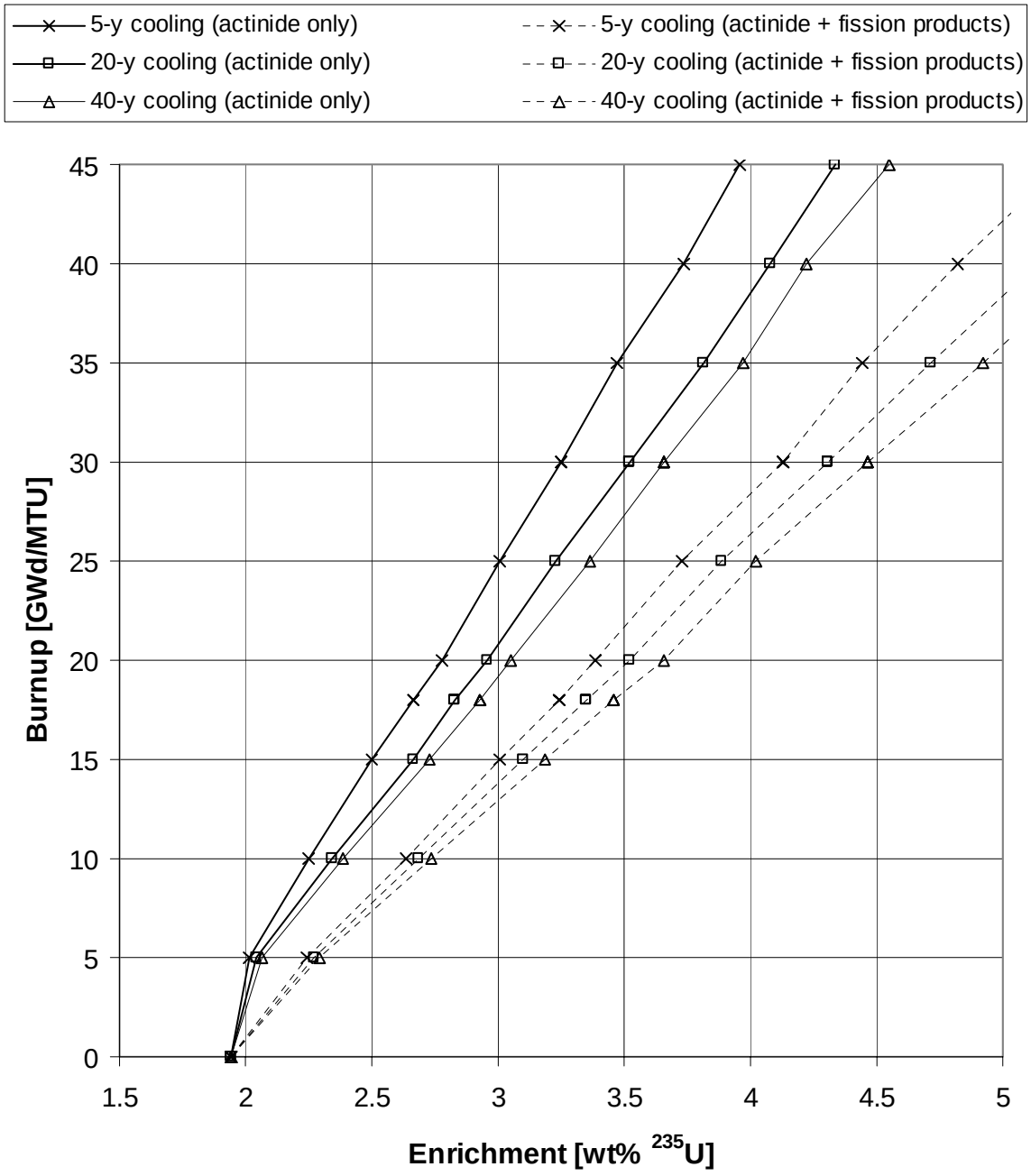

Figure 27 Effect of cooling time on burnup-credit loading curves for the GBC-32 cask

6.3 ISOTOPIC VALIDATION

6.3.1 Background

In contrast to the fresh fuel assumption, the use of burnup credit requires additional validation for calculational methods used to predict the SNF isotopic compositions that are subsequently applied in criticality calculations. Various validation approaches have been proposed, including both independent (Refs. 3, 6, 8, 42, 43) and integral (Refs. 3, 5, 44) validation of the depletion and criticality methods. To date, however, the focus for burnup credit in storage and transportation casks has been on independent validation of depletion and criticality methods, which involves qualifying calculated isotopic predictions via validation against destructive assay measurements from SNF samples and qualifying criticality methods via validation against applicable critical experiments. Thus, utilization of nuclides in a safety analysis process has been primarily limited by the availability of measured assay data and applicable critical experiments.

For independent validation of depletion methods and data, calculated isotopic predictions are compared to chemical assay data to determine biases and uncertainties for each isotope considered in the safety evaluation. The calculational bias is defined as the average measured-to-calculated ratio for a number of comparisons for a given isotope. The uncertainty in the bias is the product of the standard deviation of the bias and a tolerance factor corresponding to a desired confidence level. The uncertainty is typically accounted for at a 95% confidence level and reflects the variance of the predicted bias and the number of assay measurements available. For isotopes with relatively few measurements, the uncertainty can be large.

An important consideration is how to properly combine the uncertainties of the individual isotopes. The most conservative approach is to adjust the calculated isotopic concentration of every isotope to its statistical limit in such a way as to always create a more reactive system; concentrations of fissile isotopes are always increased, while the concentrations of absorbing isotopes are always decreased. Each isotopic concentration is multiplied by an isotopic correction factor (ICF) to adjust for the average bias in the depletion calculation and the uncertainty in the bias. If the concentration of each isotope included in the criticality calculation is adjusted to its statistical limit to account for the nuclide uncertainty, this bounding approach ensures that the predicted reactivity margin due to the uncertainties in the calculated isotopic inventories will be bounding. This approach is conservative but unrealistic, since the calculational methods and data will not produce isotopic concentrations that are biased in a direction that always results in a more reactive system (i.e., concentrations of some nuclide species will be underpredicted, while others will be overpredicted). However, such an approach is simple and easy to justify as conservative.

Recently developed best-estimate methods, which are discussed in Refs. 45 and 46, are expected to provide a more accurate, yet bounding, estimate of the effects of nuclide uncertainty by combining the uncertainties in a more realistic manner. These approaches evaluate the aggregate effect of isotopic uncertainties on k_{eff} rather than the separate effects from individual isotopes, and as a result, the approach credits compensating uncertainties in the calculated isotopic concentrations. The net uncertainty is derived directly from experimental radiochemical assay data, providing a realistic and meaningful measure of the effects of such uncertainties. With these approaches, calculated isotopic concentrations are adjusted for the average bias in the depletion calculation, while the aggregate effect of isotopic uncertainties is accounted for by reduction in the upper subcritical limit (USL).

6.3.2 Analysis

The effect of conservative isotopic validation on the predicted k_{eff} of the GBC-32 cask was estimated using bounding ICFs derived from publicly available experimental assay data for the SCALE (SAS2H) depletion analysis sequence and 44-group ENDF/B-V cross-section library. The ICFs used for this study, which are available from the open literature,[46,47] were developed for the same depletion sequence (SAS2H) and cross-section library used for the analyses in this report, and are listed in Table 8. Note that the two sets were not developed based on the same experiments; Ref. 46 includes more recent experimental data. Although it is not suggested that an applicant use ICFs that were developed by others in their safety evaluation, these published values are useful for the purpose of estimating the impact on k_{eff} values and loading curves.

The effect of the Set 1 ICFs listed in Table 8 on k_{eff} values as a function of burnup for various initial enrichments is shown in Figure 28. The results demonstrate the large effect (> 3% Δk for typical discharge burnup and enrichment combinations) associated with this simple, conservative approach (i.e., simultaneously adjusting each isotope concentration to its statistical limit) in comparison to the reference case without any isotopic validation. The effects of each of the two sets of ICFs listed in Table 8 are compared in Figure 29 for cooling times of 5 and 20 years and 4.0 wt % fuel.

To demonstrate the impact of ICFs on a loading curve for the GBC-32 cask, loading curves with and without ICFs applied are shown in Figure 30. It is clear from Figure 30 that the application of the ICFs listed in Table 8 results in a very large penalty to the loading curve. Consequently, more realistic approaches for representing the effect of nuclide uncertainties, such as those presented in Refs. 45 and 46, could provide enhanced utilization of burnup credit. Reference 46 describes several best-estimate approaches for bounding the uncertainty in k_{eff} associated with the differences between measured and computed isotopic compositions. From these approaches, Δk values, due to the uncertainties in the computed isotopic compositions, were determined for a number of different configurations and conditions, including the GBC-32 cask with and without fission products present. These Δk values can be used to account for the uncertainties in the computed isotopic compositions. The Δk values from Ref. 46 for the GBC-32 cask with and without fission products are 1.4% and 1.8%, respectively. To utilize these values for generating loading curves, the USL used to develop the loading curves is reduced by the Δk values (e.g., the USL limit of 0.94 used in this report is reduced to 0.922 and 0.926 for the cases with and without fission products present). Note that it is still necessary to adjust the calculated isotopic concentrations to account for the average bias in the depletion calculation. For this analysis, the conservatively adjusted bias values from Ref. 46 were used. Loading curves based on the best-estimate approach are compared to loading curves based on the bounding ICF approach in Figure 30, where it is shown that the best-estimate approach for bounding uncertainties in the computed isotopic compositions is significantly less conservative than the bounding ICF approach. For the best-estimate approach, separate loading curves were generated based on the conservatively adjusted bias values (adjusted to prevent positive biases, see Ref. 46 for details) and the unmodified bias values.[46] As shown in Figure 30, the effect of using the conservatively adjusted bias values is very small. This is due to the fact that few bias values require adjustment and most of those that do are near unity, and hence the adjustment is small.

Table 8 Isotopic correction factors used for analyses

Isotope[‡]	Isotopic correction factors[†] Set 1 (***Source*****:** Ref. 46)	Set 2 (***Source*****:** Ref. 47)
U-234	0.714	0.635
U-235	1.080	1.085
U-238	0.990	0.992
Pu-238	0.862	0.856
Pu-239	1.095	1.076
Pu-240	0.950	0.945
Pu-241	1.144	1.087
Pu-242	0.882	0.848
Am-241	0.461	0.609
U-236	0.932	0.910
Np-237	0.741	0.697
Am-243	0.669	0.804
Mo-95	0.000	0.000
Tc-99	0.256	0.590
Ru-101	0.000	0.000
Rh-103	0.000	0.000
Ag-109	0.000	0.000
Cs-133	0.907	0.907
Nd-143	0.978	0.962
Nd-145	0.972	0.973
Sm-147	0.883	0.695
Sm-149	0.332	0.000
Sm-150	0.879	0.619
Sm-151	0.598	0.506
Sm-152	0.321	0.755
Eu-151	0.000	0.506
Eu-153	0.719	0.641
Gd-155	0.649	0.524

[†]A value of zero indicates no data, and thus the composition is set to zero (i.e., no credit is taken for that isotope in the criticality calculations).

[‡] Consistent with the classification in Table 2, isotopes shown in bold correspond to the actinide-only nuclides.

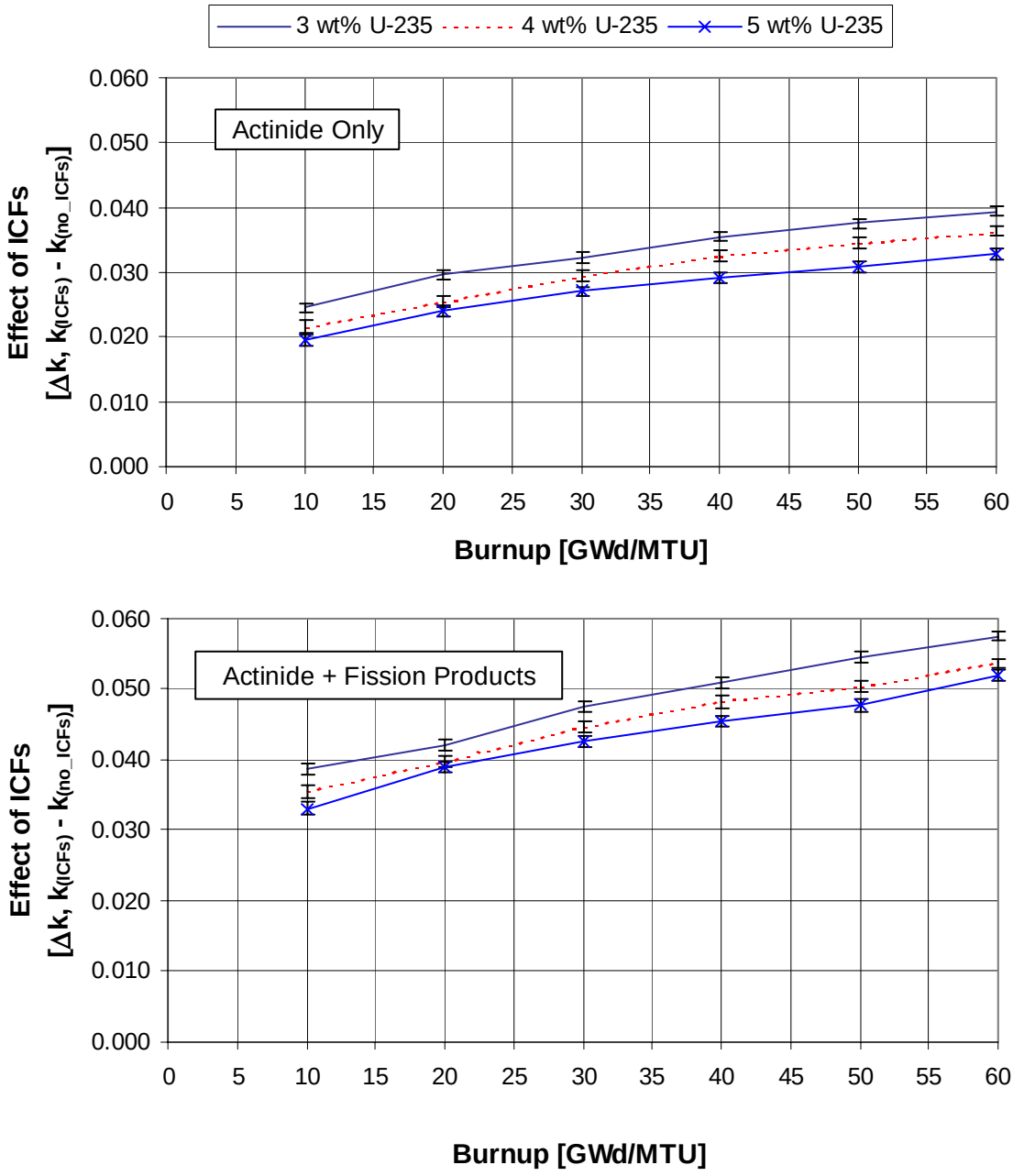

Figure 28 Comparison of the effect of the Set 1 ICFs as a function of burnup for various initial enrichments

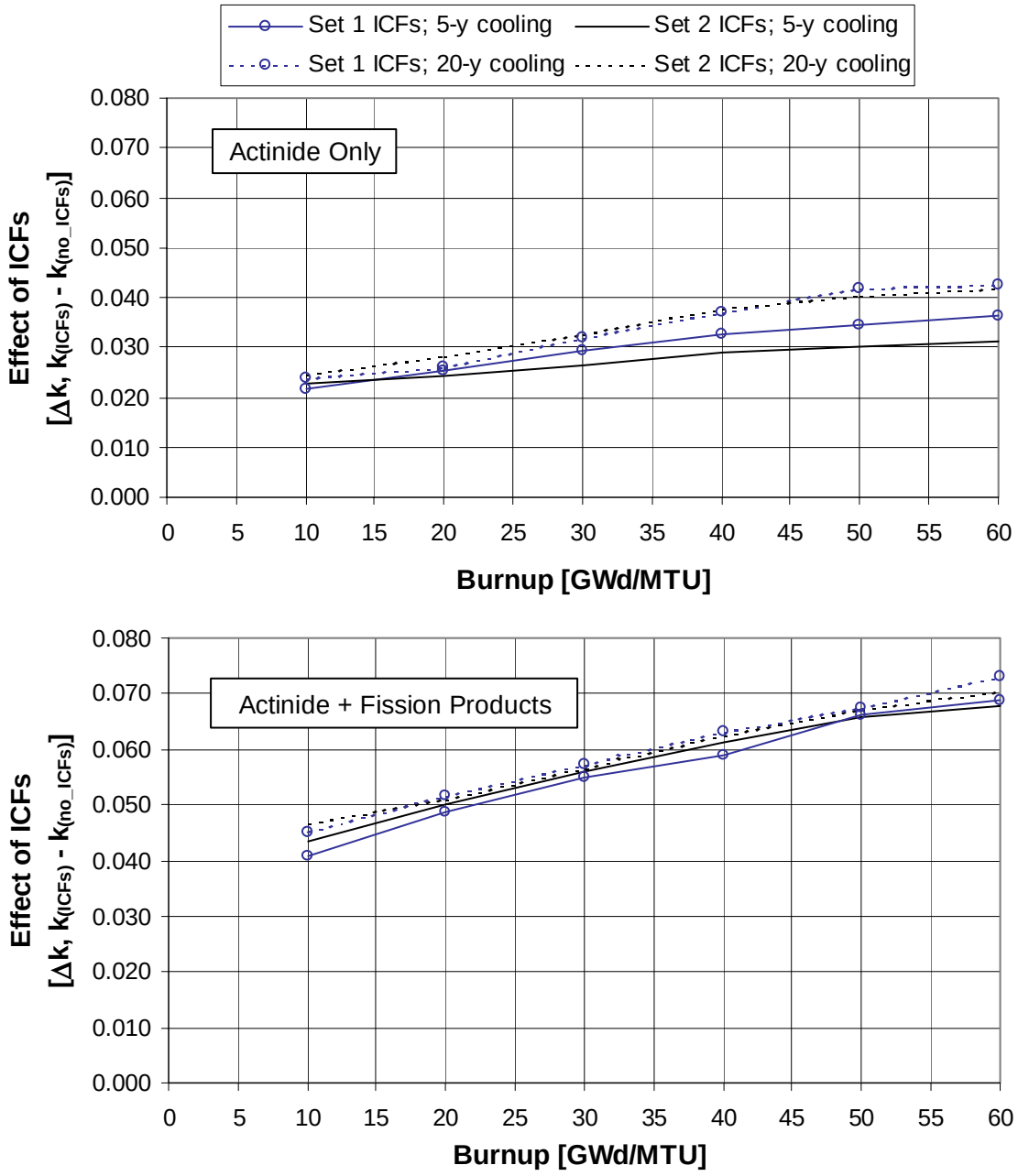

Figure 29 Comparison of the effect of ICFs for cooling times of 5 and 20 years with 4.0 wt % ^{235}U fuel

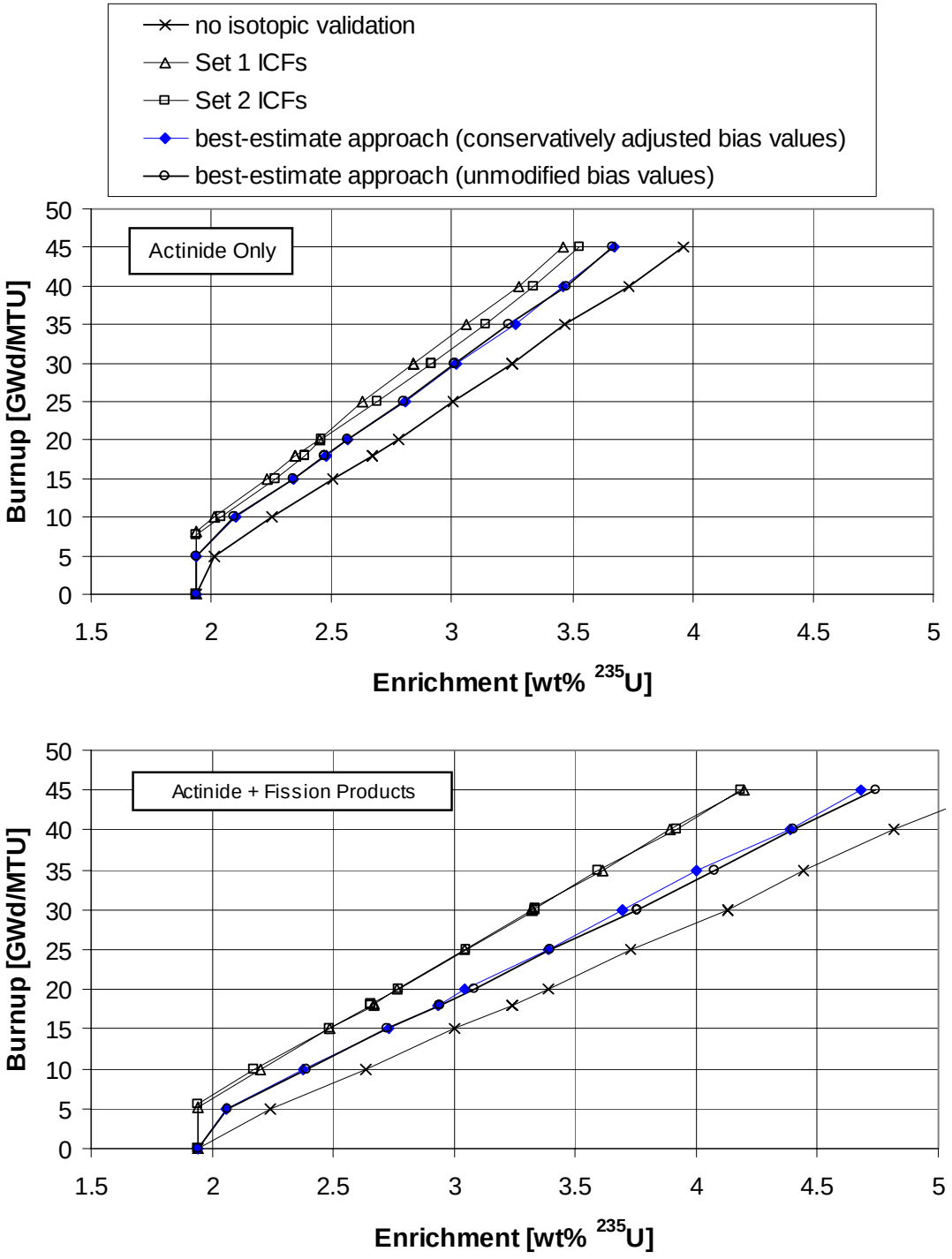

Figure 30 Comparison of the effect of isotopic validation on burnup-credit loading curves for the GBC-32 cask

6.4 "LOADING OFFSET" FOR ENRICHMENT > 4.0 WT % ^{235}U

6.4.1 Background

The applicable regulatory guidance for burnup-credit safety evaluations[16,18] recommends a loading offset equal to at least 1 GWd/MTU for every 0.1 wt % ^{235}U increase above 4 wt % ^{235}U. The maximum enrichment that may be considered in any case is 5.0 wt % ^{235}U. Therefore, spent fuel with an initial enrichment of 4.5 wt % ^{235}U would be assigned a burnup loading value that is at least 5 GWd/MTU higher than the burnup credited in the safety analysis. The loading offset was included in the regulatory guidance to account for the potential of higher uncertainties in calculated isotopic inventories with SNF having initial enrichments greater than 4.0 wt % ^{235}U. At the time the regulatory recommendation was developed, no publicly-available experimental data were available to validate computer code isotopic predictions for initial enrichments > 4.0 wt % ^{235}U or burnups > 40 GWd/MTU.

The loading offset has been identified as a potential limitation to the practical usefulness of burnup credit. However, for loading in a burnup-credit cask, the minimum burnup requirement increases with enrichment. Consequently, considering the current regulatory limit on burnup (40 GWd/MTU and the actinide-only burnup credit), the benefits associated with removing the enrichment loading offset (without removing the limit on burnup) are limited, or non-existent for high-capacity casks such as the GBC-32. This point is illustrated in Figure 31, which shows illustrative loading curves with and without the loading offset applied. On the other hand, the enrichment loading offset does provide a means to store fuel up to 5.0 wt % ^{235}U enrichment with burnup credit in lower-density cask designs (e.g., a 24-assembly cask).

6.4.2 Analysis

The loading offset, expressed in terms of Δk, is illustrated in Figure 32 for actinide-only burnup credit. The penalty associated with the loading offset is dependent on the burnup range over which it is applied – the lower the burnup range, the larger the loading offset penalty. For 5 wt % ^{235}U fuel, which is the maximum enrichment allowed, the loading offset penalty ranges from approximately 0.030 to 0.045 Δk, depending on the fuel burnup.

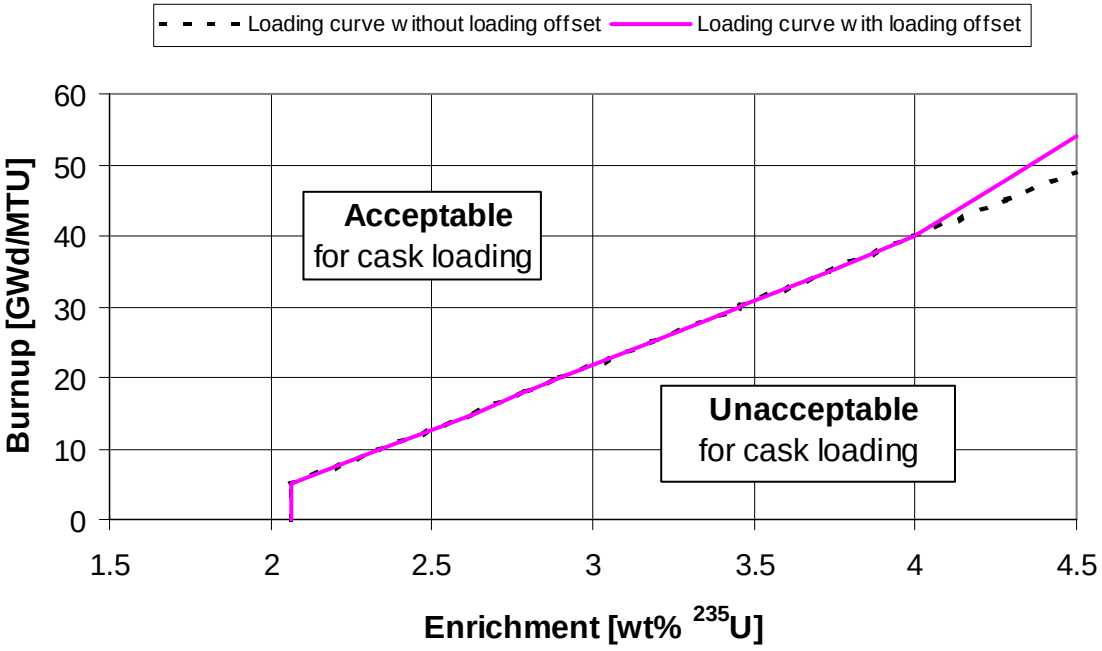

Figure 31 Illustrative loading curves depicting the effect of the loading offset

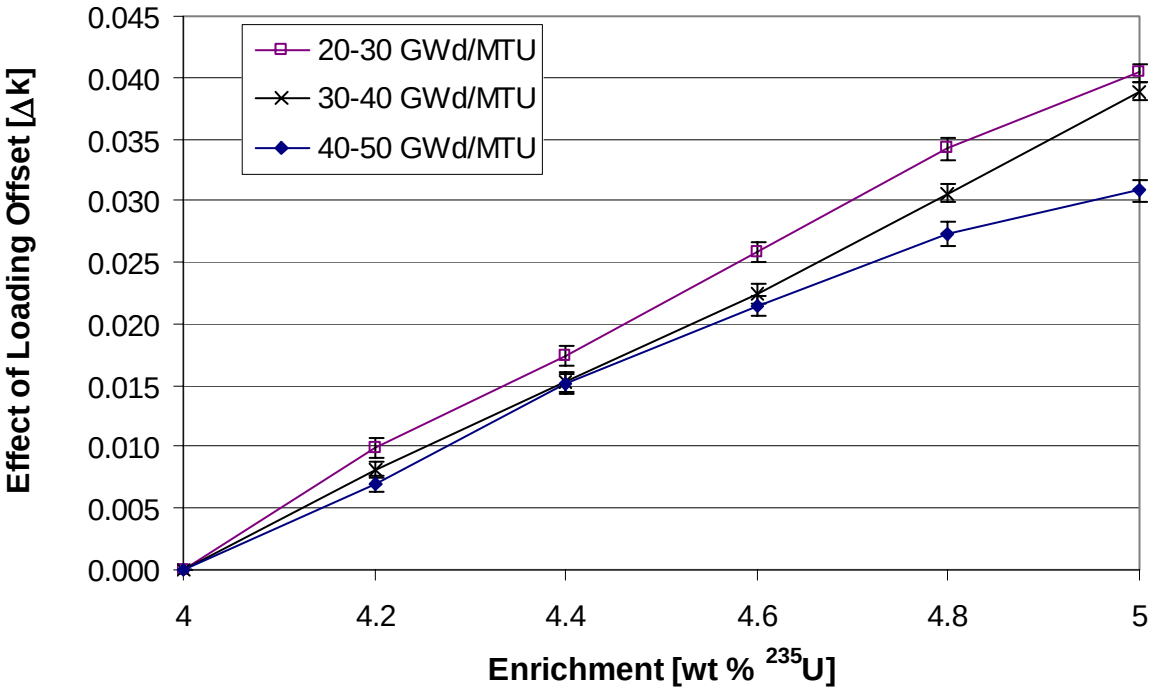

Figure 32 Effect of the loading offset for actinide-only burnup credit

6.5 FISSION PRODUCT MARGIN

6.5.1 Background

The applicable regulatory guidance[16,18] recommends limiting credit for the reactivity reduction associated with burnup to that available from actinide compositions. Moreover, the actinides are limited to those that are established by validation. Credit for the reactivity reduction due to fission products is not currently included due to the greater uncertainties associated with inventory prediction (see Section 6.3) and cross-section data for fission products. Consequently, an added margin of subcriticality exists due to the presence of fission product and actinide nuclides not included in the design-basis safety analysis. To assess the effect of fission products and gain a greater understanding of the actual subcritical margin, the regulatory guidance recommends performing design-specific analyses to estimate the additional reactivity margins available from the fission products and actinides not included in the design-basis safety analysis. Additionally, Ref. 18 states that, "the analysis methods used for determining the estimated reactivity margins should be verified using available experimental data (e.g., isotopic assay data) and computational benchmarks that demonstrate the performance of the applicant's methods in comparison with independent methods and analyses."

The GBC-32 cask was developed as a computational benchmark to provide a reference burnup-credit cask configuration for the estimation of reactivity margin available from fission products and minor actinides, and reference estimations of the additional reactivity margin as a function of initial enrichment, burnup, and cooling time are provided in Ref. 27. The findings are summarized here, while Ref. 27 provides the detailed results. For typical enrichment and discharge burnup combinations, ~70% of the total reactivity reduction associated with burnup is due to the major actinides (the Set 1 nuclides listed in Table 2), with the remaining 30% being attributed to the additional nuclides (major fission products and minor actinides; the nuclides present in Set 2 of Table 2 that are not part of Set 1). For a given burnup, an increase in the initial enrichment is shown to result in a decrease in the contribution from the major actinides and a simultaneous increase in the contribution from the additional nuclides. During the time frame of interest to cask storage and transportation (0–40 years), the reactivity reduction associated with the major actinides is shown to increase with cooling time. In contrast, the reactivity reduction associated with the fission products and minor actinides is shown to increase initially with cooling time, but then decrease somewhat in the 5- to 40-year time frame. The range (minimum and maximum) for the additional reactivity margin available from fission products and minor actinides was quantified for the burnup, initial enrichments, and cooling times considered, and is shown in Figure 33. The minimum values are shown to occur at zero cooling time and increase as a function of burnup from ~0.03 Δk at 10 GWd/MTU to ~0.08 Δk at 60 GWd/MTU.

6.5.2 Analysis

For the reference conditions considered herein (i.e., the bounding depletion parameters listed in Table 4, 5-year cooling, and axial-burnup distribution included), the reactivity reduction due to the major actinides and the actinide + fission products are illustrated in Figures 34–36 for 4.0 wt % ^{235}U enriched fuel. The impact of including the major fission products and minor actinides on loading curves for the GBC-32 cask is shown in Figure 37.

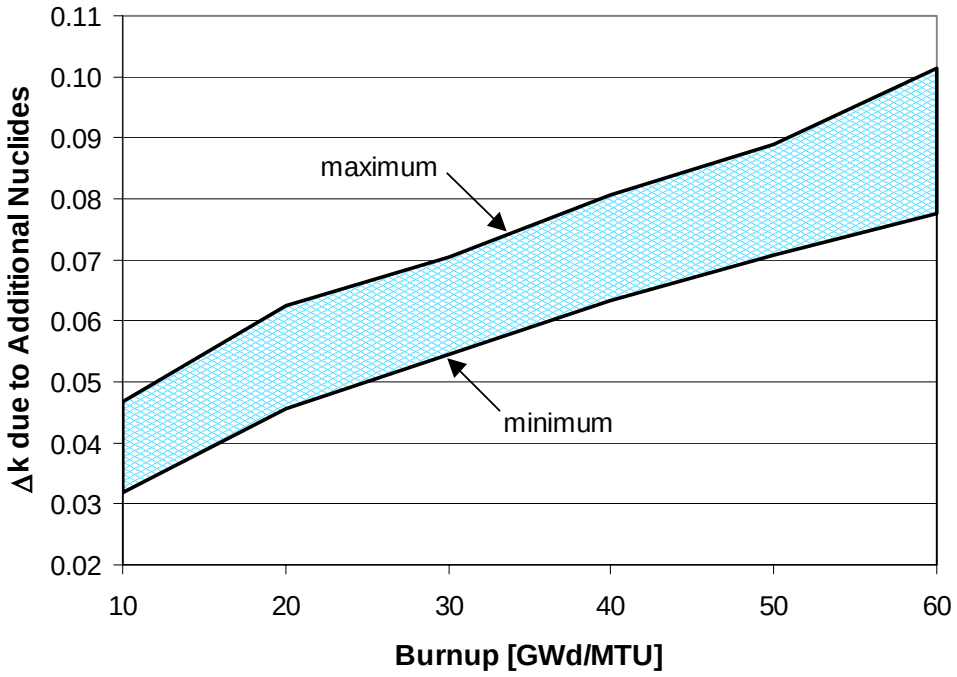

Figure 33 Range of Δ*k* values in the GBC-32 cask due to minor actinides and major fission products for all cooling times and enrichments considered (0- to 40-years cooling; 2- to 5-wt % ^{235}U enrichment)

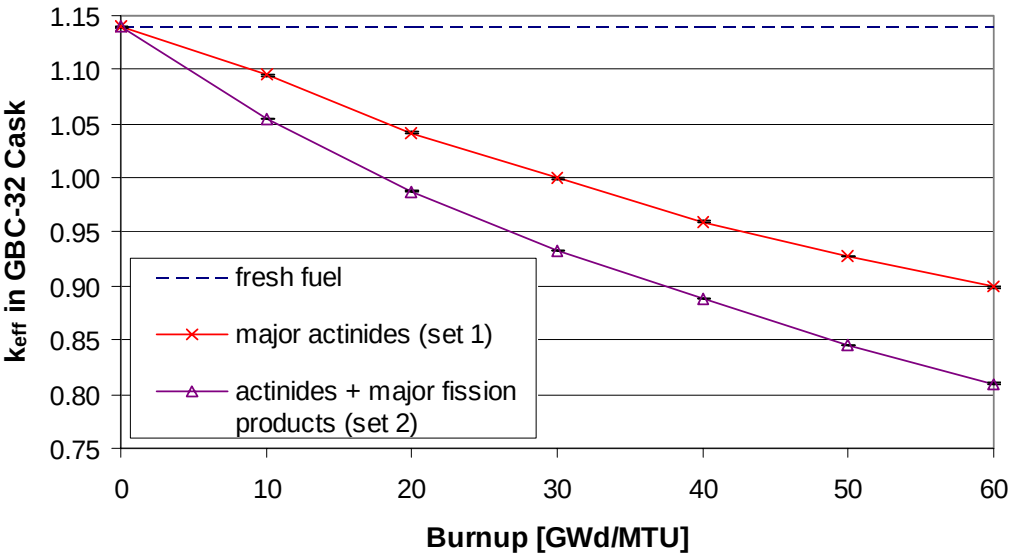

Figure 34 Values of k_{eff} in the GBC-32 cask as a function of burnup using different nuclide sets (see Table 2) and 4.0 wt % fuel

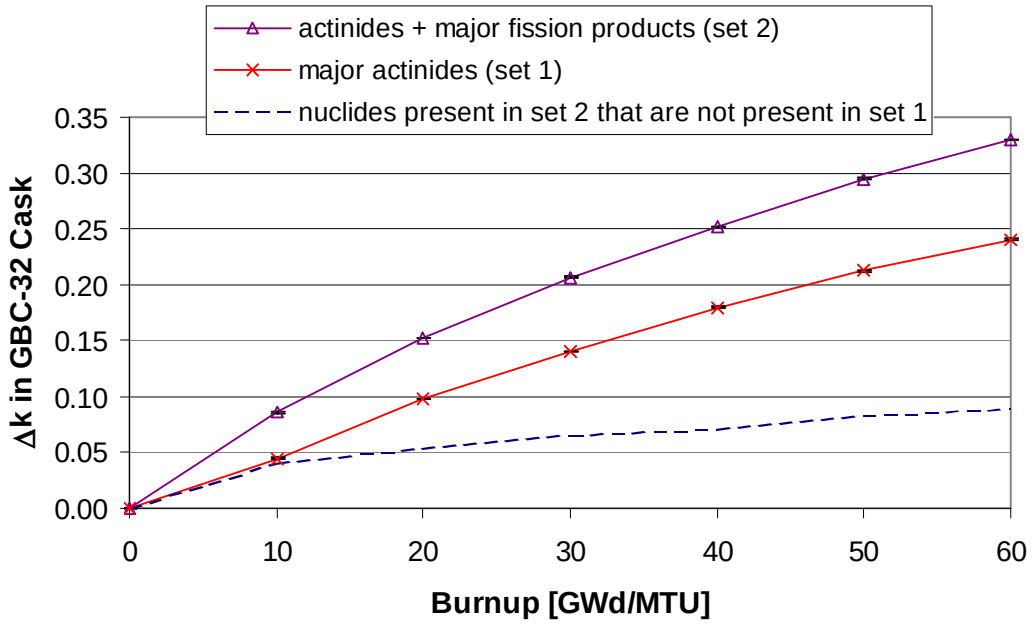

Figure 35 Δ*k* values (relative to fresh fuel) in the GBC-32 cask as a function of burnup using different nuclide sets (see Table 2) and 4.0 wt % fuel

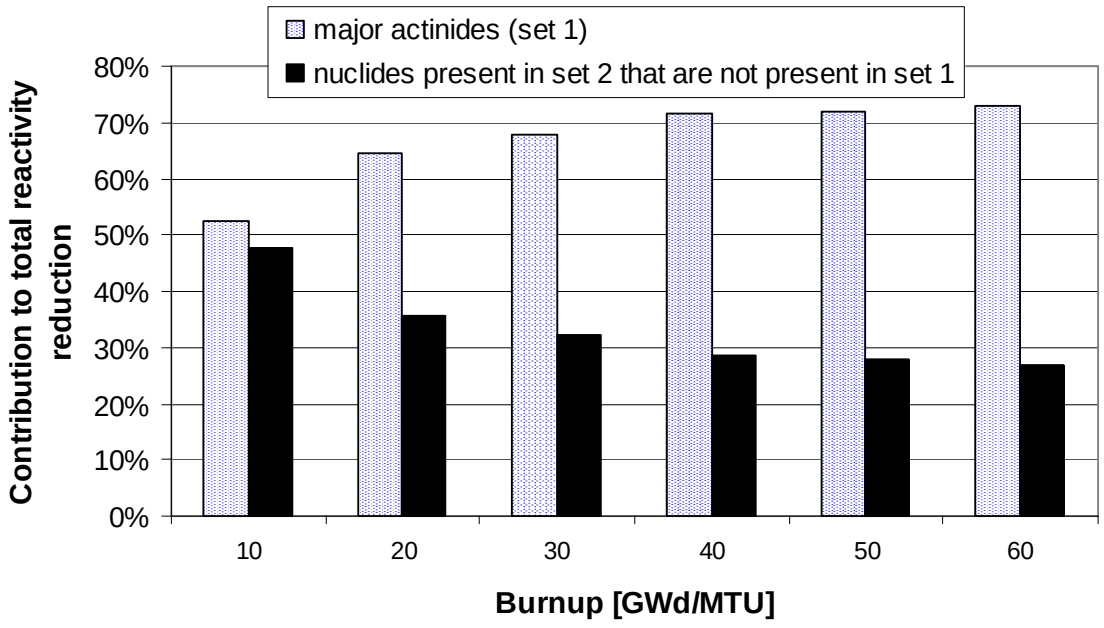

Figure 36 Components of the total reduction in k_{eff} due to burnup for the different nuclide sets (see Table 2) as a function of burnup for 4.0 wt % fuel

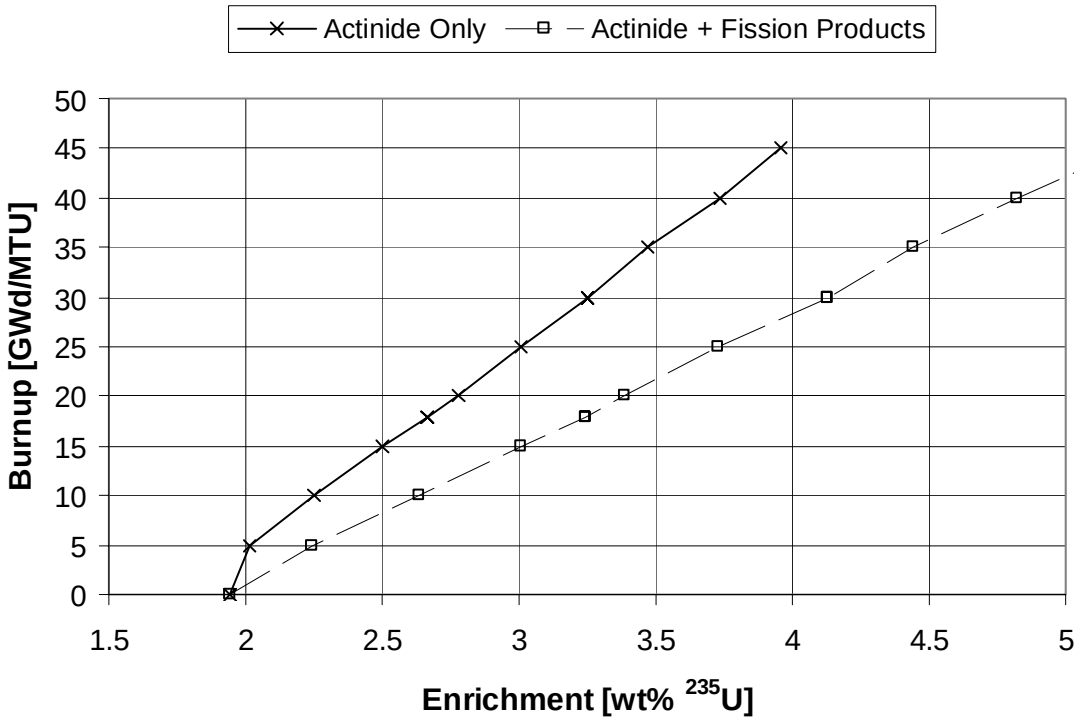

Figure 37 Comparison of the effect of fission products on burnup-credit loading curves for the GBC-32 cask

6.6 ASSEMBLY DESIGNS

Up to this point, all calculations have been based on the WE 17 × 17 fuel assembly design. The primary motivation for using this assembly design is that it is known to be one of the most-reactive PWR assembly designs. Because some assembly designs are know to be considerably less reactive than others, it may be beneficial for applicants to generate separate loading curves for unique classes of assembly designs. To investigate the potential merits, loading curves were generated for the following unique fuel assembly design configurations: (1) CE 14 × 14, (2) B&W 15 × 15, (3) CE 16 × 16, and (4) WE 17 × 17. The loading curves are shown in Figure 38, where it is clear that the minimum burnup requirements for the CE assembly designs are significantly less than the requirements for the WE or B&W fuel assembly designs. The fuel assembly specifications used for the calculations are listed in Table 9.

Table 9 PWR fuel assembly design specifications (all units in cm)

Assembly design	CE 14 × 14	B&W 15 × 15	CE 16 × 16	WE 17 × 17
Parameter				
Fuel pellet outside diameter	0.9563	0.9505	0.8255	0.7844
Cladding inside diameter	0.9754	0.9703	0.8433	0.8001
Cladding outside diameter	1.1176	1.0871	0.9703	0.9144
Rod pitch	1.4732	1.4427	1.2852	1.2598
Guide tube/thimble inside diameter	2.628	1.2700	2.2860	1.1227
Guide tube/thimble outside diameter	2.832	1.3411	2.4892	1.2040
Instrument tube inside diameter	N/A	1.2700	N/A	1.1227
Instrument tube outside diameter	N/A	1.3411	N/A	1.2040
Active fuel length	375.76	365.76	365.76	365.76
Array size	14 × 14	15 × 15	16 × 16	17 × 17
Number of fuel rods	176	208	236	264
Number of guide tubes/thimbles	5	16	5	24
Number of instrument tubes	0	1	0	1

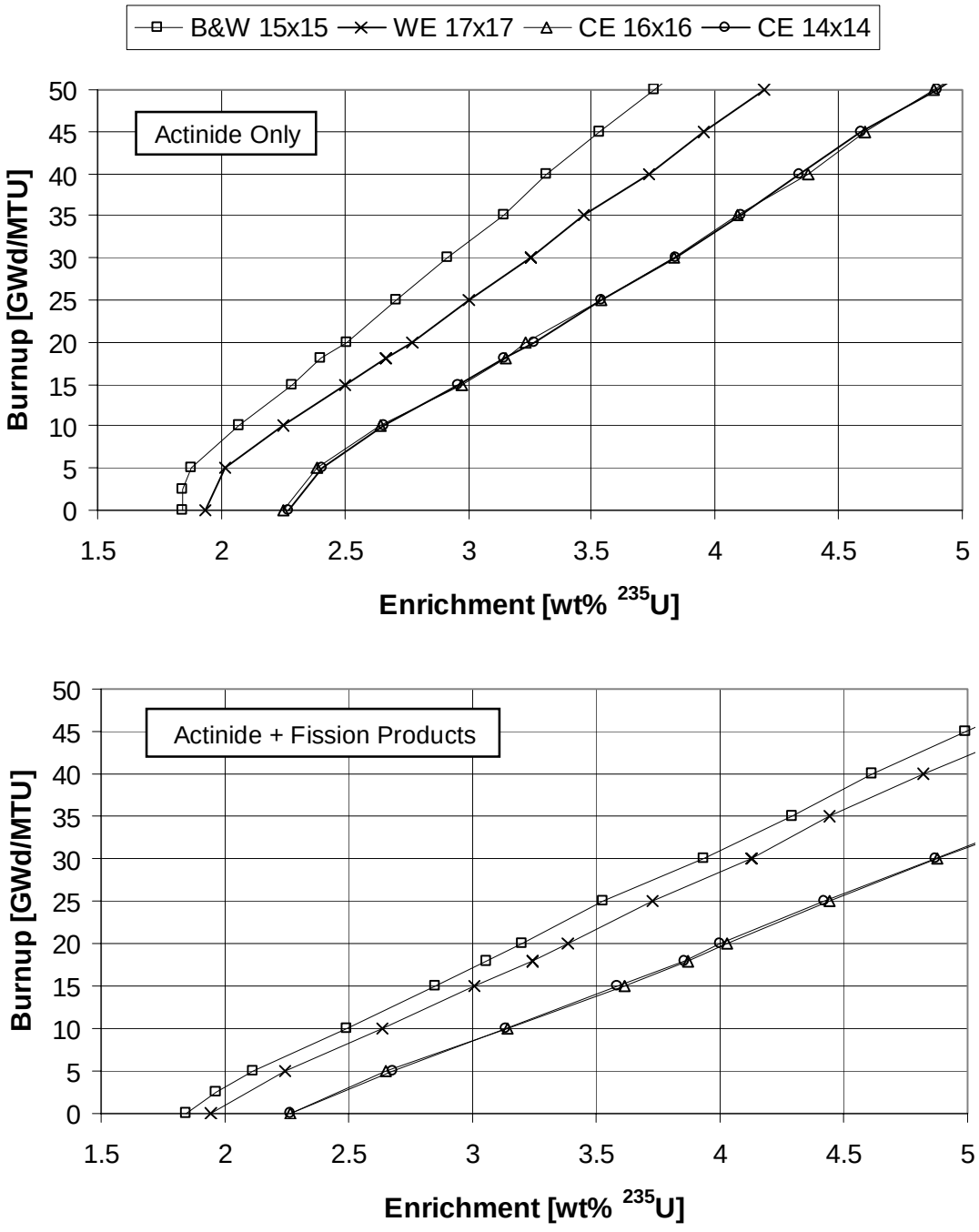

Figure 38 Comparison of loading curves for different assembly designs in the GBC-32 cask

6.7 SUMMARY OF EFFECTS ON LOADING CURVES

The results in the previous sections demonstrated the individual impact of each of the modeling assumptions considered. In this section, the effect of the individual modeling assumptions are evaluated in a cumulative manner, concluding with a loading curve that includes all of the primary bounding assumptions necessary for a burnup-credit safety evaluation. The results correspond to the high-capacity GBC-32 cask loaded with WE 17×17 fuel assemblies. Note that, as is the case throughout this report (except where explicitly stated otherwise), the loading curves correspond to an USL of 0.94, which inherently allows 1% for criticality calculational bias and uncertainty. Validation of criticality analysis methods for burnup-credit analyses is outside the scope of this report, and hence specific values for criticality calculational bias and uncertainty were not determined.

The characteristics of the cases considered are indicated in Table 10 and the resulting loading curves are given in Figure 39 for actinide-only burnup credit. From Figure 39, the calculational assumptions that have the largest increasing effect on the loading curve are (1) the use of bounding depletion parameters, (2) the use of bounding ICFs for isotopic validation, and (3) BPR/CR exposure. Bounding modeling assumptions are necessary to account for all realistic conditions that may increase the reactivity of SNF. However, improved knowledge of the uncertainties and improved information to establish bounding modeling assumptions will improve the accuracy of the estimates of subcritical margins, thereby reducing the level of conservatism. Most notably, more realistic approaches to address the validation of calculated SNF isotopic compositions including those of fission products will provide improved estimates of the subcritical margin. The impact of longer cooling times is illustrated in Figure 40.

Table 10 Explanation of calculational assumptions for the loading curves shown in Figures 39 and 40

Case	Notes	Nominal depletion parameter (Table 4)	Bounding depletion parameters (Table 4)	3 burnup-dependent axial profiles (Table 6)	3 burnup-dependent horizontal profiles (Table 7)	Set 1 ICFs included (Table 8)	BPR exposure 20 GWd/MTU	CR exposure 5 GWd/MTU
1	Reference conditions*	✔						
2	Reference conditions*		✔					
3	5-year cooling		✔	✔				
4	5-year cooling		✔	✔	✔			
5	5-year cooling		✔	✔	✔	✔		
6	5-year cooling		✔	✔	✔	✔	✔	
7	5-year cooling		✔	✔	✔	✔		✔

* 5-year cooling, axial profile from Table 1.

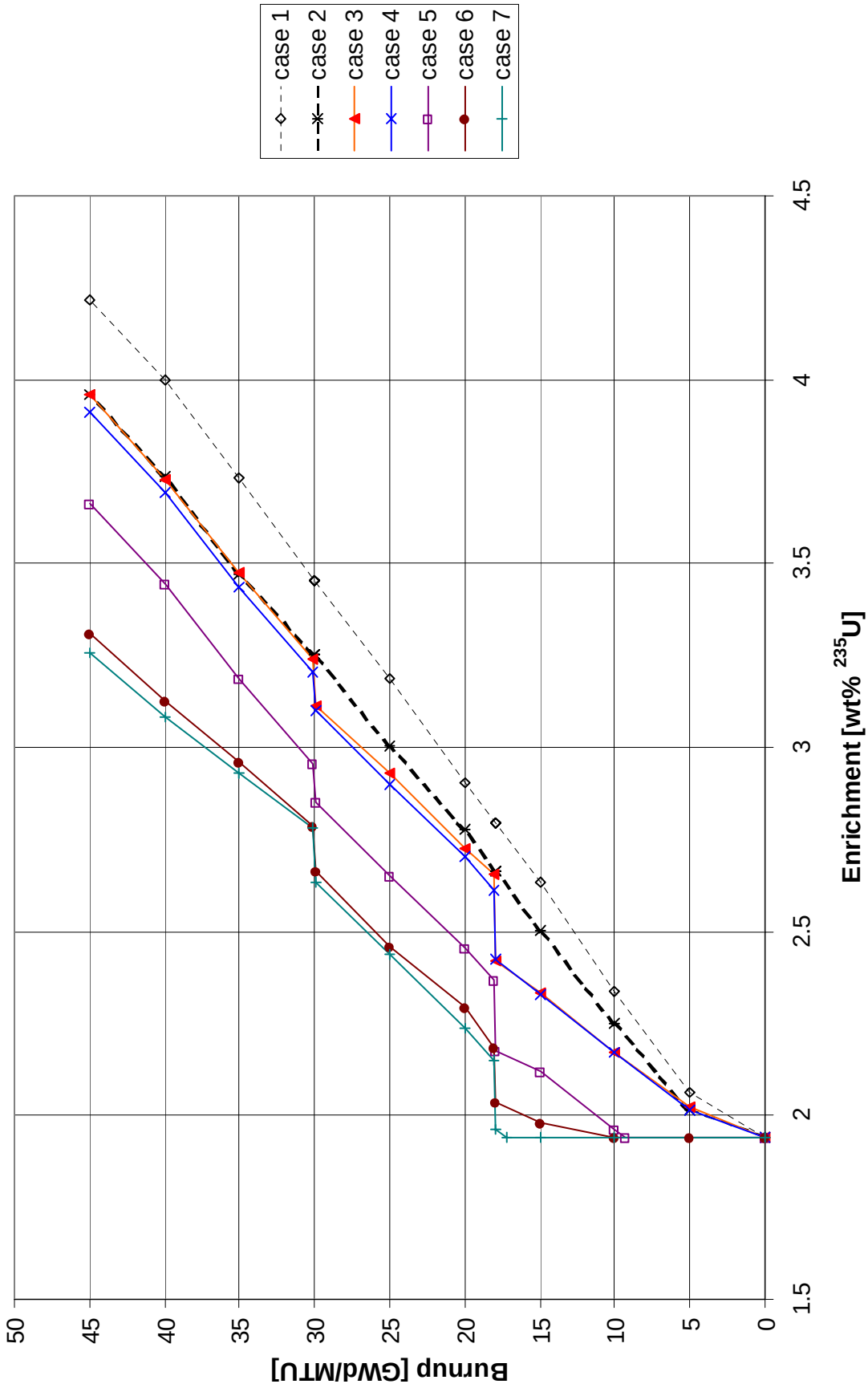

Figure 39 Cumulative effect of modeling assumptions on loading curves for actinide-only burnup credit (see Table 10 for specification of the various cases)

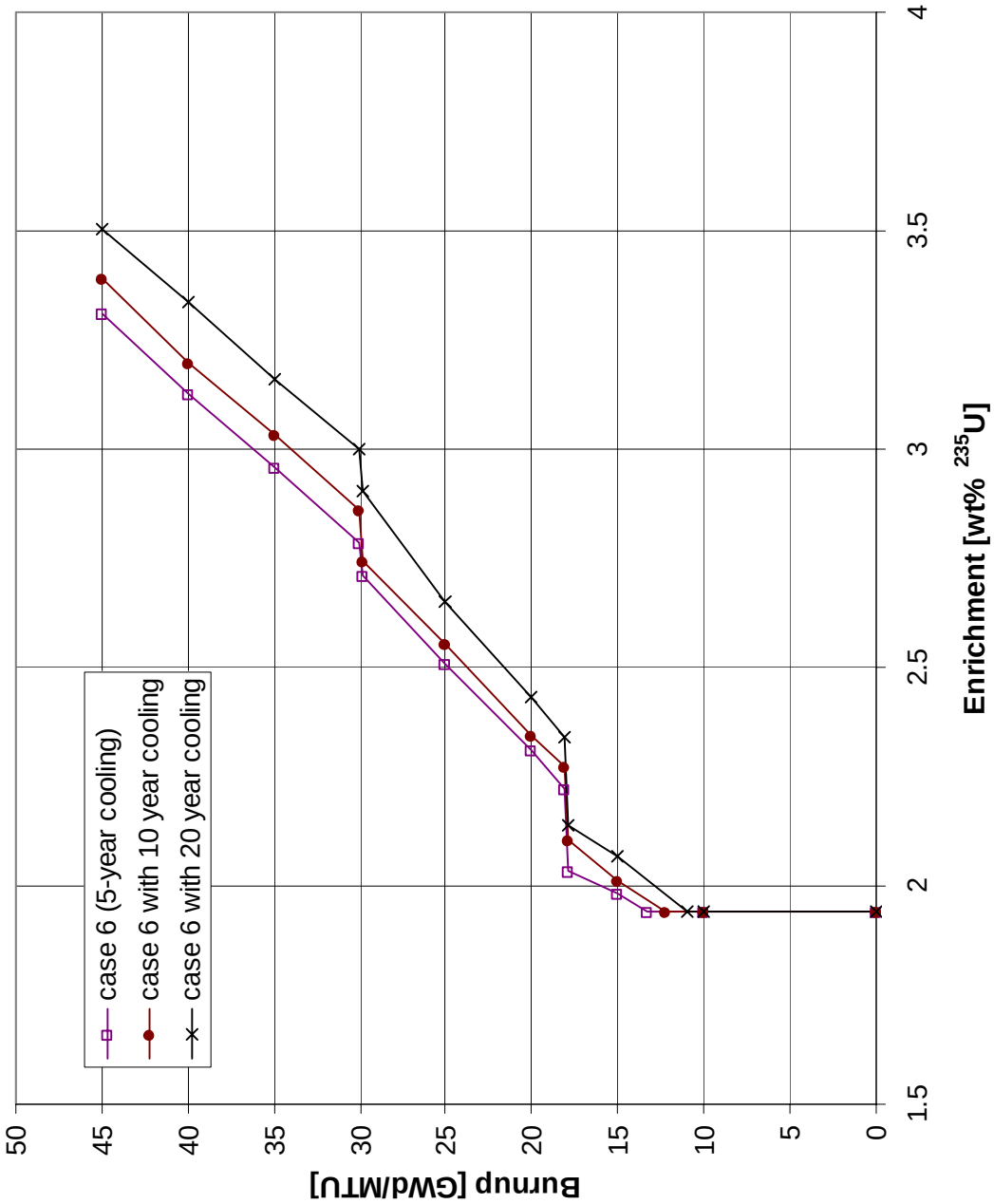

Figure 40 Effect of cooling time on loading curves for actinide-only burnup credit (see Table 10 for specification of case 6)

7 ASSESSMENT OF LOADING CURVES

In this section, the effectiveness of using burnup credit to accommodate SNF in high-capacity storage and transportation casks is assessed by comparing discharge data to loading curves for the GBC-32 cask and determining the number of SNF assemblies that meet the loading criteria. In addition, the impact of variations in the calculational assumptions on the number of SNF assemblies that are qualified for loading in the GBC-32 cask is examined. The discharge data from Ref. 19, which represents SNF assemblies discharged from U.S. PWRs through the end of 1998, are used for this evaluation.

Following the regulatory guidance,[18] separate loading curves were generated for the GBC-32 cask for each of the four assembly designs described in Section 6.6 (i.e., CE 14×14, B&W 15×15, CE 16×16, and WE 17×17). The calculations utilized the bounding depletion parameters listed in Table 4, the burnup-dependent axial and horizontal burnup distributions listed in Tables 6 and 7, respectively, 5-year cooling time, and the Set 1 ICFs listed in Table 8. Since B&W and WE reactors have used BPRs, those cases assumed BPR exposure for the first 20 GWd/MTU of burnup. Hence, the loading curves for the CE assembly designs correspond to case 5 from Table 10, while the loading curves for the B&W and WE assembly designs correspond to case 6 from Table 10. Note that the above calculational assumptions were used to enable reasonable comparisons of loading curves for the GBC-32 cask to SNF discharge data. It is not implied, nor should it be assumed, that the NRC would approve or require the above assumptions in a licensing application.

The loading curves for the four assembly types are provided in Figure 41, and the acceptability of the SNF assemblies for each fuel type is summarized in Table 11. For determining acceptability, assemblies that have enrichment > 4 wt % ^{235}U or require burnup > 40 GWd/MTU are classified as unacceptable. Application of the loading offset, which enables acceptability of assemblies with enrichments up to 5.0 wt % ^{235}U, would not have a significant impact on acceptability due to its associated increased burnup requirements. The results indicate that while burnup credit can enable the loading of a large percentage of the CE assembly types in a high-capacity 32-assembly cask, the effectiveness of burnup credit under the current regulatory guidance is minimal for the B&W and WE assembly designs considered.

To illustrate the effect of selected calculational assumptions in terms of loading acceptability, Figure 42 compares the loading curve for the WE 17×17 assembly (case 6 from Table 10) to loading curves for the following individual variations: (1) extended cooling time (20-years), (2) inclusion of the major fission products and minor actinides with the Set 1 ICFs, (3) inclusion of the major fission products and minor actinides based on best-estimate bounding isotopic validation,[46] and (4) inclusion of the major fission product and minor actinides without any correction for isotopic validation. The last case corresponds to full credit for the calculated actinide and fission product concentrations, and represents a maximum in terms of the negative reactivity. For the cases with fission products included, no explicit consideration of criticality validation with fission products was included. However, the loading curves are all based on an USL of 0.94 (as opposed to the recommended limit[1,18] of 0.95), which inherently allows 1% Δk for criticality calculational bias and uncertainty. The percentage of WE 17×17 assemblies that would be acceptable for each case is also shown in Figure 42. For these cases, the acceptable percentages are based on removal of the regulatory limits[18] on burnup and enrichment (i.e., $\leq$ 4.0 wt % ^{235}U and $\leq$ 40 GWd/MTU, in the absence of the loading offset).

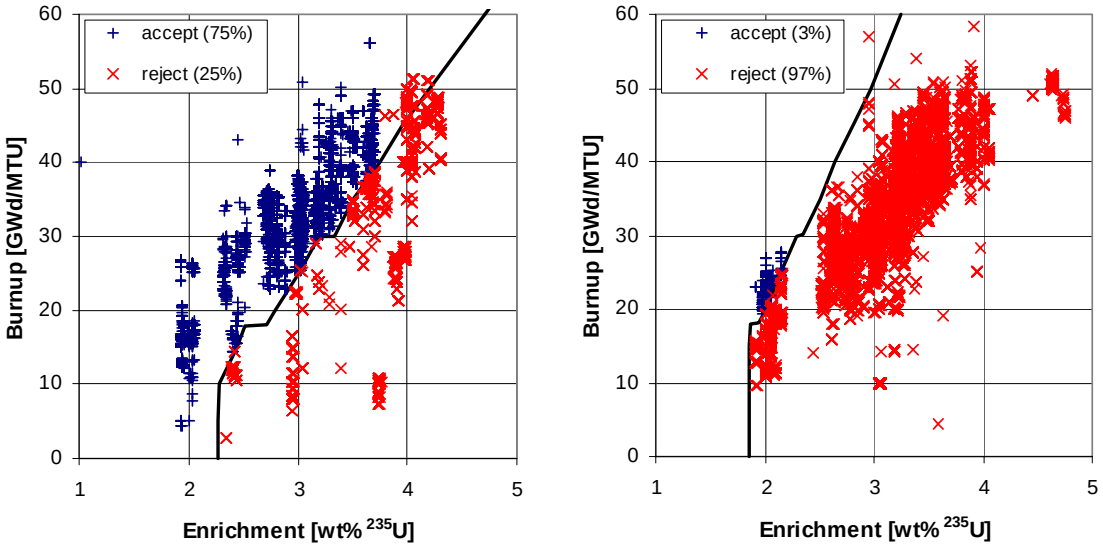

(a) CE 14×14

(b) B&W 15×15

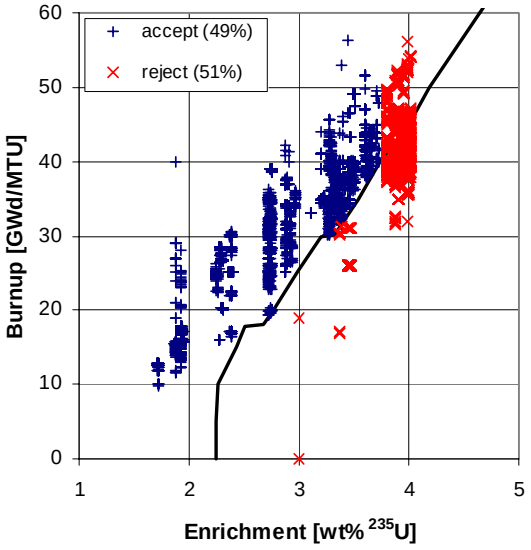

(c) CE 16×16

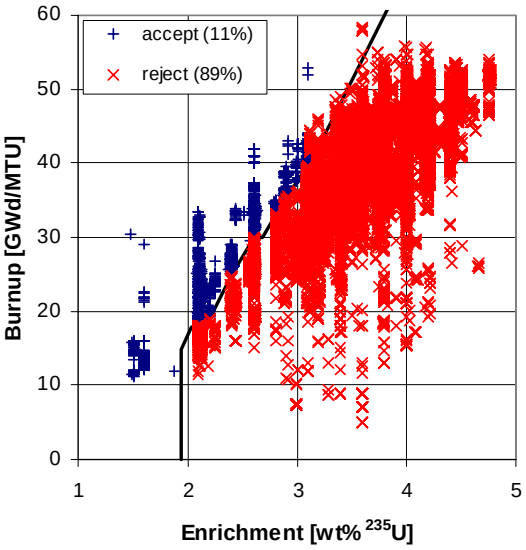

(d) WE 17×17

Figure 41 Comparison of discharged SNF assemblies to actinide-only loading curves for the GBC-32 cask

The major component that would improve the accuracy of burnup credit analyses, with supporting data for validation, is the inclusion of fission products. To illustrate the impact of including fission products, actinide + fission product burnup-credit loading curves for the four assembly types are provided in Figure 43, and the acceptability of the SNF assemblies for each fuel type is summarized in Table 12. As these results are intended to provide an assessment of the potential of expanded burnup credit, the determination of assembly acceptability ignores the current regulatory limitations on burnup and enrichment (40 GWd/MTU and 4 wt % ^{235}U, in the absence of the loading offset). With the exception of the nuclides included in the calculations, the cases shown in Figure 43 are consistent with those shown in Figure 41. Therefore, comparison of Figure 43 and Table 12 to Figure 41 and Table 11, respectively, identifies the increase in the number of SNF assemblies that are acceptable for loading with credit for the minor actinides and major fission products and removal of the current limitations on burnup and enrichment. Note that the actinide + fission product calculations included the Set 1 ICFs listed in Table 8. The results demonstrate the potential significant increase in accomodating SNF with inclusion of the major fission products and removal of the burnup and enrichment limits.

Table 11 Summary of SNF acceptability in the GBC-32 cask with actinide-only burnup credit for the four assembly types considered

Assembly type	Total number in discharge data	Number acceptable for loading	Number unacceptable for loading	Number of assemblies rejected because minimum required burnup > 40 GWd/MTU
CE 14 × 14	5453	4096 (75%)	1357 (25%)	98 (1.8%)
B&W 15 × 15	6439	189 (3%)	6250 (97%)	1 (0.02%)
CE 16 × 16	5809	2830 (49%)	2979 (51%)	796 (13.7%)
WE 17 × 17	21569	2389 (11%)	19180 (89%)	53 (0.3%)
Total	39270	9504 (24%)	29766 (76%)	948 (2.4%)

Table 12 Summary of SNF acceptability in the GBC-32 cask with actinide + fission product burnup credit and neglecting the regulatory limitation of burnup and enrichment (40 GWd/MTU, 4 wt % ^{235}U) for the four assembly types considered

Assembly type	Total number in discharge data	Number acceptable for loading	Number unacceptable for loading
CE 14 × 14	5453	5182 (95%)	271 (5%)
B&W 15 × 15	6439	2110 (33%)	4329 (67%)
CE 16 × 16	5809	5748 (99%)	61 (1%)
WE 17 × 17	21569	12598 (58%)	8971 (42%)
Total	39270	25638 (65%)	13632 (35%)

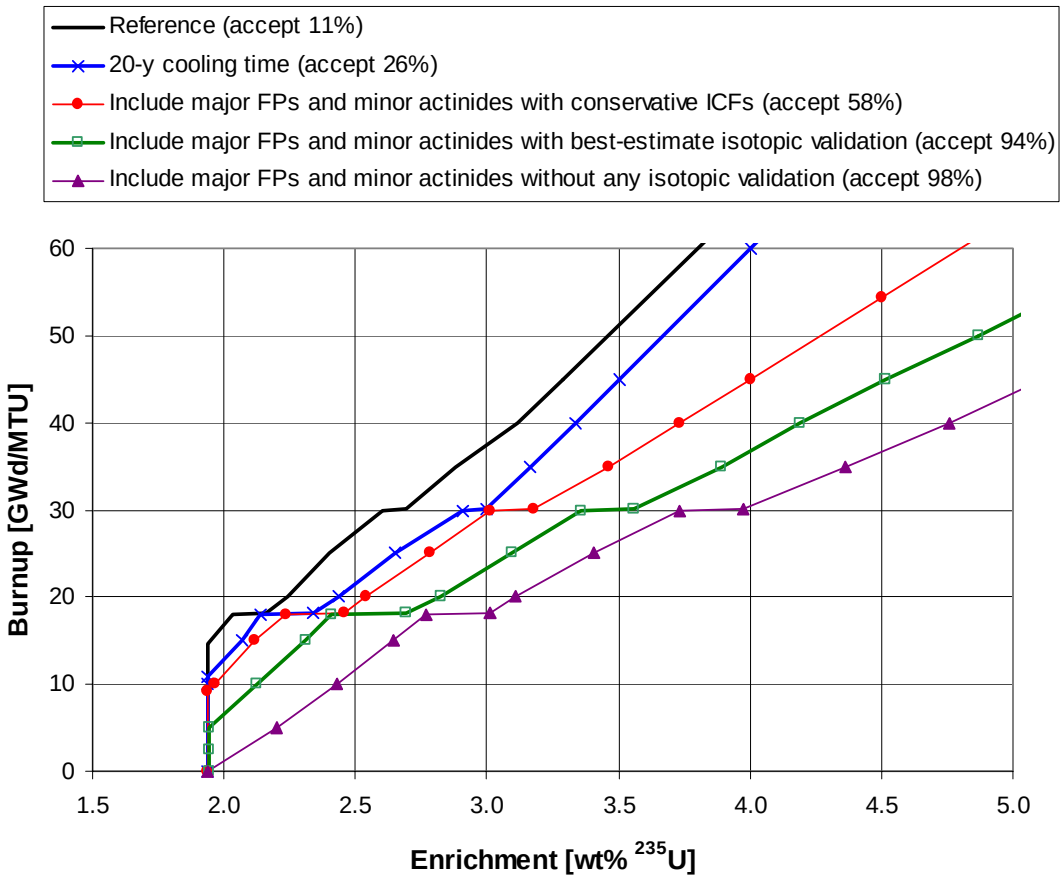

Figure 42 Effect of calculational assumptions on loading curves for the GBC-32 cask and WE 17 × 17 assemblies.

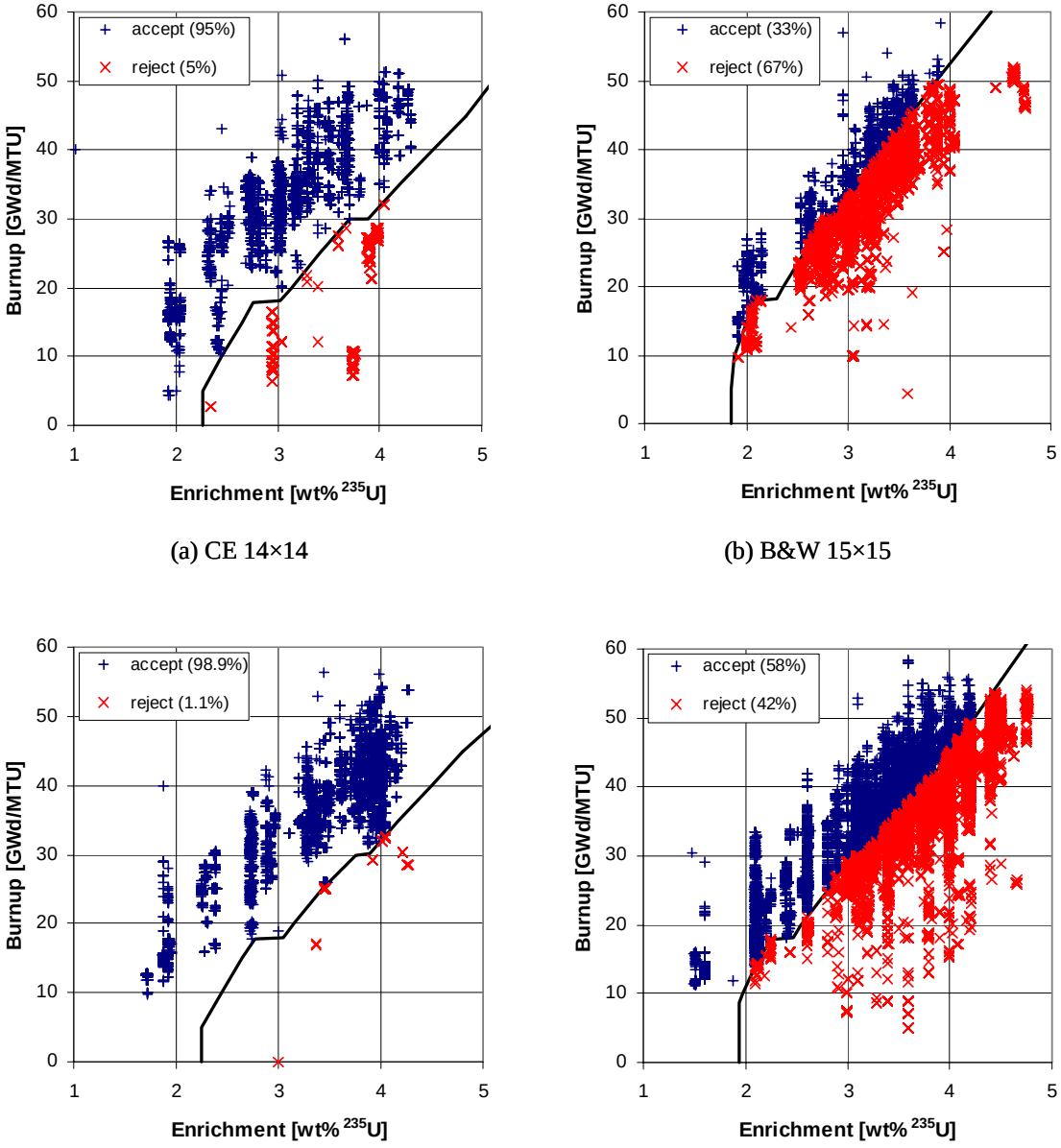

Figure 43 Comparison of discharged SNF assemblies to loading curves for the GBC-32 cask with actinide + fission product burnup credit

Besides improving the accuracy of burnup-credit analyses, cask design and utilization characteristics (e.g., assembly separation, poison loading, and the use of assembly inserts) can be optimized to lower burnup-credit loading curves. To illustrate the impact of design/utilization modifications, loading curves were generated for the GBC-32 cask with selected design (increased poison loading) and utilization (assembly inserts) modifications. The loading curves are provided in Figure 44 and are based on the WE 17×17 assembly and the case 6 modeling assumptions (from Table 10). While the increases in boron loading show notable reductions in the loading curve, the maximum possible boron loading is constrained by physical limitations that are not addressed here. Regarding cask utilization, the insertion of rods into assembly guide tubes, which displaces moderator, can effectively reduce reactivity. Three simplistic cases were considered here to illustrate the effect, including solid rods of aluminum, solid rods of stainless steel (SS), and unirradiated WE WABA BPRs. In all three cases, the rods were inserted into all guide tubes of all assemblies. The outer diameter of the solid rods was chosen consistent with that of the WE burnable poison rod designs (i.e., 0.96774 cm).[30] While the solid aluminum rods had a relatively small impact on the loading curves, the solid SS rods had a large effect – exceeding the negative reactivity effect of the major fission products. As expected, the use of poisoned insert rods (i.e., WABAs) had a very large effect. Although the use of rod inserts was not thoroughly investigated here, this type of approach offers a great deal of flexibility (e.g., the dimension, composition, and number of rods can be varied) to achieve needed reductions in reactivity in an existing cask design.

Assemblies that are not qualified for loading in a given high-capacity cask (i.e., do not meet the minimum burnup requirement for its initial enrichment value) must be stored or transported by other means. These include (1) high-capacity casks with design/utilization modifications (as described above) and (2) lower-capacity (e.g., 24-assembly) casks that utilize flux traps and/or increased fixed poison concentrations. Many lower-capacity casks are currently licensed under the fresh-fuel assumption[1] and are capable of accommodating assemblies with initial enrichments in the mid-to-low 4% range without any credit for fuel burnup. However, credit for fuel burnup can be used to enable loading of higher-enrichment assemblies (up to 5 wt % ^{235}U). To investigate the effectiveness of burnup credit for this purpose, loading curves were generated for an established 24-assembly cask design[48] with each of the four assembly designs described in Section 6.6. These loading curves are based on the case 6 modeling assumptions (from Table 10) and are illustrated in Figure 45 (note that these are the only loading curves in this report that do not correspond to the GBC-32 cask). Because the current regulatory guidance recommends a loading offset for enrichments above 4 wt % ^{235}U (see Section 6.4 for details), loading curves are shown in Figure 45 with and without the loading offset. A comparison of the loading curves in Figure 45 and the corresponding SNF discharge data shown in Figure 43 reveals that, even with the loading offset, this 24-assembly cask is capable of accepting 100% of the discharged fuel for the four assembly designs considered. Hence, the results indicate that, under the current regulatory guidance, burnup credit can enable the loading of all or very nearly all assemblies with initial enrichments up to 5 wt % ^{235}U in 24-assembly casks.

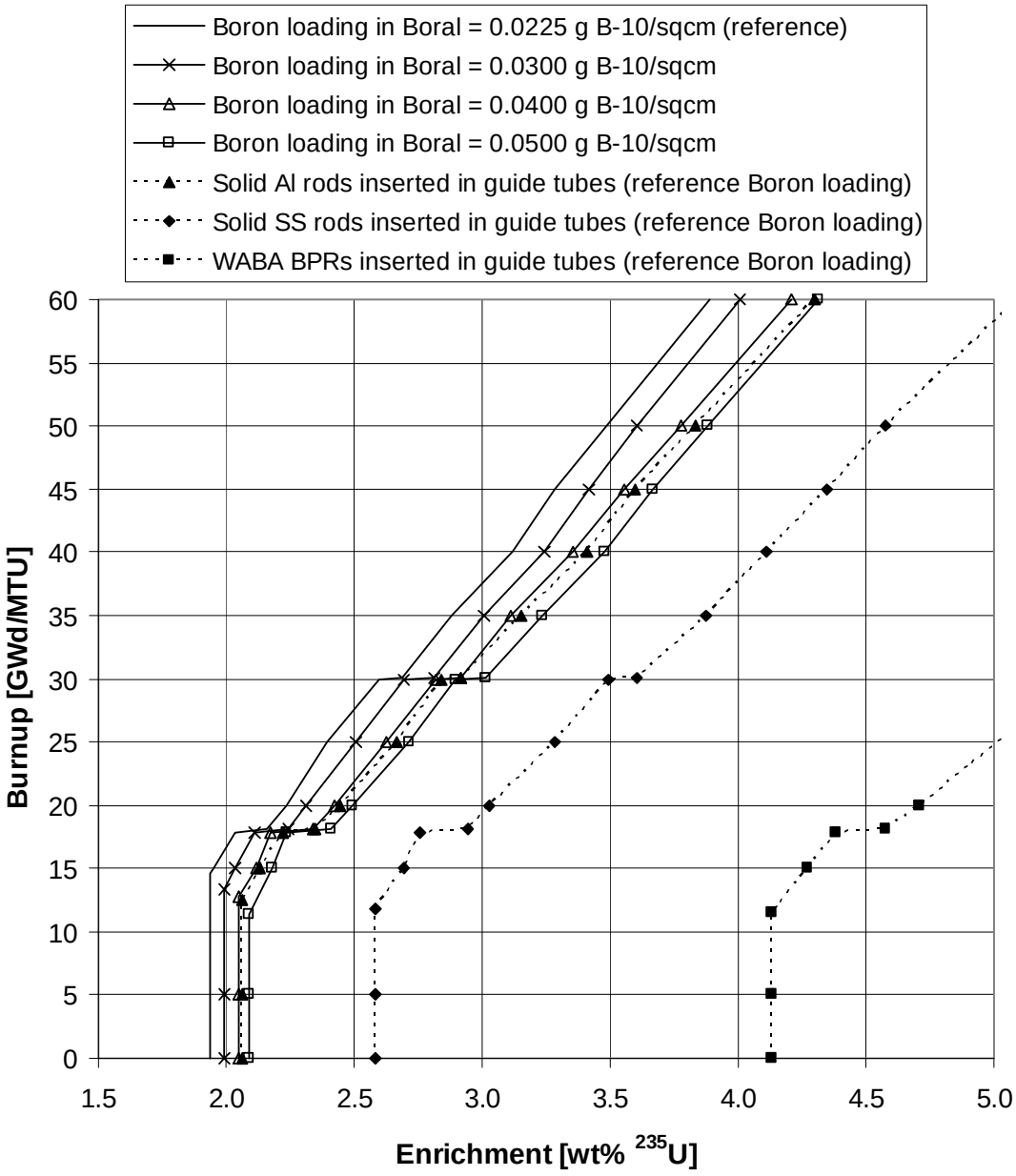

Figure 44 Effect of design and utilization modifications on loading curves for the GBC-32 cask

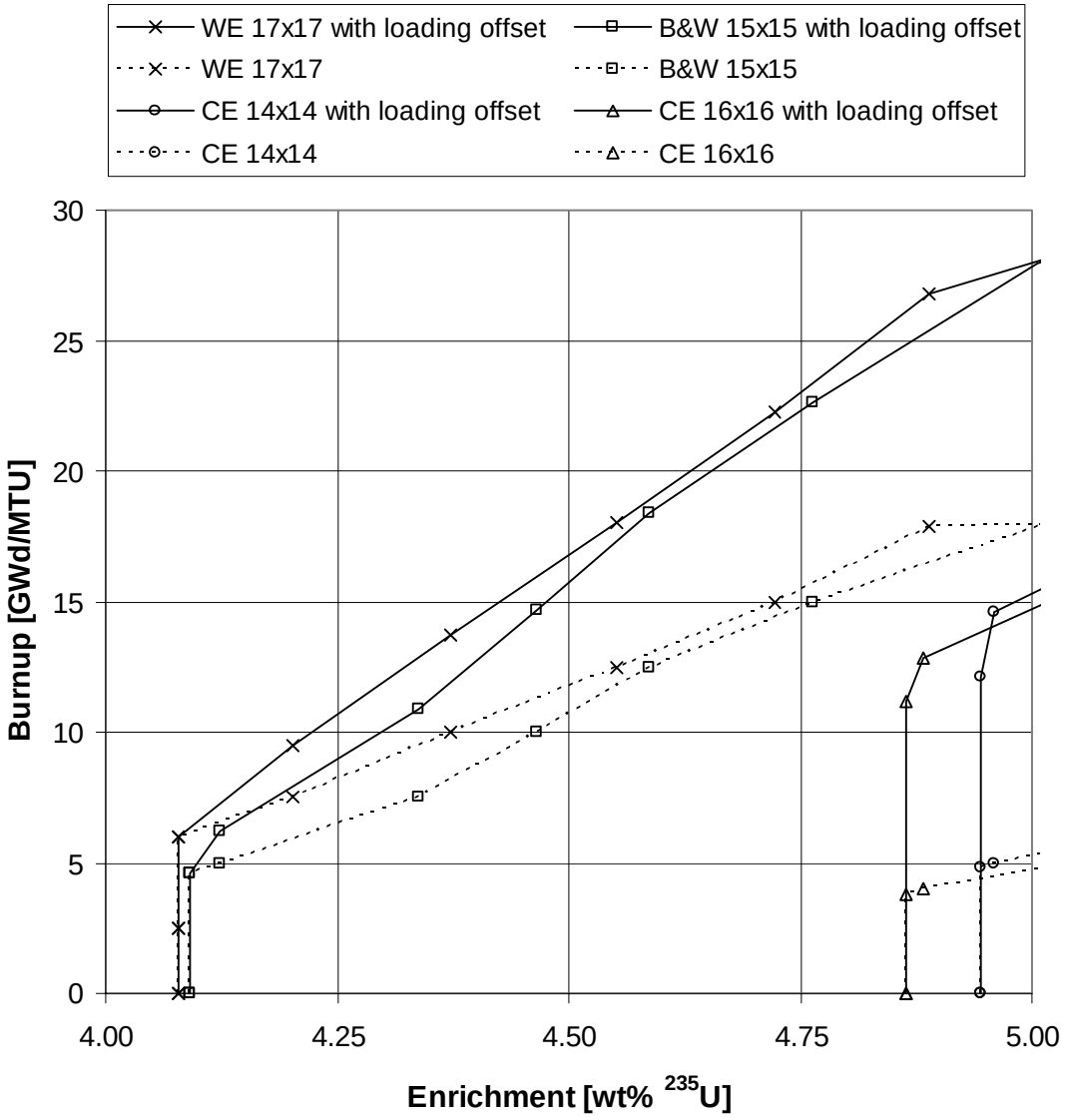

Figure 45 Burnup credit loading curves for a 24-assembly cask with and without the loading offset

8 CONCLUSIONS

Parametric studies were presented in this report to quantify the effect of variations in the calculational assumptions (depletion and criticality) required for a PWR burnup-credit criticality safety analysis. The purpose of these studies was to provide a better understanding of the importance of input parameter variations on k_{eff} values and loading curves for a prototypic high-capacity cask. This information may assist NRC staff reviewers in their evaluation of calculational assumptions used in burnup-credit applications and provide guidance with respect to technical areas where improved information will most improve the accuracy of subcritical margin estimates. Because the impact of variations in the calculational assumptions are dependent on the characteristics of the model used for the determination (e.g., nuclides include, burnup, enrichment, etc.), it is difficult and problematic to quantify Δk values that are generally applicable. With this note of caution, Table 13 summarizes Δk values associated with specific variations in the modeling parameters and characteristics considered in this study for a specific initial enrichment and burnup combination.

Comparison of actinide-only based loading curves for the GBC-32 cask to PWR SNF discharge data (through the end of 1998) leads to the conclusion that additional negative reactivity (through either increased credit for fuel burnup or cask design/utilization modifications) is necessary to accommodate the majority of SNF assemblies in high-capacity casks. However, it was shown that even minor reductions in the minimum required burnup, for a given enrichment, significantly increase the number of assemblies that may be accommodated. In other words, reductions in analysis uncertainties that enable more accurate estimates of subcritical margins will lower the burnup-enrichment loading curve, and thus expand the usefulness of burnup credit. Because the CE assemblies are considerably less reactive than the WE and B&W assemblies considered herein, loading curves for the CE assemblies are notably lower than those for WE and B&W assemblies.

Assemblies that are not qualified for loading in a given high-capacity cask (i.e., do not meet the minimum burnup requirement for its initial enrichment value) must be stored or transported by other means. These include (1) high-capacity casks with design/utilization modifications and (2) lower-capacity (e.g., 24-assembly) casks that utilize flux traps and/or increased fixed poison concentrations. Loading curves developed for actinide-only burnup credit with an established 24-assembly cask design[48] are such that all or very nearly all assemblies with initial enrichments up to 5 wt % ^{235}U are acceptable. Finally, loading curves developed for the GBC-32 cask with selected design (increased poison loading) and utilization (assembly inserts) modifications illustrate alternative means for increasing the number of assemblies acceptable for loading in high-capacity cask designs.

Future work should focus on investigating approaches for increasing the allowed inventory of SNF that can be loaded in high-capacity cask designs by increasing the accuracy of burnup-credit analyses. For example, alternative approaches for validation of the isotopic compositions should be considered. The most significant component that would provide a better estimate of k_{eff} is the accurate inclusion of fission products. Consequently, an effective approach for validation of fission products is a key element necessary for the expansion of burnup credit.

Finally, it should be noted that the results described in this report are useful for predicting trends in SNF behavior based on variations in input parameters and for assessing the relative importance of different calculational assumptions. However, caution should be taken in using specific numbers (e.g., reactivity margins), especially if calculations are performed using other computer codes, cross-section data, or cask designs.

Table 13 Summary table of Δ*k* values due to variations in calculational assumptions for a typical discharge burnup and enrichment combination (40 GWd/MTU; 4.0 wt % ^{235}U) in the GBC-32 cask

Modeling parameter/ characteristic	Assumptions used for comparison†		Δ*k* values*	
	Base assumption	Bounding assumption	Actinide-only	Actinide + fission products
Fuel temperature during depletion	850 K	1100 K	0.0045	0.0031
Moderator temperature during depletion	595 K	610 K	0.0083	0.0088
Soluble boron concentration during depletion	600 ppm	1000 ppm	0.0042	0.0038
Specific power during depletion	40 MW/MTU	60 MW/MTU	< the statistical uncertainty	0.0008
Total of all depletion parameters listed above	All values listed above	All values listed above	0.0185‡	0.0154
BPRs during depletion	None	Inserted for first 20 GWd/MTU of burnup	0.0080	0.0062
CRs during depletion	None	Fully-inserted for first 5 GWd/MTU of burnup	0.0062	0.0070
Axial-burnup variation	Uniform	Reference profile from Table 1	0.0111	0.0337
Horizontal-burnup variation	Uniform	20% gradient	0.0023	0.0021
ICFs	None	Set 1 ICFs from Table 8	0.0325	0.0482

† Except where noted otherwise, all cases correspond to 5-year cooling and include the axial-burnup distribution specified in Table 1.

* Δ*k* value equals k_{eff} value based on assumption listed in column 3 minus k_{eff} value based on assumption listed in column 2. All statistical uncertainties in the Δ*k* values are less than or equal to 0.0008.

‡ This value is not the sum of the above values, but rather the difference between two calculations that used the values indicated in columns 2 and 3.

9 REFERENCES

1. *Standard Review Plan for Dry Cask Storage Systems*, NUREG-1536, U.S. NRC, Washington D.C., January 1997.

2. T. L. Sanders, R. M. Westfall, and R. H. Jones, *Feasibility and Incentives for the Consideration of Spent Fuel Operating Histories in the Criticality Analysis of Spent Fuel Shipping Casks*, SAND87-0151, TTC-0713, UC-71, Sandia National Laboratory, August 1987.

3. T. L. Sanders, editor, "Proceedings of a Workshop on the Use of Burnup Credit in Spent Fuel Transport Casks," Washington D.C., February 21–22, 1988, SAND89-0018, TTC-0884, UC-820, Sandia National Laboratory (October 1989).

4. T. L. Sanders and R. M. Westfall, "Feasibility and Incentives for Burnup Credit in Spent Fuel Transport Casks," *Nucl. Sci. Eng.* **104**, 66–77 (1990).

5. C. V. Parks, M. D. DeHart and J. C. Wagner, *Review and Prioritization of Technical Issues Related to Burnup Credit for LWR Fuel*, NUREG/CR-6665 (ORNL/TM-1999/303), U.S. Nuclear Regulatory Commission, Oak Ridge National Laboratory, February 2000.

6. "Topical Report on Actinide-Only Burnup Credit for PWR Spent Nuclear Fuel Packages," DOE/RW-0472, Rev. 2, U.S. Department of Energy (September 1998).

7. B. H. Wakeman and S. A. Ahmed, *Evaluation of Burnup Credit for Dry Storage Casks*, EPRI NP-6494, Electric Power Research Institute (August 1989).

8. M. D. DeHart, *Sensitivity and Parametric Evaluations of Significant Aspects of Burnup Credit for PWR Spent Fuel Packages*, ORNL/TM-12973, Lockheed Martin Energy Research Corp., Oak Ridge National Laboratory, May 1996.

9. M. D. DeHart, *Parametric Analysis of PWR Spent Fuel Depletion Parameters for Long-Term Disposal Criticality Safety*, ORNL/TM-1999/99, Lockheed Martin Energy Research Corp., Oak Ridge National Laboratory, August 1999.

10. C. H. Kang and D. B. Lancaster, *Depletion and Package Modeling Assumptions for Actinide-Only Burnup Credit*, DOE/RW-0495, U.S. Department of Energy (1997).

11. M. Takano, *OECD/NEA Burnup Credit Criticality Benchmark — Result of Phase-1A*, JAERI-M 94-003 (NEA/NSC/DOC(93)22, Japan Atomic Energy Research Institute, 1994.

12. M. D. DeHart, M. C. Brady, and C. V. Parks, *OECD/NEA Burnup Credit Calculational Criticality Benchmark Phase I-B Results*, ORNL-6901 (NEA/NSC/DOC(96)-06), Lockheed Martin Energy Research Corp., Oak Ridge National Laboratory, June 1996.

13. M. Takano and H. Okuno, *OECD/NEA Burnup Credit Criticality Benchmark - Result of Phase IIA*, JAERI-Research-96-003 (NEA/NSC/DOC(61)01), Japan Atomic Energy Research Institute, 1996.

14. A. Nouri, *OECD/NEA Burnup Credit Criticality Benchmark — Analysis of Phase II-B Results: Conceptual PWR Spent Fuel Transportation Cask*, IPSN/98-05 (NEA/NSC/DOC(98)1), Institut de Protection et de Surete Nucleaire, May 1998.

15. P. M O'Leary and J. M. Scaglione, "An Empirical Approach to Bounding the Axial Reactivity Effects of PWR Spent Nuclear Fuel," *Trans. Am. Nucl. Soc.*, **84,** 352–353 (June 2001).

16. "Interim Staff Guidance – 8, Rev. 1 – Limited Burnup Credit," U.S. Nuclear Regulatory Commission, Spent Fuel Project Office, July 1999.

17. D. E. Carlson, C. J. Withee and C. V. Parks, "Spent Fuel Burnup Credit in Casks: An NRC Perspective," NUREG/CP-0169, pp. 419–436 in *Proc. of U.S. Nuclear Regulatory Commission Twenty-Seventh Water Reactor Safety Information Meeting*, October 25–27, 1999, Bethesda, MD (March 2000).

18. *Standard Review Plan for Transportation Packages for Spent Nuclear Fuel – Final Report*, NUREG-1617, U.S. Nuclear Regulatory Commission, Washington, D.C., March 2000.

19. RW-859 Nuclear Fuel Data, Energy Information Administration, December 2000.

20. I. C. Gauld and S. M. Bowman, *STARBUCS: A Prototypic SCALE Control Module for Automated Criticality Safety Analyses Using Burnup Credit*, NUREG/CR-6748 (ORNL/TM-2001/33), U.S. Nuclear Regulatory Commission, Oak Ridge National Laboratory, October 2001.

21. *SCALE: A Modular Code System for Performing Standardized Computer Analyses for Licensing Evaluation*, NUREG/CR-0200, Rev. 6 (ORNL/NUREG/CSD-2/R6), Vols. I, II, and III, May 2000. Available from Radiation Safety Information Computational Center at Oak Ridge National Laboratory as CCC-545.

22. I. C. Gauld and C. E. Sanders, "Development and Applications of a Prototypic SCALE Control Module for Automated Burnup Credit Analysis," 35238.pdf in *Proc. 2001 ANS Embedded Topical Meeting on Practical Implementation of Nuclear Criticality Safety*, November 11–15, 2001, Reno, NV [ANS Order No.: 700284; ISBN: 0-89448-659-4].

23. O. W. Hermann and C. V. Parks, "SAS2H: A Coupled One-Dimensional Depletion and Shielding Analysis Module," Vol. I, Sect. S2 of *SCALE: A Modular Code System for Performing Standardized Computer Analyses for Licensing Evaluation*, NUREG/CR-0200, Rev. 6 (ORNL/NUREG/CSD-2/R6), Vols. I, II, and III, May 2000. Available from Radiation Safety Information Computational Center at Oak Ridge National Laboratory as CCC-545.

24. L. C. Leal, O. W. Hermann, S. M. Bowman, and C. V. Parks, "Automatic Rapid Process for the Generation of Problem-Dependent SAS2H/ORIGEN-S Cross-Section Libraries," *Nucl. Technol.* **127(1)**, 1–23, July 1999.

25. S. M. Bowman and L. C. Leal, "ORIGEN-ARP: Automatic Rapid Process for Spent Fuel Depletion, Decay, and Source Term Analysis," Vol. I, Sect. D1 of *SCALE: A Modular Code System for Performing Standardized Computer Analyses for Licensing Evaluation*, NUREG/CR-0200, Rev. 6 (ORNL/NUREG/CSD-2/R6), Vols. I, II, and III, May 2000. Available from

Radiation Safety Information Computational Center at Oak Ridge National Laboratory as CCC-545.

26. L. M. Petrie and N. F. Landers, "KENO V.a: An Improved Monte Carlo Criticality Program With Supergrouping," Vol. II, Sect. F11 of *SCALE: A Modular Code System for Performing Standardized Computer Analyses for Licensing Evaluation*, NUREG/CR-0200, Rev. 6 (ORNL/NUREG/CSD-2/R6), Vols. I, II, and III, May 2000. Available from Radiation Safety Information Computational Center at Oak Ridge National Laboratory as CCC-545.

27. J. C. Wagner, *Computational Benchmark for Estimation of Reactivity Margin from Fission Products and Minor Actinides in PWR Burnup Credit*, NUREG/CR-6747 (ORNL/TM-2000/306), U.S. Nuclear Regulatory Commission, Oak Ridge National Laboratory, October 2001.

28. C. V. Parks, I. C. Gauld, J. C. Wagner, B. L. Broadhead, M. D. DeHart, and D. D. Ebert, "Research Supporting Implementation of Burnup Credit in the Criticality Safety Assessment of Transport and Storage Casks," NUREG/CP-0172, pp. 139–161 in *Proc. of U.S. Nuclear Regulatory Commission Twenty-Eighth Water Reactor Safety Information Meeting*, October 23-25, 2000, Bethesda, MD (May 2001).

29. *Disposal Criticality Analysis Methodology Topical Report*, YMP/TR-004Q, Rev. 1, DOE OCRWM (2000).

30. J. C. Wagner and C. V. Parks, *Parametric Study of the Effect of Burnable Poison Rods for PWR Burnup Credit*, NUREG/CR-6761 (ORNL/TM-2000/373), U.S. Nuclear Regulatory Commission, Oak Ridge National Laboratory, March 2002.

31. M. Maillot, E. Guillou, D. Biron, and S. Janski, "Search for an Envelope Axial Burnup Profile for Use in PWR Criticality Studies with Burnup Credit," in *Proc. ICNC'99, Sixth International Conference on Nuclear Criticality Safety*, September 20–24, 1999, Palais des Congres, Versailles, France.

32. *CRWMS M&O 1998 Summary Report of Commercial Reactor Criticality Data for Crystal River Unit 3*, B00000000-01717-5705-00060 Rev. 01, Las Vegas, NV: CRWMS M&O. MOL.19980728.0189.

33. M. D. DeHart, *SCALE-4 Analysis of Pressurized Water Reactor Critical Configurations: Volume 4 – Three Mile Island Unit 1 Cycle 5*, ORNL/TM-12294/V4, Martin Marietta Energy Systems, Inc., Oak Ridge National Laboratory, March 1995.

34. R. J. Cacciapouti and S. Van Volkinburg, "Axial Burnup Profile Database for Pressurized Water Reactors," YAEC-1937, Yankee Atomic Electric Company (May 1997). Available from Radiation Safety Information Computational Center at Oak Ridge National Laboratory as DLC-201.

35. J. C. Wagner, "Addressing the Axial Burnup Distribution in PWR Burnup Credit Criticality Safety," 35218.pdf in *Proc. 2001 ANS Embedded Topical Meeting on Practical Implementation of Nuclear Criticality Safety*, November 11–15, 2001, Reno, NV [ANS Order No.: 700284; ISBN: 0-89448-659-4].

36. C. E. Sanders and J. C. Wagner, *Parametric Study of the Effect of Control Rods for PWR Burnup Credit*, NUREG/CR-6759 (ORNL/TM-2001/69), U.S. Nuclear Regulatory Commission, Oak Ridge National Laboratory, February 2002.

37. J. C. Wagner and M. D. DeHart, *Review of Axial Burnup Distribution Considerations for Burnup Credit Calculations*, ORNL/TM-1999/246, Lockheed Martin Energy Research Corp., Oak Ridge National Laboratory, March 2000.

38. T. A. Parish and C. H. Chen, *Bounding Axial Profile Analysis for the Topical Report Database*, Nuclear Engineering Dept, Texas A&M University, May 1997.

39. C. H. Kang and D. B. Lancaster, "Actinide-Only Burnup Credit for Pressurized Water Reactor Spent Nuclear Fuel — III: Bounding Treatment of Spatial Burnup Distributions," *Nucl. Technol.* **125**, 292 (1999).

40. J. C. Wagner and C. V. Parks, *Recommendations on the Credit for Cooling Time in PWR Burnup Credit Analyses*, NUREG/CR-6781 (ORNL/TM-2001/272), U.S. Nuclear Regulatory Commission, Oak Ridge National Laboratory, January 2003.

41. *Horizontal Burnup Gradient Datafile for PWR Assemblies*, DOE/RW-0496, U.S. Department of Energy, Office of Civilian Radioactive Waste Management, May 1997.

42. M. Rahimi, E. Fuentes, D. Lancaster, *Isotopic and Criticality Validation for PWR Actinide-Only Burnup Credit*, DOE/RW-0497, U.S. Department of Energy, May 1997.

43. D. B. Lancaster, E. Fuentes, C. H. Kang and M. Rahimi, "Actinide-Only Burnup Credit for Pressurized Water Reactor Spent Nuclear Fuel — I: Methodology Overview," *Nucl. Technol.* **125**, 255 (1999).

44. J. M. Scaglione, "Spent Fuel Criticality Benchmark Experiments," in *Proc. 2001 ANS Embedded Topical Meeting on Practical Implementation of Nuclear Criticality Safety*, November 11–15, 2001, Reno, NV.

45. M. D. DeHart, *A Stochastic Method for Estimating the Effect of Isotopic Uncertainties in Spent Nuclear Fuel*, ORNL/TM-2001/83, UT-Battelle, LLC, Oak Ridge National Laboratory, September 2001.

46. I. C. Gauld, *Strategies for Application of Isotopic Uncertainties in Burnup Credit*, NUREG/CR-6811 (ORNL/TM-2001/257), U.S. Nuclear Regulatory Commission, Oak Ridge National Laboratory, 2003.

47. M. D. DeHart and O. W. Hermann, *An Extension of the Validation of SCALE (SAS2H) Isotopic Predictions for PWR Spent Fuel*, ORNL/TM-13317, Lockheed Martin Energy Research Corp., Oak Ridge National Laboratory, September 1996.

48. Safety Analysis Report for the HI-STAR 100 System, Holtec International report HI-951251, NRC Docket 71-9261, 1998.

INTERNAL DISTRIBUTION

1. S. M. Bowman, 6011, MS-6370
2. B. L. Broadhead, 6011, MS-6370
3. W. C. Carter, 6011, MS-6370
4. M. D. DeHart, 6011, MS-6370
5. M. E. Dunn, 6011, MS-6370
6. K. R. Elam, 6011, MS-6370
7. R. J. Ellis, 6025, MS-6363
8. I. C. Gauld, 6011, MS-6370
9. J. C. Gehin, 6025, MS-6363
10. S. Goluoglu, 6011, MS-6370
11. J. N. Herndon, 4500N, MS-6228
12. D. J. Hill, 4500N, MS-6228
13. D. F. Hollenbach, 6011, MS-6370
14. B. L. Kirk, 6025, MS-6362
15. S. B. Ludwig, NTRC, MS-6472
16. G. E. Michaels, 4500N, MS-6210
17. C. V. Parks, 6011, MS-6370
18. L. M. Petrie, 6011, MS-6370
19. R. T. Primm, III, 7917, MS-6399
20. B. T. Rearden, 6011, MS-6370
21. J. J. Simpson, 4500N, MS-6210
22. J. C. Wagner, 6011, MS-6370
23. R. M. Westfall, 6011, MS-6370
24. Laboratory Records-RC
    4500N, MS-6285
25. Central Research Library
    4500N, MS-6191

26–50. Return extra ORNL copies to:
W. C. Carter, 6011, MS-6370

EXTERNAL DISTRIBUTION

51. M. L. Anderson, Bechtel SAIC Company, LLC, 1261 Town Center Drive, Las Vegas, NV 89134
52. S. Anton, Holtec International, 555 Lincoln Drive West, Marlton, NJ 08053
53. A. C. Attard, U.S. Nuclear Regulatory Commission, NRR/DSSA/SRXB, MS O10-B1, Washington, DC 20555-0001
54. M. G. Bailey, U.S. Nuclear Regulatory Commission, NMSS, MS T8-F5, Washington, DC 20555-0001
55. A. B. Barto, U.S. Nuclear Regulatory Commission, NMSS/SFPO/TRA, MS O13-D13, Washington, DC 20555-0001
56. C. J. Benson, Bettis Atomic Power Laboratory, PO Box 79, West Mifflin, PA 15122
57. G. H. Bidinger, NUMEC, 17016 Cashell Road, Rockville, MD 20853
58. J. Boshoven, Transnuclear West, Inc., 39300 Civic Center Drive, Suite 280, Fremont, CA 94538
59. M. C. Brady Raap, Battelle, Pacific Northwest National Laboratory, PO Box 999 / MS K8-34, Richland, WA 99352
60. R. J. Cacciapouti, Duke Engineering and Services, 400 Donald Lynch Boulevard, Marlborough, MA 01752
61. D. E. Carlson, U.S. Nuclear Regulatory Commission, RES/DSARE/REAHFB, MS T10-F13A, Washington, DC 20555-0001
62. J. M. Conde López, Consejo de Seguridad Nuclear, Jefe de Area de Ingeniería Nuclear, Subdirección General de Technologia Nuclear, Justo Dorado, 11, 28040 Madrid, SPAIN

63. D. R. Conners, Bettis Atomic Power Laboratory, PO Box 79, West Mifflin, PA 15122
64. P. Cousinou, Institut de Protection et de Sûreté Nucleaire, Départment de Recherches en Sécurité, CECI B.P. 6 - 92265 Fontenzy-Aux-Roses, Cedex, FRANCE
65. T. W. Doering, Bechtel SAIC Company, LLC, 1261 Town Center Drive, Las Vegas, NV 89134
66. E. P. Easton, U.S. Nuclear Regulatory Commission, NMSS/SFPO/TRD, MS O13-D13, Washington, DC 20555-0001
67. F. Eltawila, U.S. Nuclear Regulatory Commission, RES/DSARE, MS T10-E32, Washington, DC 20555-0001
68. K. T. Erwin, U.S. Nuclear Regulatory Commission, NMSS/SFPO/TRB, MS O13-D14, Washington, DC 20555-0001
69. A. S. Giantelli, U.S. Nuclear Regulatory Commission, NMSS/SFPO/TRA, MS O13-D13, Washington, DC 20555-0001
70. R. N. B. Gmal, Gesellschaft für Anlagen-und Reaktorsicherheit (GRS) mbH, Leiter der Gruppe Kritikalität, Forschungsgelände, 85748 Garching b. München
71. P. Grimm, Paul Scherrer Institute, CH-5232 Villigen Psi, SWITZERLAND
72. J. N. Gulliford, BNFL, R101, Rutherford House, Risley, Warrington, Cheshire WA3 6AS
73. J. Guttmann, U.S. Nuclear Regulatory Commission, NMSS/SFPO/TRD, MS O13-D13, Washington, DC 20555-0001
74. L. A. Hassler, Framatome ANP, 3315 Old Forest Road, PO Box 10935, Lynchburg, VA 24506-0935
75. D. Henderson, Framatome ANP, 3315 Old Forest Road, PO Box 10935, Lynchburg, VA 24506-0935
76. M. W. Hodges, U.S. Nuclear Regulatory Commission, NMSS/SFPO/TRD, MS O13-D13, Washington, DC 20555-0001
77. Hae Ryong Hwang, Radiation Safety Analysis Group, KOPEC, 150, Duckjin Dong, Taejon, SOUTH KOREA 305-600
78. H. Kühl, Wissenschaftlich-Technische Ingenieurberatung GMBH, Karl-Heinz-Beckurts-Strasse 8, 52428 Jülich
79. W. H. Lake, Office of Civilian Radioactive Waste Management, U.S. Department of Energy, RW-46, Washington, DC 20585
80. D. B. Lancaster, Nuclear Consultants.com, 320 South Corl Street, State College, PA 16801
81. C. Lavarenne, Institut de Protection et de Sûreté Nucléaire, Department of Prevention and Studies of Accidents, Criticality Studies Division, CEA - 60-68, avenue de Général Leclerc, B.P. 6 - 92265, Fontenay - Aux - Roses, Cedex, FRANCE

82–86. R. Y. Lee, U.S. Nuclear Regulatory Commission, RES/DSARE/SMSAB, MS T10-K8, Washington, DC 20555-0001

87. Willington J. Lee, NAC International, 655 Engineering Drive, Norcross, GA 30092
88. M. Mason, Transnuclear, Two Skyline Drive, Hawthorne, NY 10532-2120
89. A. J. Machiels, Electric Power Research Institute, Advanced Nuclear Technology, Energy Convervation Division, 3412 Hillview Ave., Palo Alto, CA 94304-1395
90. L. Markova, Ustav jaderneho vyzkumu Rez, Theoretical Reactor Physics, Nuclear Research Institute, Czech Republic, 25068 REZ
91. Daniel Marloye, Belgonucléaire, Av. Ariane 4, B-1200, Brussels, BELGIUM
92. C. W. Mays, Framatome ANP, 3315 Old Forest Road, PO Box 10935, Lynchburg, VA 24506-0935
93. J. N. McKamy, U.S. Department of Energy, Office of Engineering Assistance and Site Interface, EH-34, 19901 Germantown Rd., Germantown, MD 20874
94. N. B. McLeod, JAI Corporation, 4103 Chain Bridge Road, Suite 200, Fairfax, VA 22030

95. D. Mennerdahl, E. Mennerdahl Systems, Starvägen 12, S-183 57 Täby, SWEDEN
96. Dr. Raymond L. Murray, 8701 Murray Hill Drive, Raleigh, NC 27615
97. K. A. Neimer, Duke Engineering & Services, 400 S. Tyron St., WC26B, PO Box 1004, Charlotte, NC 28201-1004
98. P. Noel, Bechtel SAIC Company, LLC, 1261 Town Center Drive, Las Vegas, NV 89134
99. I. Nojiri, Japan Nuclear Cycle Development Institute, Environment and Safety Division, Tokai Works, Muramatsu Tokai-mura, Naka-gun Ibaraki-ken 319-1194, JAPAN
100. J. C. Neuber, SIEMENS AG, KWU NS-B, Berliner Str. 295-303, D-63067 OFFENBACH AM MAIN, GERMANY
101. A. Nouri, OECD/NEA Data Bank, Le Seine-Saint Germain, 12 Boulevard des Iles, F-92130 Issy-les-Moulineaux, FRANCE
102. Office of the Assistant Manager for Energy Research and Development, Department of Energy Oak Ridge Operations (DOE-ORO), PO Box 2008, Oak Ridge, TN 37831
103. H. Okuno, Japan Atomic Energy Research Institute, Department of Fuel Cycle, Safety Research, 2-4 Shirakata-Shirane, 319-1195 Tokai-mura, Naka-Gun, Ibaraki-ken, JAPAN
104. N. L. Osgood, U.S. Nuclear Regulatory Commission, NMSS/SFPO/SLID, MS O13-D13, Washington, DC 20555-0001
105. V. A. Perin, U.S. Nuclear Regulatory Commission, NMSS/FCSS/SPB, MS T8-A33, Washington, DC 20555-0001
106. B. Petrovic, Westinghouse Electric Company, Science and Technology Department, 1344 Beulah Road, Pittsburgh, PA 15235
107. J. S. Philbin, Sandia National Laboratory, PO Box 5800, Mail Stop 1143, Albuquerque, NM 87185-1143
108. M. Rahimi, U.S. Nuclear Regulatory Commission, NMSS/DWM/HLWB, MS T7-F3, Washington, DC 20555-0001
109. E. L. Redmond II, Holtec International, 555 Lincoln Drive West, Marlton, NJ 08053
110. I. Reiche, Bundesamt fuer Strahlenschutz, Willi Brandt Str. 5, D-38226 SALZGITTER, GERMANY
111. C. Rombough, CTR Technical Services, Inc., 5619 Misty Crest Dr., Arlington, TX 76017-4147
112. J. E. Rosenthal, U.S. Nuclear Regulatory Commission, RES/DSARE/SMSAB, MS T10-K8, Washington, DC 20555-0001
113. C. E. Sanders, Bechtel SAIC Company, 1930 Village Center Cir 3-256, Las Vegas, NV 89134
114. A. Santamarina, Commissariat A L'Energie Atomique, Nuclear Reactor Division, Reactor Studies Department, Reactor and Cycle Physics Service, CEA/CADARACHE/DRN/DER/SPRC Bat. 230, 13108 Saint-Paul-Lez-Durance, Cedex, FRANCE
115. E. Sartori, OECD/NEA Data Bank, Le Seine-Saint Germain, 12 Boulevard des Iles, F-92130 Issy-les-Moulineaux, FRANCE
116. J. J. Sapyta, Framatome Cogema Fuels, 3315 Old Forest Road, PO Box 10935, Lynchburg, VA 24506-0935
117. M. Smith, Virginia Power Co., PO Box 2666, Richmond, VA 23261
118. N. R. Smith, AEA Technology, A32 Winfrith, Dorchester, Dorset DT2 8DH, United Kingdom
119. J. T. Stewart, Department of Environment, Transport, and Re, RMTD, 4/18, GMH, 76 Marsham Street, London SW1P 4DR, United Kingdom
120. T. Suto, Power Reactor and Nuclear Fuel Development Corporation, Technical Service Division, Tokai Reprocessing Plant, Tokai Works, Tokai-Mura, Naka-gun, Ibaraki-ken, JAPAN
121. H. Taniuchi, Kobe Steel, Ltd., 2-3-1 Shinhama, Arai-Cho, Takasago, 676 JAPAN
122. D. A. Thomas, Bechtel SAIC Company, LLC, 1261 Town Center Drive, Las Vegas, NV 89134

123. P. R. Thorne, British Nuclear Fuels plc (BNFL), Nuclear and Radiological Safety, R101 Rutherford House, Risley Warrington WA3 6AS, United Kingdom
124. J. R. Thornton, Duke Engineering & Services, 230 S. Tyron St., PO Box 1004, Charlotte, NC 28201-1004
125. S. E. Turner, Holtec International, 230 Normandy Circle East, Palm Harbor, FL 34683
126. A. P. Ulses, U.S. Nuclear Regulatory Commission, RES, MS T10-K8, Washington, DC 20555-0001
127. M. D. Waters, U.S. Nuclear Regulatory Commission, NMSS/SFPO/SLID, MS O13-D13, Washington, DC 20555-0001
128. A. Wells, 2846 Peachtree Walk, Duluth, GA 30136
129. B. H. White IV, U.S. Nuclear Regulatory Commission, NMSS/SFPO/TRD, MS O13-D13, Washington, DC 20555-0001
130. Robert Wilson, Rocky Flats Field Office, USDOE, 10808 Highway 93, Golden, CO 80403-8200
131. C. J. Withee, U.S. Nuclear Regulatory Commission, NMSS/SFPO/TRD, MS O13-D13, Washington, DC 20555-0001

NRC FORM 335 (2-89) NRCM 1102 3201, 3202

U.S. NUCLEAR REGULATORY COMMISSION

BIBLIOGRAPHIC DATA SHEET

(See instructions on the reverse)

1. REPORT NUMBER (Assigned by NRC, Add Vol., Supp., Rev., and Addendum Numbers, if any.)

NUREG/CR-6800
ORNL/TM-2002/6

2. TITLE AND SUBTITLE

Assessment of Reactivity Margins and Loading Curves for PWR Burnup-Credit Cask Designs

3. DATE REPORT PUBLISHED

MONTH	YEAR
March	2003

4. FIN OR GRANT NUMBER

W6479

5. AUTHOR(S)

J. C. Wagner and C. E. Sanders

6. TYPE OF REPORT

Technical

7. PERIOD COVERED *(Inclusive Dates)*

8. PERFORMING ORGANIZATION — NAME AND ADDRESS *(If NRC, provide Division, Office or Region, U.S. Nuclear Regulatory Commission, and mailing address; if contractor, provide name and mailing address.)*

Oak Ridge National Laboratory, Managed by UT-Battelle, LLC
PO Box 2008, Bldg. 6011, MS-6370
Oak Ridge, TN 37831-6370 USA

9. SPONSORING ORGANIZATION — NAME AND ADDRESS *(If NRC, type "Same as above"; if contractor, provide NRC Division, Office or Region, U.S. Regulatory Commission, and mailing address.)*

Division of Systems Analysis and Regulatory Effectiveness
Office of Nuclear Regulatory Research
U.S. Nuclear Regulatory Commission
Washington, DC 20555-0001

10. SUPPLEMENTARY NOTES

R. Y. Lee, NRC Project Manager

11. ABSTRACT *(200 words or less)*

This report presents studies to assess reactivity margins and loading curves for pressurized water reactor (PWR) burnup-credit criticality safety evaluations. The studies are based on a generic high-density 32-assembly cask and systematically vary individual calculational (depletion and criticality) assumptions to demonstrate the impact on the predicted effective neutron multiplication factor, k_{eff}, and burnup-credit loading curves. The purpose of this report is to provide a greater understanding of the importance of input parameter variations and quantify the impact of calculational assumptions on the outcome of a burnup-credit evaluation. This study should provide guidance to regulators and industry on the technical areas where improved information will most enhance the estimation of accurate subcritical margins. Based on these studies, areas where future work may provide the most benefit are identified. The report also includes an evaluation of the degree of burnup credit needed for high-density casks to transport the current spent nuclear fuel inventory. By comparing PWR discharge data to actinide-only based loading curves and determining the number of assemblies that meet the loading criteria, this evaluation finds that additional negative reactivity (through either increased credit for fuel burnup or cask design/utilization modifications) is necessary to accommodate the majority of current spent fuel assemblies in high-capacity casks.

12. KEY WORDS/DESCRIPTORS *(List words or phrases that will assist researchers in locating the report.)*

burnup credit, criticality safety, spent fuel, storage, transportation

13. AVAILABILITY STATEMENT

unlimited

14. SECURITY CLASSIFICATION

(This Page) unclassified

(This Report) unclassified

15. NUMBER OF PAGES

16. PRICE